Volume 9, Issue 15 - e2025915 January - December - 2025

Journal-Mathematical and Quantitave Methods

ISSN: 2531-2979

RINOE®

Journal-Mathematical and Quantitative Methods, Volume 9, Issue 15: e2025915 January – December 2025, is a Continuous publication - Journal edited by RINOE-Spain. 38 Matacerquillas, Moralzarzal - CP-28411. Madrid- Spain. WEB: www.rinoe.org journal@rinoe.org.

Editor in Chief: Segovia - Vargas, María Jesús. PhD. ISSN-2531-2979. Responsible for the latest update of this issue RINOE Computer Unit. Escamilla-Bouchán, Imelda. PhD, Luna-Soto, Vladimir. PhD. 38 Matacerquillas, Moralzarzal – CP- 28411. Madrid - Spain, last updated December 30, 2025.

RINOE Journal-Mathematical and Quantitative Methods

Definition of the Journal

Scientific Objectives

Support the international scientific community in its written production Science, Technology and Innovation in the Field of Social Sciences, in Subdisciplines of Econometric and statistical methods: Generalities, Bayesian analysis, Hypothesis testing, Estimation, Semiparametric and nonparametric methods, Statistical simulation methods; Monte Carlo methods, Econometric and statistical methods: Specific distributions; Econometric methods: Single equation models; Econometric methods: Multiple/Simultaneous equation models; Econometric and statistical methods: Special topics, Duration analysis, Survey methods, Index numbers and aggregation, Statistical decision theory, Operations research, Neural networks and related topics; Econometric modeling: Model construction and estimation, Model evaluation and testing, Forecasting and other model applications; Mathematical methods and programming: Optimization techniques, Programming models, Dynamic analysis, Existence and stability conditions of equilibrium, Computational techniques, Miscellaneous mathematical tools, Input-Output models, Computable general equilibrium models; Game theory and bargaining theory: Cooperative games, Noncooperative games, Stochastic and dynamic games, Bargaining theory, Matching theory; Data collection and Data estimation methodology: Computer programs, Methodology for collecting, Estimating, and Organizing microeconomic, Methodology for collecting, Estimating, and Organizing Macroeconomic Data, Econometric software; Design of experiments: Laboratory, Individual behavior, Laboratory, Group behavior, Field experiments.

RINOE® is a Scientific and Technological Company in contribution to the Human Resource training focused on the continuity in the critical analysis of International Research and is attached to SECIHTI-RENIECYT number 1702902, its commitment is to disseminate research and contributions of the International Scientific Community, academic institutions, agencies and entities of the public and private sectors and contribute to the linking of researchers who carry out scientific activities, technological developments and training of specialized human resources with governments, companies and social organizations.

Encourage the interlocution of the International Scientific Community with other Study Centers in Mexico and abroad and promote a wide incorporation of academics, specialists and researchers to the publication in Science Structures of Autonomous Universities - State Public Universities - Federal IES - Polytechnic Universities - Technological Universities - Federal Technological Institutes - Normal Schools - Decentralized Technological Institutes - Intercultural Universities - S & T Councils - SECIHTI Research Centers.

Scope, Coverage and Audience

RINOE Journal-Mathematical and Quantitative Methods is a Journal edited by RINOE® in its Holding with repository in Spain, is a scientific publication arbitrated and indexed with semester periods. It supports a wide range of contents that are evaluated by academic peers by the Double-Blind method, around subjects related to the theory and practice of Econometric and statistical methods: Generalities, Bayesian analysis, Hypothesis testing, Estimation, Semiparametric and nonparametric methods, Statistical simulation methods; Monte Carlo methods, Econometric and statistical methods: Specific distributions; Econometric methods: Single equation models; Econometric methods: Multiple/Simultaneous equation models; Econometric and statistical methods: Special topics, Duration analysis, Survey methods, Index numbers and aggregation, Statistical decision theory, Operations research, Neural networks and related topics; Econometric modeling: Model construction and estimation, Model evaluation and testing, Forecasting and other model applications; Mathematical methods and programming: Optimization techniques, Programming models, Dynamic analysis, Existence and stability conditions of equilibrium, Computational techniques, Miscellaneous mathematical tools, Input-Output models, Computable general equilibrium models; Game theory and bargaining theory: Cooperative games, Noncooperative games, Stochastic and dynamic games, Bargaining theory, Matching theory; Data collection and Data estimation methodology: Computer programs, Methodology for collecting, Estimating, and Organizing microeconomic, Methodology for collecting, Estimating, and Organizing Macroeconomic Data, Econometric software.

Design of experiments: Laboratory, Individual behavior, Laboratory, Group behavior, Field experiments with diverse approaches and perspectives, That contribute to the diffusion of the development of Science Technology and Innovation that allow the arguments related to the decision making and influence in the formulation of international policies in the Field of Social Sciences. The editorial horizon of RINOE® extends beyond the academy and integrates other segments of research and analysis outside the scope, as long as they meet the requirements of rigorous argumentative and scientific, as well as addressing issues of general and current interest of the International Scientific Society.

Editorial Board

Arbitration Committee

Assignment of Rights

The sending of an Article to RINOE Journal-Mathematical and Quantitative Methods emanates the commitment of the author not to submit it simultaneously to the consideration of other series publications for it must complement the Originality Format for its Article.

The authors sign the Format of Authorization for their Article to be disseminated by means that RINOE® In its Holding Spain considers pertinent for disclosure and diffusion of its Article its Rights of Work.

Declaration of Authorship

Indicate the Name of Author and Coauthors at most in the participation of the Article and indicate in extensive the Institutional Affiliation indicating the Department.

Identify the Name of Author and Coauthors at most with the CVU Scholarship Number-PNPC or SNI-SECIHTI- Indicating the Researcher Level and their Google Scholar Profile to verify their Citation Level and H index.

Identify the Name of Author and Coauthors at most in the Science and Technology Profiles widely accepted by the International Scientific Community ORC ID - Researcher ID Thomson - arXiv Author ID - PubMed Author ID - Open ID respectively.

Indicate the contact for correspondence to the Author (Mail and Telephone) and indicate the Researcher who contributes as the first Author of the Article.

Plagiarism Detection

All Articles will be tested by plagiarism software PLAGSCAN if a plagiarism level is detected Positive will not be sent to arbitration and will be rescinded of the reception of the Article notifying the Authors responsible, claiming that academic plagiarism is criminalized in the Penal Code.

Arbitration Process

All Articles will be evaluated by academic peers by the Double Blind method, the Arbitration Approval is a requirement for the Editorial Board to make a final decision that will be final in all cases. MARVID® is a derivative brand of ECORFAN® specialized in providing the expert evaluators all of them with Doctorate degree and distinction of International Researchers in the respective Councils of Science and Technology the counterpart of SECIHTI for the chapters of America-Europe-Asia- Africa and Oceania. The identification of the authorship should only appear on a first removable page, in order to ensure that the Arbitration process is anonymous and covers the following stages: Identification of the Journal with its author occupation rate - Identification of Authors and Coauthors - Detection of plagiarism PLAGSCAN - Review of Formats of Authorization and Originality-Allocation to the Editorial Board- Allocation of the pair of Expert Arbitrators-Notification of Arbitration -Declaration of observations to the Author-Verification of Article Modified for Editing-Publication.

Instructions for Scientific, Technological and Innovation Publication

Knowledge Area

The works must be unpublished and refer to topics of Econometric and statistical methods: Generalities, Bayesian analysis, Hypothesis testing, Estimation, Semiparametric and nonparametric methods, Statistical simulation methods; Monte Carlo methods; Econometric and statistical methods: Specific distributions; Econometric methods: Single equation models; Econometric methods: Multiple/Simultaneous equation models; Econometric and statistical methods: Special topics, Duration analysis, Survey methods, Index numbers and aggregation, Statistical decision theory, Operations research, Neural networks and related topics; Econometric modeling: Model construction and estimation, Model evaluation and testing, Forecasting and other model applications; Mathematical methods and programming: Optimization techniques, Programming models.

Dynamic analysis, Existence and stability conditions of equilibrium, Computational techniques, Miscellaneous mathematical tools, Input-Output models, Computable general equilibrium models; Game theory and bargaining theory: Cooperative games, Noncooperative games, Stochastic and dynamic games, Bargaining theory, Matching theory; Data collection and Data estimation methodology: Computer programs, Methodology for collecting, Estimating, and Organizing microeconomic, Methodology for collecting, Estimating, and Organizing Macroeconomic Data, Econometric software; Design of experiments: Laboratory, Individual behavior, Laboratory, Group behavior, Field experiments and other topics related to Social Sciences.

Presentation of the Content

In the first article we present, *Microcrack evaluation using modal analysis under two loading conditions on rotodynamic shafts*, by Romero-Sotelo, Francisco Javier, Rodríguez-Blanco, Marco Antonio, Pérez-Montejo, Salatiel and Álvarez-Arellano, Juan Antonio, with adscription in the Universidad Autónoma del Carmen; as next article we present, *Soil gradients and phytochemical responses in Tithonia diversifolia: design of a comprehensive utilization model by vegetative tissue in Veracruz*, by Ixmatlahua-Rodríguez, Christian Andrés, Ortiz-Celiseo, Araceli, Alejandre-Rosas, Jorge Alberto and López-Zamora, Leticia, with adscription in the Tecnológico Nacional de México. Instituto Tecnológico de Orizaba and LADISER - Universidad Veracruzana; as next article we present, *Design and maintenance analysis of wind turbine amplifier gearboxes systems exposed to lightning discharges*, by Berra-Ceballos, Raúl, Cruz-Gómez, Marco Antonio, Mejía-Pérez, José Alfredo and Castillo- Pensado, Juan Luis, with adscription in the Benemérita Universidad Autónoma de Puebla;; as final article we present, *Modelling of the lifting platform braking mechanism for autonomous vertical parking*, by Betanzos-Castillo, Francisco, Fuentes-Castañeda, Pilar, Cortez-Solis, Reynaldo and Rodriguez-Cortes, Aldo, with adscription in the Tecnológico Nacional de México – TES Valle de Bravo.

Content

Journal-Mathematical and Quantitative Methods 9[15]1-14: e1915114
Article

Microcrack evaluation using modal analysis under two loading conditions on rotodynamic shafts

Evaluación de microfisuras usando análisis modal bajo dos condiciones de carga en ejes rotodinámicos

Romero-Sotelo, Francisco Javier * [a], Rodríguez-Blanco, Marco Antonio [b], Pérez-Montejo, Salatiel [c] and Álvarez-Arellano, Juan Antonio [d]

[a] Universidad Autónoma del Carmen • NKO-8222-2025 • 0000-0003-4605-0567 • 377427
[b] Universidad Autónoma del Carmen • U-6476-2017 • 0000-0003-3641-6895 • 92331
[c] Universidad Autónoma del Carmen • LYO-9195-2024 • 0000-0002-1750-0154 • 594590
[d] Universidad Autónoma del Carmen • JRX-8666-2023 • 0000-0001-6341-417X • 273636

Classification:

Area: Engineering
Field: Engineering
Discipline: Mechanical Engineering
Subdiscipline: Vibration and acoustics

https://doi.org/10.35429/JMQM.2025.9.15.1.1.14
History of the article:
Received: October 30, 2025
Accepted: December 30, 2025

* ✉ [fromero@pampano.unacar].

Abstract

Microcracks in a component are characterized as minor imperfections that manifest in specific materials, particularly those integral to critical structures. Their diminutive size renders detection exceedingly challenging, presenting a substantial obstacle for analysts of structural systems. These microcracks frequently signify the onset of a more extensive degradation process, so they early identification is crucial. Otherwise, the mechanical integrity of the equipment could be put at risk. Currently, standard practice entails subjecting components to laboratory tests, which, although informative, are not invariably nondestructive. Considering this, the adoption of simulations based on modal analysis and the monitoring of stiffness variations under controlled loads is gaining traction, with the objective of shortening evaluation times and safeguarding the component's integrity during diagnosis.

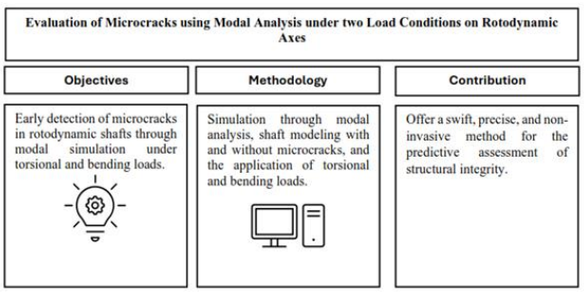

Microcrack, Modal analysis, Rigidity

Resumen

Las microfisuras en un componente se definen como pequeñas imperfecciones que aparecen en ciertos materiales, sobre todo en los que forman parte de estructuras críticas. Debido a su reducido tamaño, localizarlas resulta sumamente complicado, lo que plantea un reto significativo para quienes analizan sistemas estructurales. Estas microfisuras a menudo marcan el comienzo de un proceso de degradación más amplio, por lo que identificarlas a tiempo es vital; de lo contrario, el rendimiento mecánico de la pieza puede verse comprometido. Actualmente, la práctica habitual pasa por someter los elementos a ensayos de laboratorio, protocolos que, si bien informativos, no siempre son no destructivos. Ante este panorama, surge el aprovechamiento de simulaciones basadas en análisis modal y en el monitoreo de variaciones de rigidez bajo cargas controladas, con el fin de acortar los plazos de evaluación y proteger la integridad del componente durante el diagnóstico.

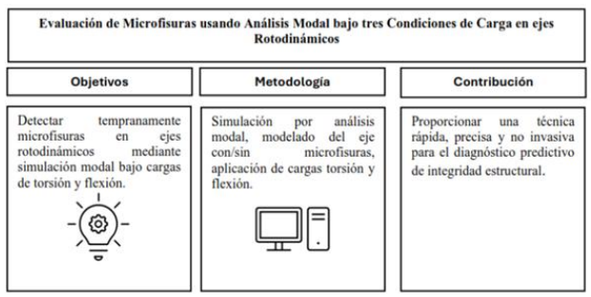

Microfisura, Análisis modal, Rigidez

Area: Promotion of frontier research and basic science in all fields of knowledge

Citation: Romero-Sotelo, Francisco Javier, Rodríguez-Blanco, Marco Antonio, Pérez-Montejo, Salatiel and Álvarez-Arellano, Juan Antonio. [2025]. Microcrack evaluation using modal analysis under two loading conditions on rotodynamic shafts. Journal-Mathematical and Quantitative Methods. 9[15]1-14: e1915114.

ISSN 2531-2979 /© 2009 The Authors. Published by RINOE-México, S.C. for its Holding Spain on behalf of Journal-Mathematical and Quantitative Methods. This is an open-access article under the license **CC BY-NC-ND** [http://creativecommons.org/licenses/by-nc-nd/4.0/]

Peer review under the responsibility of the Scientific Committee MARVID®- in the contribution to the scientific, technological and innovation **Peer Review Process** through the training of Human Resources for the continuity in the Critical Analysis of International Research.

RENIECYT Registro Nacional de Instituciones y Empresas Científicas y Tecnológicas
1702902 SECIHTI

Introduction

Timely detection of microcracks in rotor-driven shafts represents one of the most significant challenges in contemporary mechanical engineering. These components, integral to turbines, generators, and combustion engines, endure substantial dynamic forces and fluctuating operating conditions that promote the emergence of nearly imperceptible cracks. Despite their minuscule size, these defects can precipitate severe fractures if not promptly recognized, as they disrupt local rigidity, alter natural frequencies, and compromise the structural integrity of the machine. Consequently, this leads to failures that impact safety, diminish availability, and escalate maintenance expenses[Jorge et al., 2024].

Up until now, ultrasound, magnetic particle examination, or destructive metallography has been used in labs to examine these breaks. These approaches are helpful, but they require extensive periods of downtime and equipment handling, and they aren't always completely non-destructive. Also, they have big problems when trying to find faults that are less than a millimeter long. In a world where Industry 4.0 and predictive maintenance strategies are common, there is a strong need for fast, reliable, and mostly virtual ways to check the condition of an axis both during the design phase and throughout its operational lifespan. This will reduce the need for invasive physical testing. [Sinou & Lees, 2007].

Finite element analysis [FEA] serves as an invaluable technique for this purpose. By determining the natural frequencies, damping ratios, and modal shapes of the structure, it becomes possible to identify significant alterations induced by the emergence of microdefects. These discrepancies are accentuated under torsional and flexural loads, as the applied torque creates stress concentrations at the crack edges, thereby modifying the overall vibrational response. The integration of modal simulation with a comprehensive analysis of equivalent stiffness provides a robust theoretical and computational framework that correlates frequency reduction with localized stiffness degradation, establishing a foundation for quantitative damage assessment [Garcia, 2017].

This study simulates a cylindrical specimen per ASTM E8, featuring a flaw smaller than 1 mm [microcrack], and conducts modal analysis in ANSYS© Workbench for both intact and compromised conditions. The method allows for the measurement of displacements for the first bending and torsion modes, calculates the stiffness loss in the affected area, and sets warning levels that can be used in online monitoring systems. The proposed method adds value during both the design phase [confirmation of tolerances and fatigue life through simulation] and the operational phase [asset monitoring via vibration sensors] by providing quick, repeatable results that don't require direct intervention on the equipment [Garcia, 2017].

In conclusion, the methodology outlined here addresses the growing need for non-destructive methods based on simulation models that reduce downtime, improve maintenance, and enhance the reliability of critical rotating systems. These results show that modal analysis and stiffness studies work well together to locate microcracks and fully assess the structural integrity of rotary shafts.

The evaluation of microcracks under diverse loading situations by modal analysis has become a significant area of research due to its ability to detect subtle changes in the system's dynamic features. This procedure makes it easier to find cracks before they get big enough to put the shaft's structural integrity at risk [Rodríguez Bravo et al., 2022].

Literature review

Within the bibliographic review, different authors have carried out studies and experiments to determine the phenomenon or explain the behavior of a crack in an axis or rotodynamic mechanical element, in the first Dilena & Morassi [2002] they examined, using analytical models and experimental tests, the variations in the vibration modes of thin beams subjected to resonance. The results showed that the presence of a crack significantly alters the location of the nodes in these vibrational modes, possibly resulting in the displacement of the nodes allowing the location of the damage to be determined.

Expensive tools and large data sets are required to assess damage via the vibrations of iron marks.

ISSN: 2531-2979
RENIECYT: 1702902

Romero-Sotelo, Francisco Javier, Rodríguez-Blanco, Marco Antonio, Pérez-Montejo, Salatiel and Álvarez-Arellano, Juan Antonio. [2025]. Microcrack evaluation using modal analysis under two loading conditions on rotodynamic shafts. Journal-Mathematical and Quantitative Methods. 9[15]1-14: e1915114.
https://doi.org/10.35429/JMQM.2025.9.15.1.1.14

Most of the time, the uncertainties tied to models are ignored, affecting their accuracy. Alegria Gómez et al. [2024] suggests an innovative computational methodology using optimized genetic algorithms tailored to sparse and incomplete data sets. Unlike previous approaches, this model accounts for the uncertainty pertaining to shape and mass. The use of only three flexional vibration modes eliminates the need for higher modes' information. The methodology has been experimentally validated on an iron frame structure and provides proof of efficacy in the presence of multiple and illustrative damage conditions. The methodology achieved 100% success in damage identification and 80% in the estimation of severity. This indicates an outstanding level of performance, particularly for the low cost of the procedure in comparison to alternative approaches.

Nahvi & Jabbari [2005] demonstrate in their work that, by integrating experimental measurements of natural frequencies and mode shapes [Kushwaha & Patel, 2023] with an analytical model, it is possible to locate and estimate the depth of a crack in a cantilever beam: the comparison between measured frequencies and normalized frequency contours, followed by a minimization algorithm, allows to quickly and accurately identify the damaged element.

Kisa & Gurel [2006] propose a hybrid approach that combines the finite element method with component mode synthesis to modally analyze circular beams exhibiting multiple open and fixed cracks. The process fragments the beam into segments over the cracked areas and assembles them using flexibility matrices derived from fracture mechanics. This allows obtaining, in reasonable computational times and for any boundary conditions, the natural frequencies as the modal shapes of the beam vary systematically according to the position and depth of the damage. Viola et al. [2001]presented a finite element design for Timoshenko beams with open cracks and showed that, by including variations in stiffness and mass in the model and comparing the results with modal test measurements, it is possible to locate the crack with high precision and assess its severity from the recorded changes in the frequencies and modes of the structure.

Rastogi & Kumar [2009]review 40 years of studies on fatigue cracks in rotors defects that can lead to serious failures and critically assess the main strategies employed. They summarize: [1] advanced analytical and Lagrangian models that capture cyclic hardness variation due to crack "breathing"; [2] numerical techniques based on finite elements and modal synthesis that analyze many cracks at low computational cost; [3] physical testing and inversion algorithms, including AI approaches, to locate and measure damage; and [4] time-frequency signal analysis that finds sub-synchronous nonlinear components. The conclusion highlights challenges in validating in-service data, modeling growing cracks, and coupling bearing effects, to achieve more robust diagnostics in today's rotors.

Czajkowski et al. [2017] presented a Jeffcott model of a flexible, non-spinning rotor, which consists of a weightless shaft with a transverse crack near the disk and supports the system on ball bearings. With this arrangement, they numerically studied how breath-like opening in the crack modifies stiffness and thus natural frequencies. As the angular position of the rotor changes, each mode splits into two nearby peaks that only manifest themselves on damaged shafts; therefore, the systematic appearance of these modes duplicate peaks becomes an early and reliable sign for detecting cracks before the rotor goes into service.

According to the research, they agree that cracks significantly alter the modal properties of beams and rotors natural frequencies, vibration modes and nodes and that, by studying these variations through analytical models, finite elements, mode synthesis, or experimental tests, it is possible to locate the crack and assess its severity with good precision. In this sense, nodal displacement, peak frequency splitting, and the comparison of measured modal data with calibrated models emerge as early and reliable indicators of damage in rotodynamic elements.

Fundamentals of Modal Analysis

Modal analysis serves as a fundamental tool for identifying microcracks in rotating machinery. This method makes it easier to find the structure's inherent frequencies, damping coefficients, and mode shapes, as shown in figure 1. It is a strong and helpful way to describe dynamic behavior, notably in vibration research.

ISSN: 2531-2979
RENIECYT: 1702902

It is often called structural modal analysis. In essence, it is a computational method based on a mathematical model of certain parts of the structure, focusing on how they vibrate.

Box 1

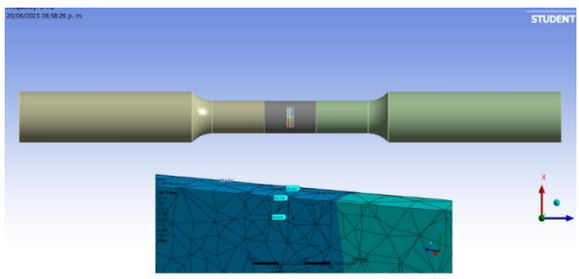

Figure 1
Modal analysis in software to assess vibrations resulting from loads or defects
Source: Own elaboration

In the classical framework of linear modal analysis, the structure is regarded as an ideal elastic system where mass *M*, damping *C*, and stiffen *K* are considered constant over time. This assumption facilitates the formulation and resolution of the problem without the need for physical testing, enabling the direct extraction of vibration modes and their natural frequencies, which act as indicators of the structure's integrity. By disregarding real loads, such as shear stresses, temperature gradients, or elastic supports, the model offers an intrinsic dynamic representation of the element, serving as a benchmark for comparison with any subsequent state.

However, the emergence of microcracks undermines the assumption that the material always maintains rigidity. Each crack introduces a localized flexibility [$\Delta K_{cracked}$] that alters the effective stiffness, resulting in the following relationship:

$$K_{cracked} = K_{intact} - \Delta K_{fissure} \quad [1]$$

As the shaft rotates, the crack functions as a diaphragm, opening under tension and closing under compression.

This phenomenon "breathes" leading to a periodic modulation of stiffness, which results in additional harmonics at submultiples of the rotational frequency and slight shifts in the natural frequencies.

Finite element analysis facilitates the integration of contact conditions at the crack edges and the superposition of realistic loads—such as torsion, combined bending, and thermal gradients. Parametric sweeps correlate the amplitude of modal displacements with the size, orientation, and depth of the crack, thereby establishing numerical thresholds for predictive maintenance. Consequently, an abstract linear model serves as a baseline against which the nonlinear effects induced by microdefects are measured, simulated, and ultimately detected while the machine remains operational.

In summary, the integration of linear modal analysis with sophisticated simulations that incorporate "breathing" microcracks a term that will be elucidated later provides a robust framework that enables: [1] the definition of the normal vibration pattern of the shaft, [2] the measurement of stiffness loss resulting from early damage, and [3] the prediction of crack progression, specifically those smaller than one millimeter, based on spectral changes before they impact the operation of critical rotodynamic machines.

Fissure Breathing Phenomenon

Crack breathing is a critical phenomenon for comprehending the behavior of structurally compromised rotodynamic shafts, specifically cracked shafts [Hossain & Wu, 2018]. This term refers to the process whereby a crack in the shaft periodically opens and closes as the component rotates. As the shaft turns, alternating forces, often resulting from bending, generate cyclic tensile and compressive stress in the damaged area. During the tensile phase, the crack opens, leading to a significant loss of load-bearing capacity in the cracked section and a reduction in its local stiffness. Conversely, when subjected to compression, the crack faces make contact, the crack closes, and stiffness is partially restored [Wang et al., 2021].

This continuous cycle of opening and closing causes a periodic modulation of the stiffness of the shaft. This rhythmic variation acts as a parametric forcing in the rotating system, which translates into vibratory components at characteristic frequencies. Specifically, the effect of the breathing fissure is usually reflected as an obvious peak in the vibration spectrum at twice the rotational speed, i.e. at 2x.

ISSN: 2531-2979
RENIECYT: 1702902

Romero-Sotelo, Francisco Javier, Rodríguez-Blanco, Marco Antonio, Pérez-Montejo, Salatiel and Álvarez-Arellano, Juan Antonio. [2025]. Microcrack evaluation using modal analysis under two loading conditions on rotodynamic shafts. Journal-Mathematical and Quantitative Methods. 9[15]1-14: e1915114.
https://doi.org/10.35429/JMQM.2025.9.15.1.1.14

In addition, spectral analysis can reveal harmonics at multiples of the rotational frequency and even subharmonic responses, all resulting from the internal modulation of the material's stiffness.

Therefore, the damaged shaft not only responds to the forced excitation at the rotational frequency, but also generates extra frequencies caused by the periodic change in its rigidity.

As a result, a shaft that exhibits a crack not only vibrates at the frequency of forced rotation, but also shows additional components generated by cyclical changes in its rigidity. Phenomena such as the prominent 2X peak and other lateral modulations then act as characteristic indicators of breakage and are key to diagnosing failures in rotating machinery. To understand these vibrations, it is necessary to face their nonlinear nature and consider the intermittent contact between the faces of the crack and the distribution of stresses in its vicinity.

As effective stiffness changes with angular position, some analytical approaches simplify it and model it with a well-determined periodic function, for example, a sine wave that repeats throughout an entire revolution. However, to reproduce the real behavior it is preferable to resort to non-linear numerical simulations that handle the phenomenon more faithfully. These advanced models, usually implemented with finite elements, include contacts that allow the opening and closing of the crack to be simulated in an explicit and realistic way at each turn [Liu et al., 2023].

A finite element model defines a surface-to-surface interaction with hard contact in the normal direction, preventing crack faces from overlapping while preventing tensile stresses from being transmitted when the crack is open.

In this manner, the model effectively captures the abrupt decrease in stiffness during crack opening and the immediate restoration of that stiffness upon closure, thereby replicating the cyclical hardness pattern observed in experimental tests. While the nonlinear formulation incorporating three-dimensional contact is regarded as the most dependable for simulating the effects of a breathing crack, its implementation necessitates extensive computation times, which constrains its practical application in industrial designs.

Therefore, the presence of a breathing crack gives the rotor [El-Mongy & Younes, 2018] a complex and non-linear dynamic behavior, with fluctuating stiffness over time; Hence, their inclusion in models is essential to understand the response of damaged rotating axes and to develop robust tools for diagnosing and detecting faults in rotating machinery[Varney & Green, 2012].

Most important modules of a modal analysis

The dynamic analysis of a structural model, in addition to comprehensively studying the transient response of that model to various external excitations, also provides invaluable information about how currently designed models respond to periodic perturbations, depending on the frequency of such perturbations[Rodríguez Bravo et al., 2022].

This information is extremely useful and practical in the design stage, as it allows structures to be optimized and possible failures to be foreseen. The evaluations are carried out within a Modal Analysis, which includes four specific resources to judge the structures accurately. These are:

1. Modal analysis, which provides an initial overview of the system's natural vibration modes [Bertero et al., 2022].

2. ARM Analysis, this procedure is superior to the classic Modal when working with large or complicated elements and calculation time is limited. It provides a detailed list of frequencies and mode shapes in the chosen band, which speeds up the design.

3. Torsion Mode analysis, which investigates how the structure rotates under torsional loads.

4. Modal visual analysis. This approach It uses the structure's torsion mode to show the deformations and behavioral states that can arise under excitations, thus providing fundamental data for design and optimization. These methods are essential to ensuring that buildings not only meet safety requirements but are also efficient and durable over the long term.

ISSN: 2531-2979
RENIECYT: 1702902

Romero-Sotelo, Francisco Javier, Rodríguez-Blanco, Marco Antonio, Pérez-Montejo, Salatiel and Álvarez-Arellano, Juan Antonio. [2025]. Microcrack evaluation using modal analysis under two loading conditions on rotodynamic shafts. Journal-Mathematical and Quantitative Methods. 9[15]1-14: e1915114.
https://doi.org/10.35429/JMQM.2025.9.15.1.1.14

Methodology

The procedure for identifying and studying microfractures using modal simulations performed in ANSYS© software begins with the creation of a three-dimensional model that defines the geometry, material properties, and a fine mesh that highlights the critical areas of the rotodynamic axis. Next, it is shown how the modal analysis was performed according to the ASTM E8 standard, determining vibrational frequencies and dynamic modes, and special attention is given to the modes that concentrate stress in susceptible regions, to then impose torsional loads of figure 2, which replicate the real conditions of the fieldwork and evaluate the stress and strain distributions.

Box 2

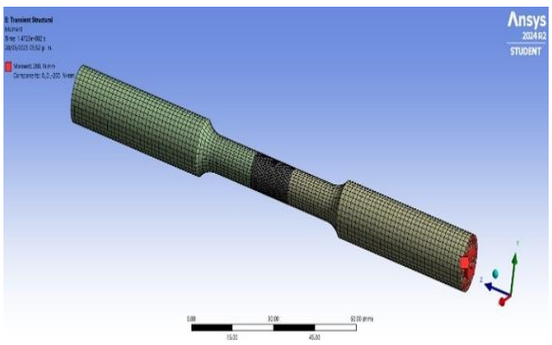

Figure 2

Definition of boundary conditions for simulation

Source: Own elaboration

Modal analysis is a fundamental technique in structural and mechanical engineering that allows characterizing the dynamic behavior of systems and structures by determining their intrinsic vibratory properties. This methodology combines solid theoretical principles with advanced experimental techniques to obtain critical modal parameters such as natural frequencies, damping factors and modal shapes, allowing them to predict their response to dynamic excitations and optimize their design to avoid resonance problems [Sinou & Lees, 2005].

Microcrack Simulation Modeling

A test specimen was designed to comply with the ASTM E8 standard for torsion tests [in simulation and future work in experimentation], in this stage will be the simulation stages, using computer-aided design software, where the first model is free of microcrack defects.

The model is a 9 mm diameter cylinder around application of the microcrack, considering an ASTM A36 steel, and appropriate boundary conditions were defined as shown in figure 3.

Box 3

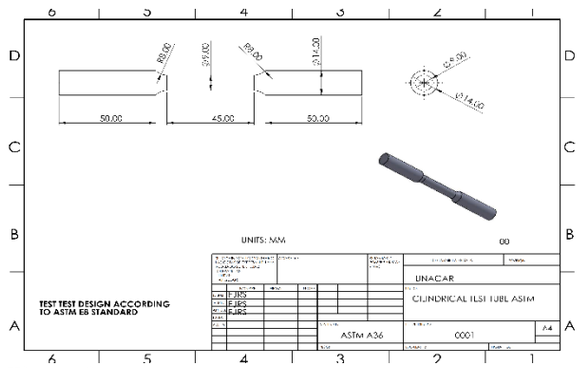

Figure 3

Shaft modeled according to ASTM E8 Standard for Vibration Testing

Source: Own elaboration

Microcracks were then incorporated into the second model to simulate potential initiation and propagation sites of microcracks and essentially determine whether microcracks smaller than 1 mm are affected by the proposed models. A modal analysis was performed to evaluate the effects of these microcracks on the natural frequencies and mode shapes of the system, which helps to detect changes in the dynamic response of the system, figure 4.

Box 4

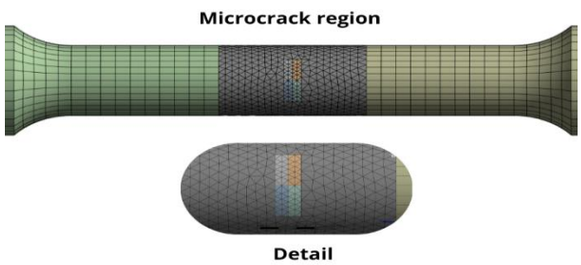

Figure 4

Modeled Shaft with Microcracks for Modal Analysis

Source: Own elaboration

Microcrack Simulation in Modal Analysis

Microcrack simulation in modal analysis using ANSYS© software allows for the study of how cracks, even small ones, affect the dynamic properties of a structure, including its vibration modes and natural frequencies.

ISSN: 2531-2979
RENIECYT: 1702902

Romero-Sotelo, Francisco Javier, Rodríguez-Blanco, Marco Antonio, Pérez-Montejo, Salatiel and Álvarez-Arellano, Juan Antonio. [2025]. Microcrack evaluation using modal analysis under two loading conditions on rotodynamic shafts. Journal-Mathematical and Quantitative Methods. 9[15]1-14: e1915114.
https://doi.org/10.35429/JMQM.2025.9.15.1.1.14

Changes in vibrational modes, displacements, and stress levels can be examined with damage models in certain regions due to the presence of microcracks. This approach is especially useful for estimating the influence of defects on the stability of a structure with respect to vibratory movements, thus aiding in the assessment of the risk of sudden and unpredictable failures and improving maintenance strategies [Gomez Peral & Fabra Rodriguez, 2022].

Experimental theoretical and technical principles are included in modal analysis. Theoretical modal analysis is based on a physical model of a dynamical system containing elements such as mass, stiffness, and damping, which are given through differential equations [Rufino-Arteaga & García-Pérez, 2025]. For a physical model to be more plausible as well, it must possess such properties in terms of their spatial distributions, and for this reason they are called matrices of mass, stiffness, and damping that are introduced into a system of differential equations of motion, as shown in Equation 2[Sadeghi, 2021]:

$$[M]\{\ddot{x}(t)\} + [C]\{\dot{x}|(t)\} + [K]\{x|(t)\} = F(t) \qquad [2]$$

M, C, K : Mass matrix, damping and stiffness, respectively.
$\ddot{x}$ $[t]$, $\dot{x}$ $[t]$, x[t]: Vectors acceleration, velocity and displacement, respectively.
F[t]: Vector force.

The modal analysis applied in the simulation offered a deeper and more detailed perspective on the natural frequencies, damping values and modal shapes that characterize the structure of the object in question. This high-level analytical technique facilitated the modification and improvement of the object's design, thus mitigating its vulnerability to different forces that arise during its use. Additionally, specific behaviors were detected that could be optimized to ensure a more efficient and safe operation of the research work in a structured way according to the scheme.

When performing modal analysis using the finite element method, it is crucial to have a model that accurately represents the geometry and other features of the system. The prudent choice of element size and type ensures that the modal shapes of the model accurately represent the natural vibrations of the system.

Specifically, elements must precisely construct the component's geometry to detect natural frequencies and insightfully and reliably characterize the associated bending and torsional modes. This allowed us a clearer understanding of the vibrational tendencies of the system as seen in Table 1.

Box 5

Table 1
Modal Vibration Modes

Frequency Mode	Without fissure [Hz]	With fissure [Hz]
Mode 1 Flex x	246.3	303.3
Mode 2 Flexion y	246.3	303.3
Mode 3 Combined Flexion	1742.9	1994.6
Mode 4 lengthways	1742.9	1994.7
Mode 5 Twist	3265.8	3466.6
Mode 6 Oscillating	4721.7	5216.9

Source: Own elaboration

It is shown in Table 1 that there are some changes in the frequencies obtained when there is microcracks in Mode 1 and 2 that are similar since they only change bending direction and give as data that there is the presence of a microcrack which by simple analysis gave us more information to determine the changes in material stiffness.

Initial calculations reveal six fundamental vibration modes, although the spectrum can be extended by combining multiple physical phenomena. Each new mode reflects variations in the material's stiffness and results in a slight shift in self-frequency, an effect that can be amplified by geometric changes, loss of mass, or the application of specific loads.

The appearance of a microfissure is a paradigmatic case that immediately alters these frequencies. Figure 5 shows the first mode in bending around the x-axis: panel 5-a illustrates the state of the material without cracking, while panel 5-b exhibits the vibrational response once the crack has been introduced, the natural frequency values are 246.3 Hz without cracking and 303.3 Hz with the presence of the microcrack resulting in a stiffness change of 18% of its frequency.

ISSN: 2531-2979
RENIECYT: 1702902

Romero-Sotelo, Francisco Javier, Rodríguez-Blanco, Marco Antonio, Pérez-Montejo, Salatiel and Álvarez-Arellano, Juan Antonio. [2025]. Microcrack evaluation using modal analysis under two loading conditions on rotodynamic shafts. Journal-Mathematical and Quantitative Methods. 9[15]1-14: e1915114.
https://doi.org/10.35429/JMQM.2025.9.15.1.1.14

In Mode 2 of bending in y-axis the values obtained in figures are shown, 6a-b, where in a without crack and b with microcrack giving as results without crack a natural frequency of 246.3 Hz without a crack and 303.3 Hz with the presence of the microcrack, resulting in a stiffness change of 18% of its frequency.

Box 6

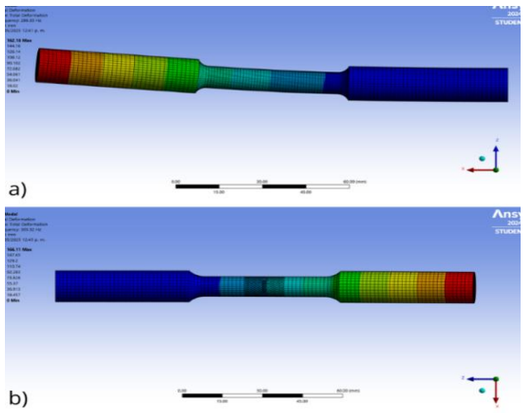

Figure 5
Vibration mode 1, in X-axis bending: [a] Without microcrack; [b] With microcrack

Source: Own elaboration

Box 7

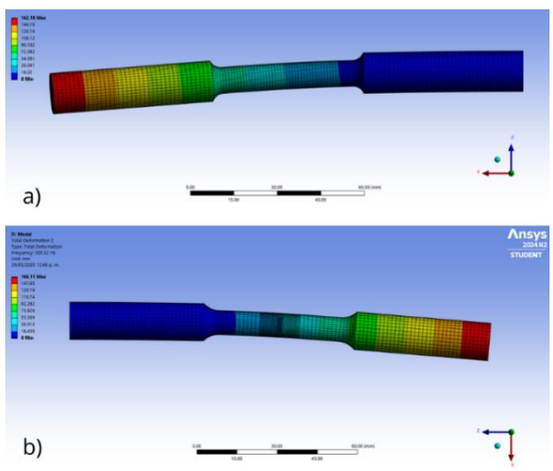

Figure 6
Vibration mode 2 in bending Y-axis: [a] Without microcrack; [b] With microcrack

Source: Own elaboration

In Mode 3, the values obtained in figure 7 are shown, under the conditions without microcrack in figure 7-a, and with microcrack in figure 7-b.

Box 8

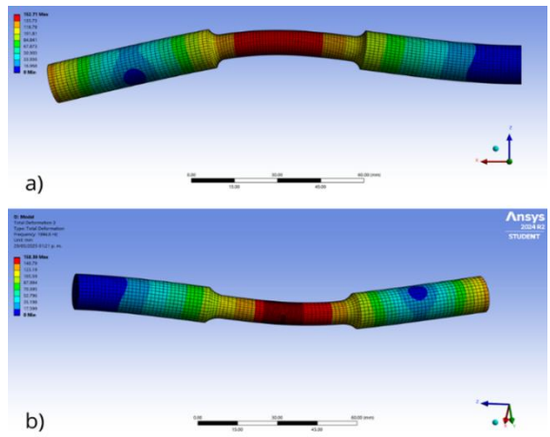

Figure 7
Vibration mode 3 in combined bending: [a] Without microcrack; [b] With microcrack

Source: Own elaboration

In Mode 5, which is the torsion mode, it is shown in figure 8, in conditions without microcrack in figure 8-a, and with microcrack in figure 8-b, resulting in a frequency of 3265.8 Hz without a crack and with a crack 3466.6 Hz with a difference of 8%.

Box 9

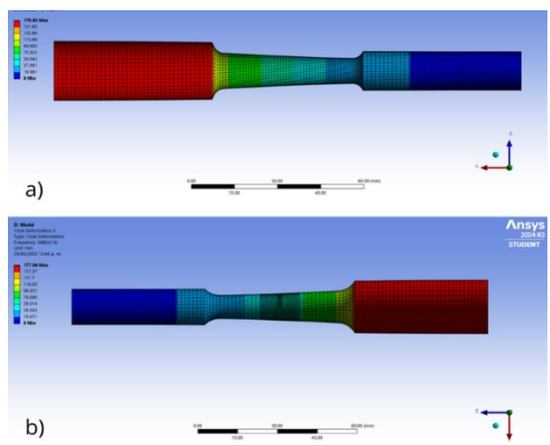

Figure 8
Torsional vibration mode 5: [a] Without microcrack; [b] With microcrack

Source: Own elaboration

Finally, figure 9 shows the chaotic Mode 6 that combines several conditions to determine the natural frequency of the material and the modeled axis, in which the conditions without microcrack figure 9-a and with microcrack figure 9-b are shown, giving as results frequencies without microcrack of 4721.7 Hz and with crack of 5216.9 Hz with a difference of 9.5 %.

ISSN: 2531-2979
RENIECYT: 1702902

Romero-Sotelo, Francisco Javier, Rodríguez-Blanco, Marco Antonio, Pérez-Montejo, Salatiel and Álvarez-Arellano, Juan Antonio. [2025]. Microcrack evaluation using modal analysis under two loading conditions on rotodynamic shafts. Journal-Mathematical and Quantitative Methods. 9[15]1-14: e1915114.
https://doi.org/10.35429/JMQM.2025.9.15.1.1.14

Box 10

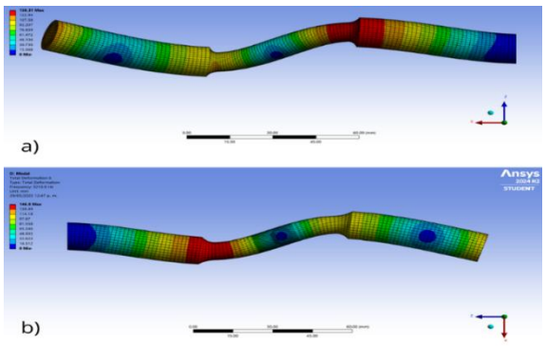

Figure 9

Vibration mode 6 in oscillating condition: [a] Without microcrack; b] With microcrack

Source: Own elaboration

Shaft stiffness analysis by simulation

The stiffness of the material is crucial for the analysis of the microcrack created in the proposed model and from where the results obtained will be evaluated in the conclusions and discussion section that will validate the proposed simulation results. In figure 10-a, the stiffness in the healthy axis or without microcrack created for its study is analyzed. figure 10-b shows the change in stiffness obtained by the modal analysis technique.

Box 11

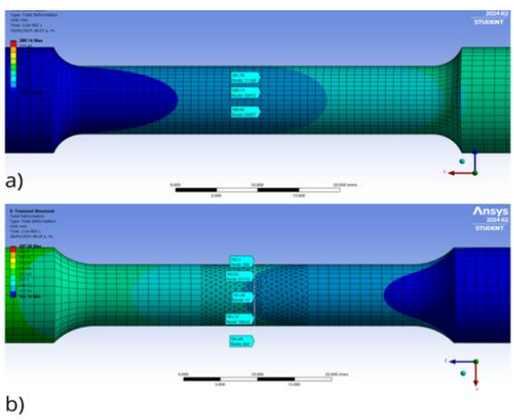

Figure 10

Stiffness Analysis: [a] Shaft without microcrack [b] Shaft with microcrack

Source: Own elaboration

The appearance of a microcrack in a material causes a gradual decline in some of its mechanical properties, including stiffness. Stiffness is defined as the resistance that a body offers against deformation due to a prescribed load and is directly related to the structural integrity of the material. The creation of a microcrack causes discontinuity that modifies stress distributions and decreases the ability of a material to withstand elastic deformations.

$$K_i = \frac{F_i}{\delta_i} \quad [3]$$

Ki: Rigidity
Fi: Applied Load
δ_i:Calculated deformation

There are different ways to analyze stiffness, depending on the type of load that is applied, such as axial, bending or torsional load, being the torsional one that will be analyzed to compare with those obtained in the general stiffness considering the deformations of the material in the simulation.

The torsional stiffness of a straight bar of uniform cross-section is defined as the ratio of the torque applied at one end to the angle of torque applied to that end, when the other end of the bar is held at rest, according to the following equation:

$$K_i = \frac{FM_x}{\theta_x} = \frac{GJ}{L} \quad [4]$$

G: Transverse elastic modulus
J: Torsional moment of inertia
L: Bar Length

Isotropic linear elastic materials obey the relationship between the transverse modulus of elasticity, Poisson's coefficient and Young's modulus.

$$G = E/2[1 + V] \quad [5]$$

E: Elastic Module
V: Poisson coefficient

The flexural stiffness of a straight bar is defined as the relationship between the bending moment applied at one of its ends and the angle of rotation experienced by that end when it undergoes deformation, considering that the bar is embedded at the opposite end.

In the case of straight bars with a uniform cross-section, two stiffness coefficients can be identified, which depend on the direction in which the bending moment is applied, whether it is aligned with a main direction of inertia or with a different one. This property of stiffness is

ISSN: 2531-2979
RENIECYT: 1702902

determined in Equations 6 and 7 [Wang et al., 2021]:

$$K_{flex,y} = 4EI_y/L^3 \quad [6]$$

$$K_{flex,z} = 4EI_x/L^3 \quad [7]$$

Iy, Iz: These are the second moments of cross-sectional area
E: Elastic Module
L=Bar Length

Results

According to Table 1, it is observed in the first instance that the frequencies determined in the modal analysis change in the first case there is no microcrack present [healthy], while in the second case there is a slightly small change, but it is related to the size of the proposed microcrack [with loads].

The stiffness change calculations were performed and will be analyzed in a section of the results, as well as the analysis of the results obtained from the modal calculation.

Results of the shaft stiffness change analysis

In figure 11 the stiffness analysis was performed according to the condition of equations 2 and 3, and from there the change in values was calculated to determine the behavior of the axis due to the type of load considered in the analysis.

The same figure shows how the stiffness of the material changes under conditions under the presence of the microcrack within the shaft, resulting in maximum values of 1.1374 N/mm to a minimum value of 1.0896 N/mm, while in the model with microcrack there is a stiffness of a maximum value of 1.0593 N/mm and minimum values of 1.0388 N/mm. resulting in a change in the stiffness of the section where the microcrack occurs, changes in stiffness of 6.87 % in the high peaks and a reduction of 4.66 % in the low peaks and validating the proposal for the generation of microcracks that allows us to determine the microcrack conditions in different mechanical elements and facilitate experimental work, in this project, a second stage is intended that considers the experimental part that will allow a better understanding of how a microcrack behaves in modal analysis and in this case how the rigidity of the material changes.

Box 12

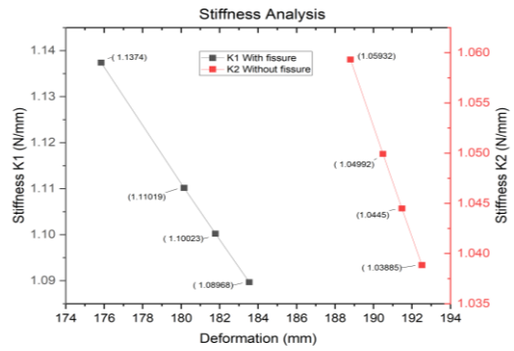

Figure 11
Stiffness analysis under torsional loading conditions on the shaft

Source: Own elaboration

Axis modal analysis results

In the most relevant phase of the study, the system's natural frequencies were determined using a modal analysis performed under loading conditions [torsion and bending], both without microcracks and with microcracks present in a specific section. The modal response was compared in both scenarios, and vibrations were recorded along the principal axes x and y. The first condition, under torsion, is presented in figures 12 and 13. From these data, a clear correlation could be established between the vibration amplitude, expressed in millimeters, and the frequencies measured in Hz.

Figure 12 shows the analysis on the x-axis under torsion conditions, where values of $4.09x10^{-6}$ mm of amplitude were obtained at a frequency of 200 Hz to 5.25 x 10^{-7} mm in the presence of a microcrack, with several peaks that allow us to relate these results with the presence of the microcrack while when there is no microcrack the only amplitude that occurs is $1.19 x10^{-7}$ mm. at a frequency of 3400 Hz.

Box 13

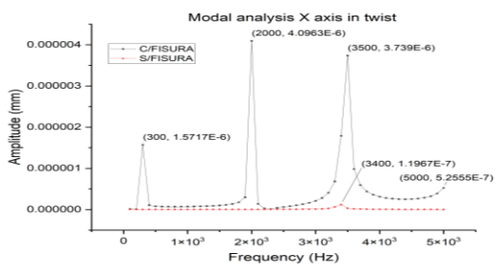

Figure 12
Modal analysis on the X axis, under defined loading conditions.

Source: Own elaboration

ISSN: 2531-2979
RENIECYT: 1702902

Romero-Sotelo, Francisco Javier, Rodríguez-Blanco, Marco Antonio, Pérez-Montejo, Salatiel and Álvarez-Arellano, Juan Antonio. [2025]. Microcrack evaluation using modal analysis under two loading conditions on rotodynamic shafts. Journal-Mathematical and Quantitative Methods. 9[15]1-14: e1915114.
https://doi.org/10.35429/JMQM.2025.9.15.1.1.14

Amplitude evaluation can be approached under various conditions; in this article, we use displacements resulting from torsion and bending. However, it is also possible to consider the change in amplitude caused by variations in stress, shaft speed, and other factors, both in the material without microcracks as well as in the presence of a microcrack, which will be the subject of another future work. The results presented in figure 13 show the measurements obtained on the y-axis; without a microcrack, the amplitude reaches 1.1148 mm at 3,500 Hz; however, with a microcrack, the value drops to 0.3072 mm, which clearly indicates the influence of the defect, showing an amplitude difference in the presence of a microcrack and without it of 66% with respect to the highest peaks. Thus, demonstrating a response to the presence of a microcrack.

Box 14

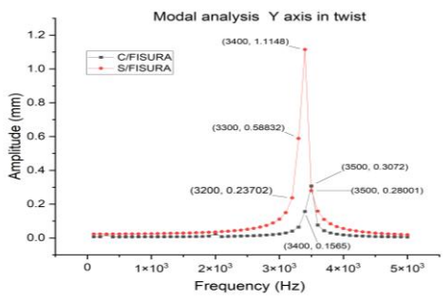

Figure 13
Modal analysis on the X axis, under bending conditions
Source: Own elaboration

The second analysis condition was that of bending along the axis, considering the same characteristics as the tests with torsional loading, determining the amplitudes and frequencies in conditions with and without the presence of microcracks.

In figure 14, the values obtained from the modal analysis of the flexural x-axis were graphed, where maximum amplitude values of 19.59 mm are obtained at a frequency of 300Hz and a value less than 2.95 mm at a frequency of 2000 Hz without fissure present, since microcracks are included, maximum values of 16.94 mm are presented at a frequency of 1300 Hz and a minimum of 1.94 mm amplitude at a frequency of 3000 Hz, showing an amplitude difference in the presence of microcrack and without it of 13.5 % with respect to the highest peaks, and a difference of 34.2 % in the low peaks. Thus, demonstrating a response to the presence of a microfissure.

ISSN: 2531-2979
RENIECYT: 1702902

Box 15

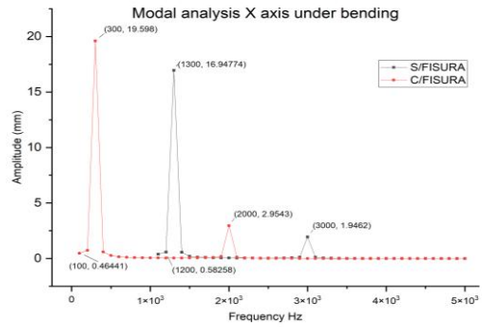

Figure 14
Modal analysis on the X axis, under bending conditions

Source: Own elaboration

In the last bending analysis, shown in figure 15, maximum values without crack of 5.17 mm amplitude are found at a frequency of 300 Hz and a minimum of 0.97 mm amplitude at a frequency of 200 Hz, with crack the values are 19.59 mm amplitude with a frequency of 300 Hz and a lowest of 2.95 mm at a frequency of 200 Hz, having a difference of 13.3 % in the high peaks, and a difference of 34.2 % in the low peaks, concluding the obtaining of values that visibly allow us to conclude that there is the presence of a microcrack.

Box 16

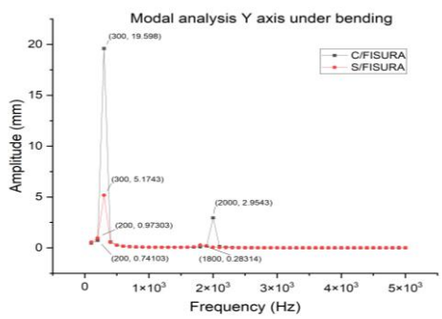

Figure 15
Modal analysis on the Y axis, under bending conditions
Source: Own elaboration

Conclusions

This study explores methodologies to identify and diagnose microcracks in components focused on rotodynamic machines, carrying out a detailed analysis through modal simulations using the ANSYS© software, with particular attention to torsional conditions and stiffness change.

Romero-Sotelo, Francisco Javier, Rodríguez-Blanco, Marco Antonio, Pérez-Montejo, Salatiel and Álvarez-Arellano, Juan Antonio. [2025]. Microcrack evaluation using modal analysis under two loading conditions on rotodynamic shafts. Journal-Mathematical and Quantitative Methods. 9[15]1-14: e1915114.
https://doi.org/10.35429/JMQM.2025.9.15.1.1.14

The findings of this work show the existence of a microcrack in a material that leads to a decrease in its rigidity compared to a homogeneous material, resulting in the discontinuity introduced by the microfracture, which facilitates the deformation of the material before the application of loads.

These results offer the possibility of extracting new features, which, under certain considerations, have a practical dimension and are highly relevant for addressing the problem of microfracture detection and understanding structural integrity in complex systems. It was revealed that the reduction in stiffness is not an independent phenomenon, but a quantifiable parameter directly related to the microcrack, as well as to its size, orientation, density, and the intrinsic properties of the material. This relationship is manifested in how the material's deformation capacity is altered by external loads, establishing a direct link with the dimensions of the microcracks and the characteristics of the material in question.

Based on these findings, future studies should focus on experimentally confirming the stiffness-frequency relationships in full-dimensional rotodynamic shafts under their realistic operating conditions. Ultra-sensitive vibration monitoring, coupled with classification algorithms, can improve the boundary thresholds established in this work by considering environmental factors such as temperature, lubrication conditions, and the changing morphology of growing cracks. Furthermore, unexplored aspects of respiratory crack contact dynamics that incorporate thermomechanical processes in finite element models could uncover additional useful frequency separation patterns for early warning diagnostics. Such multidisciplinary approaches would strengthen the theoretical basis for microcrack detection while simultaneously accelerating its implementation in proactive maintenance frameworks for critical industrial assets.

Declarations

Conflict of interest

The authors declare no interest conflict. They have no known competing financial interests or personal relationships that could have appeared to influence the article reported in this article.

Author contribution

Conceptualization, R-S,F.J. and R-B,M.A.; methodology, R-S,F.J.; software, R-S,F.J.; validation, M.A.R.-B and P-M,S.; formal analysis, P-M,S; investigation, R-S,F.J.; resources, R-S,F.J.; data curation, P-M,S.; writing—original draft preparation, P-M,S.; writing—review and editing, P-M,S.; visualization, R-B,M.A.; supervision, P-M,S.; project administration, R-B,M.A.; funding acquisition, R-S,F.J. All authors have read and agreed to the published version of the manuscript.

Availability of data and materials

There is the institutional support of the Universidad Autónoma del Carmen to use the necessary equipment for simulation with specialized software and experimentation in vibration equipment, as well as the Doctorate in Engineering Sciences of the Faculty of Engineering as part of the Doctoral training of the main author.

Funding

It receives funding from the Faculty of Engineering of UNACAR and the thesis director of this project.

Acknowledgements

The authors deeply appreciate the financial support provided by both the Secretaria de Ciencia, Humanidades, Tecnología e Innovación SECIHTI and the Universidad Autónoma del Carmen UNACAR. According to the catalog Marvid, this work belongs to the Engineering area, Mechanical Engineering Discipline, Vibration and Acoustics subdiscipline of Engineering Area VII.

Abbreviations

FEA	Finite element analysis
ASTM	American Society for Testing and Materials

References

Background

Czajkowski, M., Bartoszewicz, B., & Kulesza, Z. [2017]. Modal analysis of a rotor with a cracked shaft. *Journal of Vibroengineering*, *19*[1], 150–159.

ISSN: 2531-2979
RENIECYT: 1702902

Romero-Sotelo, Francisco Javier, Rodríguez-Blanco, Marco Antonio, Pérez-Montejo, Salatiel and Álvarez-Arellano, Juan Antonio. [2025]. Microcrack evaluation using modal analysis under two loading conditions on rotodynamic shafts. Journal-Mathematical and Quantitative Methods. 9[15]1-14: e1915114.
https://doi.org/10.35429/JMQM.2025.9.15.1.1.14

Dilena, M., & Morassi, A. [2002]. Identification of Crack Location In Vibrating Beams From Changes In Node Positions. *Journal of Sound and Vibration*, *255*[5], 915–930.

El-Mongy, H. H., & Younes, Y. K. [2018]. Vibration analysis of a multi-fault transient rotor passing through sub-critical resonances. Journal of Vibration and Control, 24[14], 2986–3009.

Gómez Peral, I., & fabra Rodriguez, M. [2022]. Análisis Modal de un Eje. Universidad Miguel Hernández de Elche, repositorio de Tesis.

Nahvi, H., & Jabbari, M. [2005]. Crack detection in beams using experimental modal data and finite element model. *International Journal of Mechanical Sciences*, *47*[10], 1477–1497.

Kisa, M., & Gurel, M. A. [2006]. Modal analysis of multi-cracked beams with circular cross section. *Engineering Fracture Mechanics*, *73*[8], 963–977.

Bertero, S., Tarazaga, P. A., & Sarlo, R. [2022]. In situ seismic testing for experimental modal analysis of civil structures. *Engineering Structures*, *270*, 114773.

Gomez Peral, I., & Fabra Rodriguez, M. [2022]. Análisis Modal de un Eje.

Hossain, M., & Wu, H. [2018]. Crack breathing behavior of unbalanced rotor system: A quasi-static numerical analysis. *Journal of Vibroengineering*, *20*[3], 1459–1469.

Jorge, A. R. F., Gouveia, E. B., da Cunha, M. J., Cavallini, A. A., & Freitas, L. C. G. [2024]. Rotodynamics Multi-Fault Diagnosis through Time Domain Parameter Analysis with MLP: A Comprehensive Study. 2024 *International Workshop on Artificial Intelligence and Machine Learning for Energy Transformation [AIE]*, 1–6.

Alegría, Gómez. F. [2024]. Análisis y diagnóstico del estado de posible falla de estructuras de armazón de acero en prevención de excitación sísmica. Tecnológico Nacional de México, Tesis de Doctorado.

Basics

García, L. M., Lourdes, M., Ruiz De Aguirre, R., Belén, M., & Abella, M. [2017]. Estudio numérico y experimental de un eje giratorio fisurado. Determinación del Factor de Intensidad de Tensiones.

Kushwaha, N., & Patel, V. N. [2023]. Nonlinear dynamic analysis of two-disk rotor system containing an unbalance influenced transverse crack. Nonlinear Dynamics, 111[2], 1109–1137. https://doi.org/10.1007/S11071-022-07893-7/METRICS

Liu, Q., Cao, S., & Lu, Z. [2023]. An Improved Crack Breathing Model and Its Application in Crack Identification for Rotors. *Machines*, *11*[5].

García R. [2017], Análisis estático y dinámico de un rotor de pruebas para simulación de fallas, SOMIM, Ciudad de México.

Rastogi, V., & Kumar, C. [2009]. A brief review on dynamics of a cracked rotor. *International Journal of Rotating Machinery*, *2009*.

Rodríguez Bravo, H., Ángel Castillo Cabrera, J., & Fernando Torres Chimal Miroslava Cano Lara, F. [2022]. Diseño Y Análisis Modal De Frame Tubular Para Car Cross Por El Método De Elemento Finito [FEM].

Rufino-Arteaga, O. E., & García-Pérez, O. A. [2025]. Análisis modal experimental en un prototipo de la semiala de un avión usando equipo de bajo costo. *Pädi Boletín Científico de Ciencias Básicas e Ingenierías Del ICBI*, *12*[24], 28–39.

Sadeghi, F. [2021]. Structural Health Monitoring of Composite Bridges by Integrating Model-based and Data-driven Methods.

Sinou, J. J., & Lees, A. W. [2005]. The influence of cracks in rotating shafts. *Journal of Sound and Vibration*, *285*[4–5], 1015–1037.

Sinou, J. J., & Lees, A. W. [2007]. A non-linear study of a cracked rotor. *European Journal of Mechanics, A/Solids*, *26*[1], 152–170.

Varney, P., & Green, I. [2012]. Crack detection in a rotor dynamic system by vibration monitoring-part II: Extended analysis and experimental results. *Journal of Engineering for Gas Turbines and Power*, *134*[11].

ISSN: 2531-2979
RENIECYT: 1702902

Romero-Sotelo, Francisco Javier, Rodríguez-Blanco, Marco Antonio, Pérez-Montejo, Salatiel and Álvarez-Arellano, Juan Antonio. [2025]. Microcrack evaluation using modal analysis under two loading conditions on rotodynamic shafts. Journal-Mathematical and Quantitative Methods. 9[15]1-14: e1915114.
https://doi.org/10.35429/JMQM.2025.9.15.1.1.14

Viola, E., Federici, L., & Nobile, L. [2001]. Detection of crack location using cracked beam element method for structural analysis. Theoretical and Applied Fracture Mechanics, 36[1], 23–35.

Wang, Y., Xiong, X., & Hu, X. [2021]. Machines Vibration and Stability Analysis of a Bearing-Rotor System with Transverse Breathing Crack and Initial Bending.

ISSN: 2531-2979
RENIECYT: 1702902

Romero-Sotelo, Francisco Javier, Rodríguez-Blanco, Marco Antonio, Pérez-Montejo, Salatiel and Álvarez-Arellano, Juan Antonio. [2025]. Microcrack evaluation using modal analysis under two loading conditions on rotodynamic shafts. Journal-Mathematical and Quantitative Methods. 9[15]1-14: e1915114.
https://doi.org/10.35429/JMQM.2025.9.15.1.1.14

Journal-Mathematical and Quantitative Methods 9[15]1-12: e2915112
Article

Soil gradients and phytochemical responses in *Tithonia diversifolia*: design of a comprehensive utilization model by vegetative tissue in Veracruz

Gradientes edáficos y respuestas fitoquímicas en Tithonia diversifolia: diseño de un modelo de utilización integral por tejido vegetativo en Veracruz

Ixmatlahua-Rodríguez, Christian Andrés [a], Ortiz-Celiseo, Araceli [b], Alejandre-Rosas, Jorge Alberto [c] and López-Zamora, Leticia [d*]

[a] Tecnológico Nacional de México. Instituto Tecnológico de Orizaba • NRY-5426-2025 • 0009-0007-7186-8543• 431434
[b] Tecnológico Nacional de México. Instituto Tecnológico de Orizaba • KYR-9025-2024• 0000-0003-3236-9462• 56228
[c] Tecnológico Nacional de México. Instituto Tecnológico de Orizaba • ONI-5775-2025 • 0000-0002-6726-8453• 350246
[d] LADISER - Universidad Veracruzana Facultad de Ciencias Químicas • NRY-5471-2025 • 0000-0002-1252-4966

Classification:

Area: Engineering
Field: Chemical enginnering
Discipline: Chemical Engineering
Subdiscipline: Bioengineering

https://doi.org/10.35429/JMQM.2025.9.15.2.1.12
History of the article:
Received: October 30, 2025
Accepted: December 30, 2025

* ✉ leticia.lz@orizaba.tecnm.mx

Abstract

Tithonia diversifolia [Hemsl.] A. Gray, an underutilized native plant, has industrial and antibiotic potential thanks to its richness in secondary metabolites and fatty acids. In this research, vegetative tissues [flower, leaf, stem and root] from three locations [Orizaba, Ixtaczoquitlán and Rafael Delgado, Veracruz], with different soil conditions were analyzed: Hydrogen Potential [pH], Organic Matter [OM], Electrical Conductivity [EC] and Texture [T], evidencing differentiated phytochemical profiles. High levels of palmitic acid [up to 26.80±16.72µg in the flower] and stearic acid [up to 18.81±11.43µg] were noted, both with antimicrobial applications. The leaves have a high protein [27.25 ± 0.14%] content for livestock use, and the stem and root are used as soil improvers. This characterization highlights the value of the T. diversifolia plant genetic resource for its use in the agroindustrial, livestock, agricultural, and pharmaceutical sectors, promoting its revaluation through vegetative tissue, productive areas with a sustainable agroecological approach that can be incorporated into silvopastoral systems.

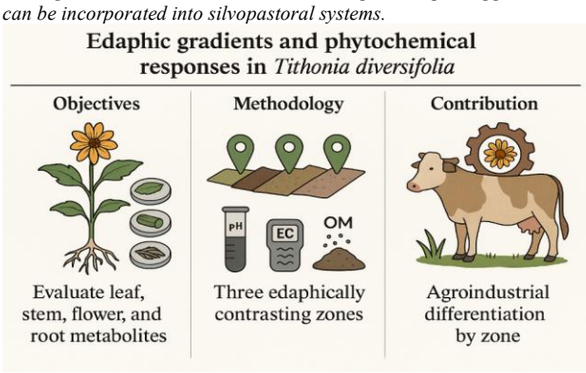

Phytochemical profiling, edaphic gradients, *Tithonia diversifolia*

Resumen

Tithonia diversifolia [Hemsl.] A. Gray, planta nativa subutilizada, posee un potencial industrial y antibiótico debido a su riqueza en metabolitos secundarios y ácidos grasos. En esta investigación, se analizaron los tejidos vegetativos [flor, hoja, tallo y raíz] provenientes de tres localidades [Orizaba, Ixtaczoquitlán y Rafael Delgado, Veracruz], con distintas condiciones edáficas: Potencial de Hidrógeno [pH], Materia Orgánica [MO], Conductividad Eléctrica [CE] y Textura [T], evidenciando perfiles fitoquímicos diferenciados. Destacaron contenidos elevados de ácido palmítico [hasta 26.80 ± 16.72 µg en flor] y esteárico [hasta 18.81 ± 11.43 µg], ambos con aplicaciones, antimicrobianas, en hojas posee un alto contenido de proteínas [27.25 ± 0.14 %] para uso pecuario, el uso de tallo y raíz, como mejoradores de suelos, esta caracterización resalta el valor del recurso fitogenético de *T. diversifolia* para su aprovechamiento en sectores: agroindustrial, pecuario, agrícola y farmacológico, promoviendo su revalorización por tejido vegetativo, área productiva con enfoque agroecológico sustentable que se incorpore a sistemas silvopastoriles.

Perfil fitoquímico, gradientes edáficos, *Tithonia diversifolia*

Area: Promotion of frontier research and basic science in all fields of knowledge

Citation: Ixmatlahua-Rodríguez, Christian Andrés, Ortiz-Celiseo, Araceli, Alejandre-Rosas, Jorge Alberto and López-Zamora, Leticia. [2025]. Soil gradients and phytochemical responses in *Tithonia diversifolia*: design of a comprehensive utilization model by vegetative tissue in Veracruz. Journal-Mathematical and Quantitative Methods. 9[15]1-12: e2915112.

Introducción

Tithonia diversifolia [Hemsl.] A. Gray, commonly known as Mexican sunflower, is a herbaceous species native to Mexico that has been categorized by the National Commission for the Knowledge and Use of Biodiversity [Comisión Nacional para el Conocimiento y Uso de la Biodiversidad; CONABIO, 2009] as a rustic plant or even classified as a weed in various agricultural systems due to its rapid growth and high colonization capacity. However, recent research has revalued its agro-industrial and ecological potential, highlighting its adaptability to diverse soil types, rich phytochemical content, and outstanding bromatological properties.

As a forage species, *T. diversifolia* exhibits high biomass production and significant levels of crude protein, reaching up to 29% on a dry matter basis, positioning it as a strategic resource for sustainable silvopastoral systems [Uu-Espens *et al*., 2021; Rivera *et al*., 2021]. Additionally, its application in phytoremediation has been documented, demonstrating an efficient accumulation of heavy metals such as lead and zinc without compromising vegetative growth [Kekere *et al*., 2020]. In the medicinal and ethnobotanical realm, *T. diversifolia* is widely used in rural communities for its anti-inflammatory, antioxidant, and antimicrobial properties, which are attributed to bioactive compounds including flavonoids, quinones, and phenolic acids [Monroy, 2025; Souza-Silva *et al*., 2020].

Additionally, ecological modeling under climate change scenarios [2041–2080] has projected a slight expansion in the potential distribution of *T. diversifolia* in Mexico, with an estimated increase from 30.7% to 32.4% of the national territory, favored by its high tolerance to intense precipitation and elevated temperatures. This adaptive behavior suggests that its dispersal could be enhanced, consolidating its strategic role in resilient productive systems and in the restoration of degraded landscapes under a sustainable agroecological approach [Durán *et al*., 2020; Pérez *et al*., 2025].

Complementarily, physiological modeling studies such as Bayona [2023] demonstrate that thermal and radiation variations can significantly modulate the productivity and quality of agricultural species, highlighting the importance of analyzing the edaphoclimatic and metabolic response *T. diversifolia* under contrasting environmental scenarios.

This study aimed to analyze the presence of key secondary metabolites, moisture content, and fatty acid composition in four vegetative tissues [leaf, stem, flower, and root] of *T. diversifolia* from three wild populations across three locations in central Veracruz [Orizaba, Ixtaczoquitlán, and Rafael Delgado], considering their soil gradients. Variables such as pH, electrical conductivity [EC], organic matter, and soil texture directly influenced the production of secondary metabolites and nutritional parameters. It was observed that alkaline soils with high EC, as in Rafael Delgado, favored the accumulation of unsaturated compounds and fatty acids; whereas acidic to neutral soils in Ixtaczoquitlán and Orizaba produced lower amounts but considerable ash and protein contents, indicators of forage nutritional value. It was hypothesized that the edaphic environment modulates the agro-industrial use potential by tissue type, with differentiated applications in regional silvopastoral systems, antimicrobials, fertilizers, and soil improvement.

Materials and Methods

Georeferencing soil sampling

The study was conducted across three representative locations in the central region of the state of Veracruz, Mexico. The first site was situated in the community of Cuautlapan, municipality of Ixtaczoquitlán, at an altitude of 990 meters above sea level [masl] with geographic coordinates 18°52'23.91" N and 97°01'33.16" W. The second site was in Rincón Grande, municipality of Orizaba, located at 1,182 masl, with coordinates 18°52'45.12" N and 97°00'38.25" W. Lastly, the third sampling point was established in Jalapilla, municipality of Rafael Delgado, at an altitude of 1,177 masl, positioned at coordinates 18°49'25.57" N and 97°05'03.01" W [Google Earth, 2024].

ISSN: 2531-2979
RENIECYT: 1702902

Ixmatlahua-Rodríguez, Christian Andrés, Ortiz-Celiseo, Araceli, Alejandre-Rosas, Jorge Alberto and López-Zamora, Leticia. [2025]. Soil gradients and phytochemical responses in Tithonia diversifolia: design of a comprehensive utilization model by vegetative tissue in Veracruz. Journal-Mathematical and Quantitative Methods. 9[15]1-12: e2915112.
https://doi.org/10.35429/JMQM.2025.9.15.2.1.12

These locations were selected for their stable wild populations of *T. diversifolia* occurring under contrasting agroecological conditions, enabling the assessment of edaphoclimatic influences on phytochemical composition and biomass utilization potential [CONABIO, 2009].

Soil samples were collected using a systematic transect design, randomly selecting 30 *T. diversifolia* plants per location. For each plant, soil adhering to the roots was extracted at an approximate depth of 20 cm.

Subsamples were homogenized to form a composite sample of 1 kg per locality, collected in duplicate [M1 and M2], and analyzed in triplicate according to NOM-021-RECNAT-2000 standards.

Soil analysis

Soil analyses were conducted at the Laboratory of the Faculty of Chemical Sciences, Veracruzana University [FCQ-UV], considering the following parameters: Organic Matter [OM] was measured using 10 g of soil, estimated by the Walkley-Black method modified by Kjeldahl. Soil texture was determined using the Bouyoucos method; 50 g of soil was dispersed in 100 mL of 0.5% sodium hexametaphosphate solution. Fraction readings were taken with a Bouyoucos hydrometer G.L.-5 at 60 VIRESA® at established intervals, allowing the quantification of sand, silt, and clay percentages.

For pH and Electrical Conductivity [EC], 20 g of soil were weighed and analyzed in soil:water [1:2] and soil:1N KCl [1:2] suspensions, continuously stirred for 30 minutes. Measurements were performed using a Hanna® Instruments H198130 multiparameter potentiometer [pH/EC/TDS, high range]. EC readings were obtained from the same solutions used for pH determination, to facilitate comparative analysis across acidic, neutral, and alkaline soils and their respective cation exchange capacities.All analyses followed the criteria established by Kome *et al*. [2018] and Quispe *et al*. [2019], adhering strictly to the guidelines of NOM-021-RECNAT-2000.

Sampling of plant tissues

A representative sampling area was delimited by selecting 30 uniform *T. diversifolia* plants per locality. The geographic location of each site was recorded for systematic documentation. Approximately 1,000 g of each vegetative tissue at physiological maturity, healthy and free of visible damage, were collected from each plant across the three localities. The vegetative material was washed with sterile distilled water to remove surface residues and subsequently air-dried by spreading each tissue sample evenly on clean mesh screens for 10 days in partial shade, at an average temperature of 22.88 ± 1.99 °C.

Moisture analysis

Moisture content determination was carried out at the Chemistry Laboratory of the Instituto Tecnológico de Orizaba [ITO], using previously dehydrated material from the vegetative tissues of *T. diversifolia*, following the methodology described by Montejo-Sierra *et al*. [2018]. Exactly 1.1 g of each sample was weighed and analyzed using an Ohaus® MB27 moisture analyzer. The procedure was performed in triplicate to ensure accuracy.

Ash and Protein Analysis.

Ash content was quantified by direct incineration in a muffle furnace, following the specifications of NMX-Y-362-SCFI-2019, which allowed estimation of total mineral content. Crude protein was estimated using the Kjeldahl method, according to NOM-F-68-S-1980, based on the determination of total nitrogen and its conversion to protein using the standard factor. All analyses were conducted in triplicate.

Secondary metabolites by High Performance Thin Layer Chromatography [HPTLC].

The chromatography was carried out in the Phytochemical Laboratory of the Center for Research and Advanced Studies of Irapuato [CINVESTAV, Unit Irapuato]. For the elution and visualization of metabolites, the High-Performance Thin-Layer Chromatography [HPTLC] technique was employed. Extracts diluted with 80% hydro-methanol were applied in aliquots of 10 µL onto silica gel 60 F254 plates with aluminum backing [250 µm thick, 10 × 20 cm, Sigma Aldrich].

ISSN: 2531-2979
RENIECYT: 1702902

Applications were performed using a CAMAG Automatic TLC Sampler 4 at a rate of 10 µL/sec and a bandwidth of 6.5 mm.

The software was programmed such that the first application was positioned 10 mm from the lower edge [X-axis] and 15 mm from the lateral edge [Y-axis].

The mobile phase consisted of a solvent system of ethyl acetate, formic acid, acetic acid, and water in the ratio 50:5.5:5.5:13 [v/v]. Before chromatographic development, the plates were dried for 30 seconds, followed by pretreatment of the chamber with the mobile phase at 20% relative humidity at room temperature. Subsequently, the plates were dried again for 5 minutes.

For the visualization of phytochemical compounds, a CAMAG TLC Visualizer [Switzerland] under white light was used, coupled with the visionCATS software version 2.0.15069.1, which enabled the digital capture of the chromatographic profiles [Wagner and Bladt, 2009].

Analysis by Gas Chromatography coupled with Mass Spectrometry [GC/EIMS]

Derivatization of extracts

Residual methanol in the extracts was removed by evaporation under a nitrogen stream within a fume hood. Subsequently, 20 µL of pyridine and 100 µL of N,O-bis[trimethylsilyl] trifluoroacetamide [BSTFA] were added as derivatizing agents. The samples were incubated for 30 minutes at 80 °C in a Thermomixer Comfort [Eppendorf®]. Finally, 100 µL of HPLC-grade isooctane was added to analysis vials to proceed with instrumental analysis. Each sample was processed in triplicate.

GC/EIMS Analytical Conditions

T. diversifolia samples were analyzed using gas chromatography coupled with electron impact ionization mass spectrometry [GC/EIMS]. An Agilent Technologies 7890A gas chromatograph coupled to a Hewlett Packard 5975C mass spectrometer was employed. Chromatographic separation was achieved using a DB-1MS column [J&W Scientific]. Ultra-high purity helium [99.9999%] served as the carrier gas at a constant flow rate of 1 mL/min.

Derivatized samples [200 µL] were injected using an Agilent Technologies 7683B automatic injector at 150 °C.

The oven temperature program started at 150 °C for 0.5 min, then increased at 12.5 °C/min to 310 °C, held for 2.5 minutes. Perfluorotributylamine [PFTBA] was used as a mass calibration standard [Agilent Technologies], covering a detection range of 50 to 800 atomic mass units [amu]. Compound processing and identification were carried out using MSChem, NIST, and AMDIS software.

Quantification of fatty acids

A calibration curve was constructed on the gas chromatography-mass spectrometry system using linoleic acid standard [Sigma-Aldrich] at a known concentration [µg/µL]. The resulting polynomial equation was $y = 7\times10^{9}$ $X= 5\times10^{7}$, with a coefficient of determination $R^2=0.98$

This calibration curve was used to determine the concentrations of the different fatty acids present in the samples.

Statistical Analysis of Data

The chemical data derived from protein analysis [dry basis] and fatty acids obtained by GC/EIMS were subjected to statistical analysis using Minitab software version 18 [LLC, 2018].

Results

This study was conducted using a comparative approach between contrasting edaphological zones, with independent variables consisting of soil physicochemical parameters [see Table 1]: pH, electrical conductivity [EC], organic matter [OM], and texture [TS].

The dependent variables were moisture percentage, secondary metabolites, fatty acids, ash, and protein content, evaluated in four vegetative tissues [leaves, stems, flowers, and roots] *T. diversifolia* from three wild populations.

The pH values determined in the soils from the three localities [Orizaba, Ixtaczoquitlán, and Rafael Delgado] [Table 1] reflect significant edaphic gradients, consistent with previous findings where pH and electrical conductivity [EC] emerge as key factors in soil dynamics and microbiota.

ISSN: 2531-2979
RENIECYT: 1702902

Box 1

Table 1

Organic Matter, Texture, pH and Electrical Conductivity, content of soils from 3 locations in Veracruz.

	pH - H_2O		pH - KCl		Electrical Conductivity [EC]			
Localidad	M1	M2	M1	M2	M1- [dS/m]	M2- [dS/m]	O.M.	Soil texture
Orizaba	6,34 ± 0,20	6,27 ± 0,19	5,58 ± 0,12	5,54 ± 0,10	0,35 ± 0,10	0,27 ± 0,02	8.63 ± 0.10	Sandy Loam
Ixtac zoquitlán	7,07 ± 0,46	6,84 ± 0,41	6,22 ± 0,60	6,19 ± 0,61	0,47 ± 0,21	0,44 ±0,23	2.72 ± 0.08	Sandy Clay Loam
Rafael Delgado	7,20 ± 0,11	7,22 ± 0,06	6,71 ± 0,12	6,75 ± 0,16	0,60 ± 0,29	1,21 ± 1,20	2.74 ± 0.06	Clay Loam

In this study, Rafael Delgado exhibited the highest pH values [7.20 ± 0.11] and EC [up to 1.21 ± 1.20 mS/cm], conditions that favor biochemical processes oriented towards the synthesis of secondary metabolites [Flores-Sánchez *et al*., 2023], in agreement with reports for adaptive species in neutral-alkaline soils. Meanwhile, Ixtaczoquitlán, with intermediate pH [7.07 ± 0.46] and lower EC [0.47 ± 0.21], showed greater water retention, resulting in favorable stomatal moisture for growth and green biomass accumulation.

The low organic matter [OM] content in Ixtaczoquitlán [2.72 ± 0.08%] and Rafael Delgado [2.74 ± 0.06%] versus the highest value in Orizaba [8.63 ± 0.10%] and the differing soil textures [from sandy loam to clay loam] directly influenced the physical and chemical soil properties. An intermediate OM content combined with loam-clay texture balances good aeration and water storage, ideal for nutrient availability and water distribution fundamental agronomic principles.

These results indicate that soils with better structure and higher organic matter stabilize pH and EC, optimizing growth conditions and phytochemical expression *T. diversifolia* [Pant *et al*., 2021]. Moisture content in the vegetative tissues [see Table 2] of *T. diversifolia* showed clear variation among localities, mainly influenced by edaphic factors such as soil pH, EC, and texture.

Box 2

Table 2 Percentage of moisture in *T. diversifolia* tissues

Tissues	Orizaba % Humidity	Ixtaczoquitlán % Humidity	Rafael Delgado % Humidity
Leaf	6.7 ± 0.52	7.0 ± 0.52	8.8 ± 0.52
Stem	7.9 ± 0.52	9.7 ± 0.52	9.7 ± 0.52
Root	7.6 ± 0.52	9.7 ± 0.52	9.7 ± 0.52
Flower	8.8 ± 0.52	9.7 ± 0.52	10.0 ± 0.00

Rafael Delgado exhibited the highest moisture values in nearly all tissues, particularly in the flower with 10%, which may be attributed to its greater water retention capacity linked to its loam-clay texture and higher electrical conductivity [1.21 ± 1.20 mS/cm]. This condition favors nutrient and water availability in the rhizosphere, facilitating water accumulation in vegetative structures [Holguín-Villanueva *et al*., 2023]. The stems and roots from Ixtaczoquitlán and Rafael Delgado showed the same moisture content [9.7 ± 0.52%], indicating possible physiological adaptability of the plant to maintain water reserves in underground and supporting organs, especially in soils with intermediate texture and higher retention capacity. Orizaba, in contrast, exhibited the lowest moisture values across all tissues, with an average leaf moisture of 6.7 ± 0.52%, consistent with its sandy loam texture, which limits soil water retention. These values suggest that the soil could be suitable for use as a soil conditioner or mulch [Li *et al*., 2024].

These results are important from a forage perspective, as moisture contents between 7–10% after drying guarantee good stability for silage, reducing the risk of undesirable fermentation and rot, thereby enhancing storage and use during scarcity periods. Furthermore, the flower and leaf tissues, with high moisture content, represent valuable fractions for formulating supplements rich in metabolites and with good digestibility [Ferrer et al., 2021; Montoya-Flores *et al*., 2022].

Ash values ranged between 6.36% and 15.23%, indicating significant variability in mineral accumulation based on sampling location [see Table 3]. The highest ash content in Ixtaczoquitlán [15.23 ± 0.02%] may be related to EC and nutrient retention capacity, which favors the absorption of essential minerals. Previous studies indicate that adaptive herbaceous species such as *T. diversifolia*, under fertile edaphic conditions, present higher mineral concentrations in tissues, translating to greater nutritional value for forage [Pant *et al*., 2021]. A greater ash content denotes a higher amount of elements extracted from the soil, making it a good fertilizer or natural soil texture enhancer; apparent soil density increased significantly, as did moisture, porosity, and nutrient content [N, P, K, Ca, Mg], thereby improving crop growth and yield [Li *et al*., 2020].

ISSN: 2531-2979
RENIECYT: 1702902

Ixmatlahua-Rodríguez, Christian Andrés, Ortiz-Celiseo, Araceli, Alejandre-Rosas, Jorge Alberto and López-Zamora, Leticia. [2025]. Soil gradients and phytochemical responses in Tithonia diversifolia: design of a comprehensive utilization model by vegetative tissue in Veracruz. Journal-Mathematical and Quantitative Methods. 9[15]1-12: e2915112.
https://doi.org/10.35429/JMQM.2025.9.15.2.1.12

Box 3

Table 3

Ashes and Proteins in leaves of *T. diversifolia*

Análisis	Orizaba [%]	Ixtaczoquitlán [%]	R. Delgado [%]
Ashes	6.36 ± 0.23	15.23 ± 0.02	13.91 ± 0.22
Proteins [Dry Basis]	20.12 ± 0.03	25.56 ± 0.23	27.25 ± 0.14
Proteins [Wet Basis]	13.23 ± 0.13	16.19 ± 0.16	17.76 ± 0.07

The crude protein levels on a dry and wet basis also show differences among the populations. Ixtaczoquitlán [25.56 ± 0.23 / 16.19 ± 0.16%] and Rafael Delgado [27.25 ± 0.14 / 17.76 ± 0.07%] present higher values, supporting their use as high-quality forage feed. Rivera *et al*. [2021] report averages between 28–29% crude protein in *T. diversifolia*, especially in genotypes selected for similar altitudes. Furthermore, studies on the inclusion of this species in ovine diets demonstrated significant increases in crude protein intake without compromising digestibility or animal health [Adetola *et al*., 2021], reaffirming its nutritional suitability according to the described edaphic variations. The chromatographic folios in Figure 1 show the presence of four main types of metabolites in almost all samples: Flavonoids [Fl], Phenols [F], Quinones [Q], and Coumarins [C]. Bands corresponding to leaves [Oh, Ih, RDh] and flowers [Of, If, RDf] exhibit greater intensity in compounds of higher polarity [high Rf], suggesting a superior accumulation of flavonoids and phenols in stems [Ot, It, RDt] and roots [Or, Ir, RDr], especially in flowers from Orizaba and Rafael Delgado. Coumarins appear in flowers and leaves, and quinones in leaves [Oh, Ih, RDh] and stems [Ot, It, RDt], indicating adaptive responses induced by specific edaphic conditions.

Box 4

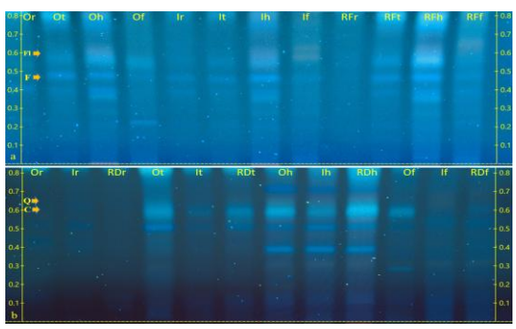

* Or, Ot, Oh, and Of refer to the root, stem, leaf, and flower tissues, respectively, from Orizaba. Similarly, Ir, It, Ih, and If denote the root, stem, leaf, and flower tissues from Ixtaczoquitlán. The abbreviations RDr, RDt, RDh, and RDf correspond to the root, stem, leaf, and flower tissues from Rafael Delgado.

Figure 1

Chromatographic profiles of four vegetative tissues from three wild populations of *T. diversifolia*

High-Performance Thin-Layer Chromatography [HPTLC] enabled the identification of key metabolites *T. diversifolia*, highlighting flavonoids [Fl], phenols [F], quinones [Q], and coumarins [C], with well-defined bands reflecting their differential abundance across tissues and locations [see Table 4]. Notably, flowers and leaves from the three populations exhibited intense bands with retention factors [Rf] typical of more polar flavonoids and phenols.

Box 5

Table 4

Presence of secondary metabolites in plant tissues of *T. diversifolia.*

Metabolite	MeOH extract 80%			
	Flower	Leaves	Steams	Roots
Phenols	+	+	+	+
Flavonoids	+	+	+	-
Coumarins	+	+	-	-
Quinones	-	+	+	-

These molecules have high biological value due to their antioxidant, anti-inflammatory, and antibacterial activities, indicating considerable agro-industrial potential as sources of bioactives for phytotherapeutic formulations or natural biopesticides [Kaurinovic and Vastag, 2021; Tessema *et al*., 2022].Coumarins and quinones, associated with allelopathic and biostimulant properties, are valuable for incorporation into bioproducts aimed at soil improvement or as organic mulch for weed suppression.

This finding is consistent with the plant's adaptive behavior to soils with higher electrical conductivity and pH [as found in Rafael Delgado], where the production of these protective metabolites is intensified.

This tissue-specific pattern, reinforced by the visual resolution of the chromatographic profile, supports the design of a differential utilization model: leaves and flowers as sources for phytochemical inputs and natural antioxidants; roots and stems as bio-stimulant agents or soil enhancers.

Thus, the integral use of *T. diversifolia* aligns with sustainable valorization strategies in agroecological and silvopastoral systems aimed at organic agriculture, reducing production costs.

ISSN: 2531-2979
RENIECYT: 1702902

Ixmatlahua-Rodríguez, Christian Andrés, Ortiz-Celiseo, Araceli, Alejandre-Rosas, Jorge Alberto and López-Zamora, Leticia. [2025]. Soil gradients and phytochemical responses in Tithonia diversifolia: design of a comprehensive utilization model by vegetative tissue in Veracruz. Journal-Mathematical and Quantitative Methods. 9[15]1-12: e2915112.
https://doi.org/10.35429/JMQM.2025.9.15.2.1.12

As shown in Table 5, the main fatty acids present in the vegetative parts of *Tithonia diversifolia* were identified and differentiated by locality. Table 6 presents the mass-based quantification, expressed as micrograms per gram of dry weight [µg/g DW], for the four analyzed vegetative tissues [leaf, stem, root, and flower] across the three study sites.

Box 6

Table 5

Main fatty acids present in the vegetative tissues of three populations of *T. diversifolia*

No.	Rt	Fatty acid	Vegetative organs from all localities	Use
1	39.665	C16:0 Palmitic Acid	Leaf, flower, steam and root	Antimicrobial Surfactant
2	43.152	C:18:0 Stearic Acid	Leaf, flower, steam and root	Antimicrobial Surfactant
3	42.535	C18:2n6 Linoleic Acid	Leaf, flower, steam and root	Antimicrobial, pharmaceutical, cosmetic, and food
4	42.62	C18:3n3 Alpha Linoleic Acid	Leaf	Antimicrobial, nutritional, and precursor to other compounds

Rt* Retention time

This quantification enabled an accurate comparison of the relative concentration of each fatty acid in the tissues, considering both the edaphic environment and the physiological role of the plant organ. Quantifying these compounds is essential, as fatty acids fulfill structural and defensive functions in plants, as well as possessing biotechnological potential as bio-stimulants, antimicrobials, or nutraceutical ingredients [Dongmo *et al*., 2021]. This type of analysis contributes to assessing the differential utilization of each tissue according to its specific lipid composition.

Box 7

Table 6

Quantification in µg of important fatty acids present in plant tissues of *T. diversifolia*, in the three locations.

Plant Tissue	Fatty Acid	Orizaba Weight [µg/g DW]	Ixtaczoquitlán Weight [µg/g DW]	Rafael Delgado Weight [µg/g DW]
Flower	Palmitic Acid	13.76 ± 0.63	16.06 ± 1.84	26.80 ± 16.72
Flower	Stearic Acid	10.22 ± 0.60	7.27 ± 3.48	18.81 ± 11.43
Flower	Linoleic Acid	6.30 ± 0.43	5.58 ± 4.58	9.77 ± 8.90
Leaf	Palmitic Acid	11.34 ± 1.01	11.40 ± 0.49	19.61 ± 3.75
Leaf	Stearic Acid	8.12 ± 0.54	8.66 ± 0.50	12.99 ± 2.01
Leaf	Linoleic Acid	3.55 ± 0.24	3.02 ± 0.07	7.28 ± 1.48
Leaf	Alpha Linoleic Acid	4.86 ± 0.42	3.83 ± 0.06	9.72 ± 1.97
Steam	Palmitic Acid	11.74 ± 1.22	18.52 ± 9.05	20.92 ± 10.81
Steam	Stearic Acid	8.18 ± 0.73	10.71 ± 2.53	12.23 ± 3.14
Steam	Linoleic Acid	2.75 ± 0.16	3.06 ± 1.25	2.91 ± 1.18
Root	Palmitic Acid	10.99 ± 6.63	14.21 ± 0.57	18.31 ± 6.99
Root	Stearic Acid	7.53 ± 4.42	10.68 ± 0.48	8.89 ± 5.82
Root	Linoleic Acid	2.90 ± 0.40	2.13 ± 0.04	2.35 ± 0.47

Gas chromatography coupled with mass spectrometry [GC-MS] phytochemical studies of plants like Moringa oleifera have extensively characterized fatty acid content, establishing benchmark reference parameters. High content is defined as concentrations above 15 µg/g of dry tissue, especially in seeds, as reported by Gharsallah *et al*. [2022] and Cervera-Chiner *et al*. [2024], dominated by fatty acids such as palmitic, oleic, and stearic acids, associated with potential applications in biofuels and natural pharmaceuticals.

Moderate content [5–15 µg/g dry weight] has been observed in vegetative structures like leaves or bulbs, where lipid profiles [Hosni *et al*., 2022] fulfill structural or bioactive functions, in accordance with El-Naggar *et al*. [2023]. Low content [<5 µg/g dry weight] is common in flowers or non-storage tissues, maintaining a lighter profile potentially involved in antioxidant or defensive activity. This classification guides biochemical interpretation of lipid content in non-conventional species like *T. diversifolia.*

Palmitic, stearic, linoleic, and α-linolenic acids were identified with tissue-specific profiles [flower, leaf, stem, root] and locality [Orizaba, Ixtaczoquitlán, Rafael Delgado].

Their biotechnological potential was assessed according to benchmark classification, enabling determination of whether a tissue serves as a rich, useful, or marginal source of specific fatty acids.

Flowers from Rafael Delgado showed high accumulation of palmitic acid [26.80 ± 16.72 µg] and stearic acid [18.81 ± 11.43 µg], while Orizaba and Ixtaczoquitlán maintained moderate levels. These long-chain saturated fatty acids are recognized for antimicrobial activity against Gram-positive and Gram-negative bacteria, targeting the cell membrane structure of pathogens. Their combination in petals, along with polyphenols and flavonoids per HPTLC analysis, positions them as natural biopesticides or ingredients for cosmetics and sanitizers [Kim *et al*., 2021].

In Ixtaczoquitlán, palmitic [16.06 ± 1.84 µg] and stearic [7.27 ± 3.48 µg] levels were high-moderate, highlighting compositional consistency useful for standardized products.

ISSN: 2531-2979
RENIECYT: 1702902

Orizaba, with palmitic [13.76 ± 0.63 µg] and stearic [10.22 ± 0.60 µg], falls within the upper-moderate range, viable for general bio-inputs. Linoleic acid was moderate [5.58 ± 4.58 µg] in all cases, useful as an anti-inflammatory or antioxidant.

Leaves of Rafael Delgado presented high palmitic acid [19.61 ± 3.75 µg] and moderate α-linolenic acid [9.72 ± 1.97 µg], suggesting protective or regulatory functions against oxidative stress, given that α-linolenic acid is an essential polyunsaturated fatty acid known to interfere with bacterial fatty acid synthesis by inhibiting key enzymes like FabI, explaining its antimicrobial action. Stearic acid [12.99 ± 2.01 µg] was moderate, enhancing its utility in bioactive formulations, also attractive for cosmetic [moisturizing] and livestock supplement industries targeting ruminal microbiota modulation [Roopa *et al*., 2020].

Palmitic acid concentrations were similar between Orizaba [11.34 ± 1.01 µg] and Ixtaczoquitlán [11.40 ± 0.49 µg], with stearic acid slightly predominant in Ixtaczoquitlán [8.66 ± 0.50 µg] vs. Orizaba [8.12 ± 0.54 µg]. α-Linolenic acid maintained stable moderate levels in both [3.55 ± 0.24 µg in Orizaba and 3.83 ± 0.06 µg in Ixtaczoquitlán], indicating balanced potential for foliar bioprotectors or mild phytopharmaceutical agents useful in agroecological practices prioritizing sustainability and low toxicity. In stems, palmitic acid was high in Ixtaczoquitlán [18.52 ± 9.05 µg] and Rafael Delgado [20.92 ± 10.81 µg], matching benchmark criteria for a rich source with applications in silage, lipid supplementation, or structural mulch. Stearic acid [10.71 ± 2.53 µg] was moderate, while linoleic acid remained low [<3 µg], indicating minor direct antioxidant role but synergistic antimicrobial potential as documented in other plant systems [Rouvier *et al*., 2025]. Orizaba, though with lower values [palmitic 11.74 ± 1.22 µg], remained in the moderate range suitable for intermediate-use biomass. High palmitic acid content was determined in roots from Rafael Delgado [18.31 ± 6.99 µg] and Ixtaczoquitlán [14.21 ± 0.57 µg], suggesting lipid reserve accumulation with potential for biological control products, soil bioprotectors, or slow-release mulch systems, while Orizaba showed moderate level [10.99 ± 6.63 µg], possibly related to denser or less porous soil characteristics. Stearic acid was moderate across all three sites.

Linoleic acid was low [<3 µg] in roots at all sites, limiting its biochemical prominence in this tissue but potentially participating as a cofactor in soil lipid synergies [Ferreira *et al*., 2019].

Conclusions

The results obtained demonstrate that *T. diversifolia*, a species traditionally considered a weed, possesses highly differentiated agro-industrial and bioeconomic potential by tissue and locality, closely linked with edaphic gradients.

Edaphic analyses conclude that in Orizaba, leaves could be used for forage production, especially in systems requiring conservation by ensiling without additives. The stems and roots from Ixtaczoquitlán are recommended as mulch, green manure, or living cover due to their capacity to conserve moisture, suppress weeds, and enrich soil; stems also could complement forage because of their high protein content.

Phytochemical profile determination revealed that in Orizaba, flowers are rich in phenols and quinones, suggesting applications in essential oil and natural cosmetics industries. In Ixtaczoquitlán, leaves showed high flavonoid presence, with pharmacological and antioxidant implications. Finally, in Rafael Delgado, the phytochemical profile reflected phenols, flavonoids, quinones, and coumarins with potential antimicrobial, antibacterial, or natural sanitizing properties.

Differentiated fatty acid profiles were identified in *T. diversifolia*, highlighting palmitic, stearic, linoleic, and α-linolenic acids distributed specifically in flower, leaf, stem, and root tissues, modulated by local edaphoclimatic conditions. Fatty acid profile differentiation indicates that in Rafael Delgado, flowers exhibit the highest palmitic acid concentration, useful in bioherbicide or natural antipathogen formulations. Leaves showed elevated stearic and α-linolenic acids, important for phytopharmaceutical, cosmeceutical, and agricultural bio-stimulant formulations. Stems and roots in Ixtaczoquitlán and Rafael Delgado showed palmitic and stearic acids, suggesting possible use in biofertilizers, soil improvers, bioactive extracts, and lignocellulosic waste valorization with biological activity.

ISSN: 2531-2979
RENIECYT: 1702902

Ixmatlahua-Rodríguez, Christian Andrés, Ortiz-Celiseo, Araceli, Alejandre-Rosas, Jorge Alberto and López-Zamora, Leticia. [2025]. Soil gradients and phytochemical responses in Tithonia diversifolia: design of a comprehensive utilization model by vegetative tissue in Veracruz. Journal-Mathematical and Quantitative Methods. 9[15]1-12: e2915112.
https://doi.org/10.35429/JMQM.2025.9.15.2.1.12

The distribution pattern also revealed Ixtaczoquitlán had the lowest standard deviation among replicates, suggesting greater metabolic stability in fatty acid synthesis, whereas Orizaba showed higher variability, especially in palmitic acid, possibly linked to microvariations in edaphic and management conditions, opening the possibility to adjust cultivation and harvest techniques for the desired metabolic product.

This integrative approach, based on accessible analytical technologies adapted to local conditions, allows designing viable technology transfer proposals for small producers, utilizing underused phytogenetic resources with low input requirements and high edaphic adaptability. The incorporation of *T. diversifolia* into silvopastoral production schemes, biofertilization, and compound extraction contributes to lowering production costs, promoting synthetic input substitution, and fostering a circular and sustainable agricultural economy in Veracruz.

The tissue- and locality-specific phytochemical-functional analysis highlighted how the edaphic conditions of each zone [Orizaba, Ixtaczoquitlán, and Rafael Delgado] differentially modulate this species' metabolic pathways, directly influencing the accumulation of secondary metabolites, fatty acids, and key phenolic compounds of functional and economic value.

Declarations

Conflict of interest

The authors declare that there is no conflict of interest. They maintain no financial, personal, or professional relationships that could influence the conduct or interpretation of this research.

They also do not receive incentives from private or commercial entities related to the use of *T. diversifolia*.

Author Contributions

Ixmatlahua-Rodríguez, Christian Andrés: Conceptualization of the project, methodological design, field sampling, compound analysis, and manuscript writing.

Ortiz-Celiseo, Araceli: Phytochemical analysis in the laboratory, table preparation, results interpretation, and technical discussion.

Alejandre-Rosas, Jorge Alberto: Processing of edaphic data, literature integration, and introduction writing.

López-Zamora, Leticia: Institutional coordination, validation of results, scientific correction of the text, conclusions, and final editing of the document.

Data Availability

All data generated or analyzed during this study are available upon request from the reader, including raw matrices, pigment tables, chromatograms, and edaphic results. No commercial analysis platforms were used.

Funding

This project was funded by the scholarship number 2023-000002-01NACF-03692 awarded by the Secretaría de Ciencia, Humanidades, Tecnología e Innovación [SECIHTI], under the graduate studies support program.

Acknowledgments

We thank the technical support from soil and bioactive compound analysis laboratories of the participating institutions, as well as the collaboration of local producers for access to sampling sites.

Abbreviation

CE	Electrical Conductivity
HPTLC	High-Performance Thin-Layer Chromatography
MO	Organic Matter
Rf	Retention Factor
T. diversifolia	*Tithonia diversifolia*
UV	Ultraviolet

References

Background

Bayona Penagos, L. V. [2016]. "Efecto de la variabilidad climática en producción y calidad en pera variedad triunfo de Viena [*Pyrus communis L.*]" Maestría en Ciencias Agrarias. Universidad Nacional de Colombia.

ISSN: 2531-2979
RENIECYT: 1702902

CONABIO, Comisión Nacional para el Conocimiento y Uso de la Biodiversidad, [2009]. Ficha técnica de *T. diversifolia*

Durán Puga, Noé, Loya Olguín, José Lenin, Ruiz Corral, José Ariel, González Eguiarte, Diego Raymundo, García Paredes, Juan Diego, Martínez González, Sergio, Crespo González, Marcos Rafael. [2020]. Impacto del cambio climático en la distribución potencial de *T. diversifolia* [Hemsl.] A. Gray en México. Revista Mexicana de Ciencias pecuarias, 11[Supl. 2], 93-106.

Kekere, O., Ademoye, A. M., Kareem, I. A., Ekundayo, T. O. [2020]. Assessment of Tithonia diversifolia With Mycorrhizal Bioaugmentation in Phytoremediation of Lead and Zinc Polluted Soils. African Journal of Applied Research, 6[1], 1–12. Retrieved from

Kome, G. K., Enang, R. K., Yerima, B. P. K., and Lontsi, M. G. R. [2018]. Models relating soil pH measurements in H_2O, KCl and $CaCl_2$ for volcanic ash soils of Cameroon. Geoderma Regional, 14, e00185.

Montejo-Sierra, I. L., Lamela-López, L., López-Vigoa, O. [2018]. Deshidratación del follaje, al sol ya la sombra, de tres plantas forrajeras proteicas. Pastos y Forrajes, 41[1], 21-29.

Quispe, R. M., Alegria, L. G., Castro, J. C., Ramos, O. E. R. [2019]. Evaluación quimiométrica del material de referencia interno [MRI] de suelos agrícolas en dos municipios provinciales de La Paz. Revista Boliviana de Química, *versión On-line* ISSN 0250-5460

Rivera, J. E., Ruíz, T. E., Chará, J., Gómez-Leyva, J. F., Barahona, R. [2021]. Biomass production and nutritional properties of promising genotypes of Tithonia diversifolia. *Tropical Grasslands-Forrajes Tropicales, 9*[3], 280–291.

Souza-Silva, G. A. de, da Silva, A. R., de Oliveira, E. G., Almeida-Bezerra, J. W. [2020]. Ethnopharmacological Potential of Tithonia diversifolia [Hemsl] A. *Gray*. *Research Society and Development, 9*[10], e8339108370.

Uu-Espens, C., Casanova-Lugo, F., Canul-Solís, JR, Chay-Canul, A., Piñeiro-Vázquez, Á., Yam-Chale, C., ... Oros-Ortega, I. [2021]. Variación estacional del rendimiento y calidad del forraje de *Tithonia diversifolia* a diferentes alturas de corte. AIA avanza en investigación agrícola , *25* [3], ágs-204.

Básicas

Google Earth Pro, [2024]. Consultado en noviembre 2024.

NMX-Y-362-SCFI-2019. Determinación de cenizas en alimentos.

NOM-021-RECNAT-2000. [2002, 31 de diciembre] Norma Oficial Mexicana que establece las especificaciones de fertilidad, sanidad y clasificación de suelos. Estudios, muestreo y análisis.

Monroy Forero, C. A. [2025]. Caracterización fitoquímica y actividad biológica de *Bactris gasipaes* y *Euterpe oleracea* y su posible aplicación para el desarrollo de una formulación cosmética. Programa de biología, Escuela de Ciencias Básicas y Aplicadas, Universidad de la Salle

NOM-F-68-S-1980. Determinación de Proteínas en Alimentos Consultado en noviembre 2024.

Pérez, D.R., González, F.M., Rodríguez Araujo, M.E., Rajnoch, G., Valfré-Giorello, T., Farinaccio, F., Lagos, J., Farina, J., Hernández, J., Paredes, D., Turuelo, N., Contreras, J., Coila, D., Álvarez, A., Sguazzini, A. [2025]. Abordajes y debates para la restauración ecológica de la Argentina: Charlas magistrales, simposios, mesas de trabajo, foros de debate, y participación en el III Encuentro Nacional de Restauración Ecológica de la Argentina [ENREA III], I Simposio Internacional de Prácticas de Restauración Ecológica y I Taller de Restauración Ecológica en la Diagonal Árida de la Argentina y Tierras Secas de Latinoamérica . Daniel Roberto Pérez Editor. ISBN 978-631-00-6989-0.

Wagner, H., and Bladt, S. [2009]. Plant Drug Analysis Second Edition Springer Dordrecht Heidelberg pp.195-254, ISBN

ISSN: 2531-2979
RENIECYT: 1702902

Ixmatlahua-Rodríguez, Christian Andrés, Ortiz-Celiseo, Araceli, Alejandre-Rosas, Jorge Alberto and López-Zamora, Leticia. [2025]. Soil gradients and phytochemical responses in Tithonia diversifolia: design of a comprehensive utilization model by vegetative tissue in Veracruz. Journal-Mathematical and Quantitative Methods. 9[15]1-12: e2915112.
https://doi.org/10.35429/JMQM.2025.9.15.2.1.12

Discussion

Adetola, O. O., Odetola, O. M., Orimogunje, A. A., Ijadunola, T. I., Adetoro-Awopetu, B. O. [2021]. Feeding effect of varying levels of sunflower [Tithonia diversifolia] leaf-blood meal mixture on blood profile and carcass quality of weaned rabbits. *Ghanaian Journal of Animal Science, 12*[1], 75–84.

Cervera-Chiner L, Pageo S, Juan-Borrás M, García-Mares FJ, Castelló ML, Ortolá MD. [2024] Fatty Acid Profile and Physicochemical Properties of *Moringa oleifera* Seed Oil Extracted at Different Temperatures. Foods. 13[17], 2733.

PMID: 39272499; PMCID: PMC11395537.
Dongmo, A. N., Nguefack, J., Dongmo, J. B. L. [2021]. Chemical characterization of an aqueous extract and the essential oil of Tithonia diversifolia and their biocontrol activity against seed-borne pathogens of rice. *Journal of Plant Diseases and Protection,* 128[6], 703–713.

El-Naggar, H.M., Shehata, A.M., Morsi, MA.A. [2023] Micropropagation and GC–MS analysis of bioactive compounds in bulbs and callus of white squill. In Vitro Cell.Dev.Biol.-Plant 59, 154–166.

Ferreira-Farías, A. L., Lobato Rodrigues, A. B., Lopes Martins, R., de Menezes Rabelo, É., Ferreira Farias, C. W., Moreira da Silva de Almeida, S. S. [2019]. Chemical characterization, antioxidant, cytotoxic and microbiological activities of the essential oil of leaf of *Tithonia diversifolia* [Hemsl] A. Gray [Asteraceae]. Pharmaceuticals, 12[1], 34.

Ferrer, J. M., Méndez, R. V., González, N. F. [2021]. Efecto de la altura de corte sobre el rendimiento y calidad bromatológica de *Tithonia diversifolia*. Livestock Research for Rural Development, 33[3].

Flores-Sánchez, I. D., Sandoval-Villa, M., Soto-Hernández, R. M. [2023]. Effects of electrical conductivity and pruning on secondary metabolite contents in fruits of Jaltomata procumbens. *Journal of Herbs, Spices & Medicinal Plants*, 29[4], 389–405.

Gharsallah K, Rezig L, B'chir F, Bourgou S, Achour NB, Jlassi C, Soltani T, Chalh A. [2022] Composition and Characterization of Cold Pressed *Moringa oleifera* Seed Oil. J Oleo Sci. 71[9]:1263-1273. PMID: 36047239

Holguín-Villanueva, C. M., Chaves-Quirós, A., Alvarado-Sanabria, O. [2023]. Evaluation of *Tithonia diversifolia* silage with microbial additives on chemical composition and fermentation profile. Agronomy, 14[7], 1386.

Hosni, T., Abbes, Z., Abaza, L., Medimagh, S., Ben Salah, H., & Kharrat, M. [2022]. Biochemical characterization of seed oil of Tunisian sunflower [Helianthus annuus L.] accessions with special reference to its fatty acid composition and oil content. Journal of Food Quality**,** 2022, 1–8.

Kaurinovic, B., Vastag, D. [2021]. Densitometric quantification and optimization of polyphenols in Phyllanthus maderaspatensis using a validated HPTLC method. Journal of Analytical Methods in Chemistry, 2021, 1–10.

Kim, Y.-G., Lee, J.-H., Park, S., Kim, S., Lee, J. [2021]. Inhibition of polymicrobial biofilm formation by saw palmetto oil, lauric acid and myristic acid. Microbial Biotechnology, 15**[**2], 590–602.

Li, R., Li, Q., Zhang, J., Liu, Z., Pan, L., Huang, K. [2020]. Effects of organic mulch on soil moisture and nutrients in karst areas of southwest China. *Polish Journal of Environmental Studies, 29*[6], 4161–4174.

Li, X., Zhang, H., Chen, L., Wang, Y. [2024]. Mulching enhances soil nutrients and moisture retention in dryland agriculture. *Agronomy for Sustainable Development, 44*[3], 1–14.

Montoya-Flores, A., Rivera-Cabrera, F., Rodríguez-Vázquez, R. [2022]. Valor nutricional de *Tithonia diversifolia* en sistemas silvopastoriles tropicales. Revista Mexicana de Ciencias Pecuarias, 13[4], 833–847.

Pant P., Pandey S., Dall'Acqua S. [2021]. The influence of environmental conditions on secondary metabolites in medicinal plants: A literature review. *Chemistry & Biodiversity*, 18[11], e2100345.

ISSN: 2531-2979
RENIECYT: 1702902

Ixmatlahua-Rodríguez, Christian Andrés, Ortiz-Celiseo, Araceli, Alejandre-Rosas, Jorge Alberto and López-Zamora, Leticia. [2025]. Soil gradients and phytochemical responses in Tithonia diversifolia: design of a comprehensive utilization model by vegetative tissue in Veracruz. Journal-Mathematical and Quantitative Methods. 9[15]1-12: e2915112.
https://doi.org/10.35429/JMQM.2025.9.15.2.1.12

Roopa, M. S., Shubharani, R., Rhetso, T., Sivaram, V. [2020]. Comparative analysis of phytochemical constituents, free radical scavenging activity and GC–MS analysis of leaf and flower extract of Tithonia diversifolia [Hemsl.] A. Gray. *International Journal of Pharmaceutical Sciences & Research,* 11[10], 5081–5090.

Rouvier, F., Abou, L., Wafo, E., Brunel, J. M. [2025]. Linoleic Fatty Acid from Rwandan Propolis: A Potential Antimicrobial Agent Against Cutibacterium acnes. Current Issues in Molecular Biology, 47[3], 162.

Tessema, F. B., Gonfa, Y. H., Asfaw, T. B., Tadesse, M. G., Bachheti, R. K. [2022]. Targeted HPTLC profile, quantification of flavonoids and phenolic acids, and antimicrobial activity of Dodonaea angustifolia leaves and flowers. Frontiers in Plant Science, 13, 825.

ISSN: 2531-2979
RENIECYT: 1702902

Ixmatlahua-Rodríguez, Christian Andrés, Ortiz-Celiseo, Araceli, Alejandre-Rosas, Jorge Alberto and López-Zamora, Leticia. [2025]. Soil gradients and phytochemical responses in Tithonia diversifolia: design of a comprehensive utilization model by vegetative tissue in Veracruz. Journal-Mathematical and Quantitative Methods. 9[15]1-12: e2915112.
https://doi.org/10.35429/JMQM.2025.9.15.2.1.12

Journal-Mathematical and Quantitative Methods 9[15]1-16: e3915116
Article

Design and maintenance analysis of wind turbine amplifier gearboxes systems exposed to lightning discharges

Análisis de diseño y mantenimientos de sistemas de cajas de engranes amplificadoras de turbinas de aerogeneradores expuestas a descargas por rayo

Berra-Ceballos, Raúl* [a], Cruz-Gómez, Marco Antonio [b], Mejía-Pérez, José Alfredo [c] and Castillo-Pensado, Juan Luis [d]

[a] Benemérita Universidad Autónoma de Puebla • NKP-4234-2025 • 0009-0005-6920-2430 • 2131975
[b] Benemérita Universidad Autónoma de Puebla, • S-3098-2018 • 0000-0003-1091-8133 • 349626
[c] Benemérita Universidad Autónoma de Puebla • G-3354-2019 • 0000-0002-4090-8828 • 473808
[d] Benemérita Universidad Autónoma de Puebla • NOF-1935-2025 • 0000-0002-1172-4843 • 670346

Classification:

Area: Engineering
Field: Engineering
Discipline: Mechanical Engineering
Subdiscipline: Energy

https://doi.org/10.35429/JMQM.2025.9.15.3.1.16
History of the article:
Received: October 30, 2025
Accepted: December 30, 2025

* ✉ [raul.berrac@alumno.buap.mx]

Abstract

The global demand for electrical energy from alternative sources has positioned wind power as the most feasible option. The aim of this research was to analyze the design and maintenance of wind turbine gearbox systems exposed to lightning strikes. On the other hand, state-of-the-art gearboxes have an average replacement frequency of 0.4 times the lifespan of the wind turbine. However, those lacking these technologies will experience longer downtimes, impacting their efficiency and profitability. A mixed-mechanism analysis was performed to evaluate gearbox design and maintenance parameters, identifying critical factors such as intermittent torque and lightning strikes. An analysis of existing gearbox design methods prompted the proposal of an alternative method that meets the goals of sustainable development and modernization. The optimization of this technology will be the future work focus.

Design and maintenance analysis of wind turbine amplifier gearboxes systems exposed to lightning discharges.		
Objectives	**Methodology**	**Contribution**
It evaluated how atmospheric discharges affect the design, reliability and maintenance of gearboxes in wind turbines.	A modeling of the gearbox system was carried out considering loads induced by lightning discharges. Analysis of failures reported in operation.	Optimize maintenance strategies to increase gearbox life and reliability.

Gearboxes in wind turbines, Lightning discharges in gearboxes in wind farms, Autonomous balancing and leveling system.

Resumen

El requerimiento global de energía eléctrica de fuentes alternativas, ha posicionado la generación eólica como la de mayor factibilidad. El objetivo de esta investigación fue analizar el diseño y mantenimiento de sistemas de cajas de engranes de aerogeneradores expuestas a descargas por rayo. Por otro lado, las cajas de engranes de última tecnología tienen frecuencia de sustitución promedio 0.4 de la vida útil del aerogenerador. Sin embargo, los que no cuentan con estas tecnologías experimentaran mayores tiempos muertos impactando su eficiencia y rentabilidad. Un análisis mixto fue realizado en la evaluación de parámetros de diseño y mantenimientos a cajas de engranes, identificando factores críticos; par torsor intermitente y descargas por rayo. Un análisis de métodos existentes de diseño de cajas de engranes fue el detonante para proponer un método alternativo que cumpla con los objetivos del desarrollo sustentable y modernidad. La optimización de esta tecnología será motivo de trabajos futuros.

Análisis de diseño y mantenimientos de sistemas de cajas de engranes amplificadoras de turbinas de aerogeneradores expuestas a descargas por rayo.		
Objetivos	**Metodología**	**Contribución**
Se evaluó cómo las descargas atmosféricas afectan el diseño, la confiabilidad y el mantenimiento de las cajas de engranajes en aerogeneradores.	Se realizo un modelado del sistema de caja de engranes considerando cargas inducidas por descargas de rayo. Análisis de fallas reportadas en operación.	Optimizar estrategias de mantenimiento para aumentar la vida útil y confiabilidad de la caja de engranes.

Cajas de engranes en aerogeneradores, descargas de rayo en cajas de engranes en parques eólicos, sistema autónomo de equilibrio y nivelación

Area: Promotion of frontier research and basic science in all fields of knowledge

Citation: Berra-Ceballos, Raúl, Cruz-Gómez, Marco Antonio, Mejía-Pérez, José Alfredo and Castillo- Pensado, Juan Luis. [2025]. Design and maintenance analysis of wind turbine amplifier gearboxes systems exposed to lightning discharges. Journal-Mathematical and Quantitative Methods. 9[15]1-16: e3915116.

Introduction

Wind energy is expanding the global electric power generation industry with greater efficiency within the area of sustainable development and zero emissions. To achieve these goals, turbine size continues to increase in all dimensions, capacities, and control through artificial intelligence. This predicts exponential growth for future generations of wind farms with technological improvements in all their components. Banihabib, R., & Assadi, M. [2023].

In recent decades, there has been a major shift in wind turbine technology, leading to the variable-speed wind turbine with a multi-stage gearbox. This type of turbine features a gearbox between the low-speed rotor and a higher-speed electrical generator [usually a doubly fed induction generator]. The purpose of the gearbox is to increase the rotor's rotational speed before powering the generator. In a wind turbine, the gearbox increases the blade rotational speed by 15 to 20 revolutions per minute [RPM] to reach the speed required by the generator.

Wind turbines without gearboxes are called variable-speed direct-drive wind turbines. The synchronous generator is powered directly by the rotor. There are two types of generators for direct-drive wind turbines: permanent magnet generators and electrically excited synchronous generators.

Wind turbines, both onshore and offshore, are exposed to different environments and phenomena that determine the types of failures in wind turbines. In the case study of gearbox systems, the main phenomena related to failure are wear and lightning strikes, which are decisive factors in the wind turbine's lifespan. Alves Ribeiro, J., et al. [2025], Arias Velásquez, R. M. [2024], Farrando, M., et al. [2024] and Verma, P., & Kumar, N. [2021].

The annual lightning strike rate, according to some real-time storm tracking sites, reports an average of 0.6 to 1 cloud-to-ground lightning strike per turbine per year. However, multi-megawatt turbines in exposed hilltop or offshore locations experience around 10 direct lightning strikes per year. This generates a high frequency of lightning strikes on wind turbines, where the rotational axis and its components are part of the discharge channel to the ground system.

The gears of a wind turbine amplifier box exposed to a lightning strike experience an intense, ultra-rapid burst of energy. The combination of heat, pressure, and electromagnetic fields from the arc concentrates the damage in tiny points, which can damage the entire gear train. Electrical arcs can exceed 20,000 kA. They develop melt craters, brittle cast layers, and heat-affected zones. The rapid expansion of the plasma generates shock fronts, and the metal peels off in microflakes around the pit. Gears exposed to plasma may suffer from: Surface erosion, sputtering, ion bombardment, sharp tooth edges, high energy neutrals and radicals, return currents, passing through lubricated spaces, lubricant degradation, attack of oils by plasma reactive [O, OH, F, Cl], vacuum or low pressure plasmas, thermal and mechanical stress, localized heating of discharges, induce thermal cycles, microcracks, increased friction, change in surface roughness, different wear phenomena. Alipio et al. [2021], Araya, N., et al. [2025], Fridman et al. [2007] and Verma, P., & Kumar, N. [2021].

The aim of this research was to analyze the design and maintenance of wind turbine gearbox systems exposed to lightning strikes. An analysis of existing gearbox design methods was the catalyst for proposing an alternative method that meets the goals of sustainable development and modernity.

How can we achieve efficient wind turbine gearbox designs and maintenance programs that meet sustainable development goals, focusing on equalizing the lifespan of amplifying gearboxes with that of wind turbines, increasing electricity generation and the profitability of wind energy in an environment with frequent lightning strikes?

The improvement proposals for wind turbine gearboxes were developed based on the authors' experience and considered real-time monitoring databases with machine learning and comparison of classified characterization models for interpretation and decision-making. The optimization of this technology will be the subject of future work

Research methodology

This research adopted a mixed approach, applying both quantitative and qualitative technologies, utilizing systematic processes, as well as records and estimated data.

ISSN: 2531-2979
RENIECYT: 1702902

Berra-Ceballos, Raúl, Cruz-Gómez, Marco Antonio, Mejía-Pérez, José Alfredo and Castillo- Pensado, Juan Luis. [2025]. Design and maintenance analysis of wind turbine amplifier gearboxes systems exposed to lightning discharges. Journal-Mathematical and Quantitative Methods. 9[15]1-16: e3915116.
https://doi.org/10.35429/JMQM.2025.9.15.3.1.16

The aim of this investigation was to analyze the design and maintenance of wind turbine gearbox systems exposed to lightning strikes. To this end, the application of the quantitative method was relevant in identifying control variables involved in previous studies evaluating gearbox design and maintenance parameters, identifying critical factors such as intermittent torque and lightning strikes.

An analysis of existing gearbox design methods was the trigger for proposing an alternative method that meets the goals of sustainable development and modernity. Quantitative indices from gearbox design reports under current international regulatory frameworks determine, based on variables such as revolutions per minute, torque, load, lubrication type, diametral pitch adjustment, mechanical vibration frequency, and material mechanical properties, the design factors for traditional bearing and gear methods. Analysis of wind turbine operating curves based on mixed-methodology records determined that state-of-the-art gearboxes have an average replacement frequency of 0.4 times the lifespan of the wind turbine, which decreases the efficiency and productivity of the wind farm. Furthermore, the experiences of wind farm personnel qualitatively identify that damage to wind turbine amplifier boxes is primarily due to wear and lightning strikes, which cause a loss of efficiency in the wind turbine system.

This was linked to scientific reports, contrasting experience and statistics that were considered as the application of the mixed method, which allowed the possibility of obtaining results from the estimation of variables, which played an important role in decision-making to evaluate the useful life of a generator's gearbox. A mixed analysis was performed in the evaluation of design parameters and maintenance of gearboxes, identifying critical factors, intermittent torque and lightning discharges through quantitative and qualitative methods. The operational data resulting from this research determined that the improvement proposals for wind turbine gearboxes were carried out through the experience of the authors and considering real-time monitoring databases with machine learning and comparison of classified characterization models of gearbox systems with uses in the aerospace industry for interpretation and decision-making.

Finally, using a mixed method, an analysis of the control variables was carried out, which allowed us to address the question of how to achieve efficient gearbox designs for wind turbines and maintenance programs that meet sustainable development objectives, focusing on achieving equal lifespans of amplifying gearboxes with those of wind turbines, increasing electricity generation and the profitability of wind energy in an environment with frequent lightning strikes.

This research proposes a design of amplifying gearboxes for wind turbines using specialized techniques from the aerospace industry to generate thin-film coatings for ultrasonic equipment. It quantitatively evaluates technical parameters adaptable to the wind energy industry, allowing for increased mechanical properties in bearings and gear shafts to supply an expanding and growing wind energy industry with continuous threats of lightning strikes. Additionally, an autonomous gyroscopic balancing and leveling system was proposed for the equipment anchoring system inside the machine room. This system will reduce impacts on rotodynamic systems in the face of intermittent wind gusts and bending of the wind turbine base pedestal, greatly reducing impact cracking of materials and reducing abrasive, adhesive, and corrosive wear, fatigue failures, and surface pitting.

Qualitative methods were used to estimate the feasibility of these technologies for modern wind turbines. Quantitative and qualitative methods show that coating the wind turbine machine room equipment, mainly the amplifier box, with high mechanical strength thin films and gyroscopically balancing and leveling using autonomous systems reduces the impact between gear systems, bearings, and bushings. Furthermore, when used as a channel in the lightning discharge phenomenon, plasma is generated, but the ceramic coatings act as a protector of the substrate, experiencing less damage to its microstructure. In addition to this, the autonomous gyroscopic balancing and leveling systems have reduced impacts, which increases the useful life of the wind turbine gearbox in all its components. [Akgül, 2024, Al-Bedhany, J. H., et al. [2024], Doostmohammadi, M., et al. [2020], Farrando, M., et al. [2024] and Fridman et al. [2007].

ISSN: 2531-2979
RENIECYT: 1702902

Berra-Ceballos, Raúl, Cruz-Gómez, Marco Antonio, Mejía-Pérez, José Alfredo and Castillo- Pensado, Juan Luis. [2025]. Design and maintenance analysis of wind turbine amplifier gearboxes systems exposed to lightning discharges. Journal-Mathematical and Quantitative Methods. 9[15]1-16: e3915116.
https://doi.org/10.35429/JMQM.2025.9.15.3.1.16

Classification of gearboxes for wind turbines.

Multi-stage gearboxes for multi-megawatt wind turbines can be classified as two-stage planetary + single-stage helical [three stages total], three-stage parallel helical, compound configurations combining spur and helical gears, magnetic torque, cycloidal, hydrodynamic, and direct drive.

Wind turbine gearbox types include: Planetary [planetary gears around the ring gear, generating ratios of 30:1 to 100:1, compact, high torque capacity], Parallel Shaft [multi-mesh spur/helical gears, ratios of 30:1 to 90:1, simpler design, easier maintenance], and Hybrid [variable combination of planetary and parallel stages balances size, weight, and reliability].

The gear set [planetary or parallel] is made of high-strength alloy steel, the bearings are designed for axial and radial loads, seals and filters keep the lubricant clean, and advanced synthetic oils maintain the film under high pressures and temperature fluctuations. Adedeji, P. A., et al. [2024] and Araya, N., et al. [2025].

Active magnetic bearings; these bearings use electromagnetic fields to levitate and stabilize rotors, allowing for frictionless operation and self-balancing.

Magnetic transmissions: torque is transmitted via magnetic coupling, without mechanical contact; wear-free, lower torque density, zero gearbox failures, the need for lubrication is virtually eliminated, and availability and energy efficiency increase by approximately 10%. These have disadvantages: they are in the development stage, require a very large nacelle footprint, and require a high initial cost due to rare-earth magnets or large mass.

Cycloidal [strain wave] transmissions—a crescent-shaped rotor flexing on a stationary ring—generate very high reductions per stage, are less field-proven, and require complex seals. Hydrodynamic transmissions feature fluid coupling and torque converter stages, smooth torque transfer, overload protection, lower efficiency, and bulkiness.

Direct drive systems, by not having a gearbox, reduce mechanical noise and the number of rotating components.

Furthermore, this type of wind turbine has a single main bearing for the rotor and generator assembly, further reducing the number of moving parts and reducing maintenance and repair costs. Gearbox vs. Direct Drive. Direct drive systems have permanent magnets made of rare earths, neodymium, and can be used in small-scale wind turbines, but they also have applications in high-power wind turbines, both offshore and onshore. Previous studies have determined that direct-drive wind turbines of 7-10 MW require larger and heavier generators. In this case, a single- or two-stage gearbox is the best option and offers the same operating conditions.

Previous studies contrast mechanical transmissions with direct drives, where the role of mass, materials, and affordability influence the cost of the support structure. These groups of developers defend different positions, highlighting their advantages in terms of service life, indicating that the gearbox-based wind turbine is almost at its peak efficiency, while direct-drive turbines have more room for improvement.

The previous proposals are in dispute; however, both proposals have significant growth potential within their areas and combined, will be superior in future technology developments. But the problem to overcome is lightning strikes, for which neither proposal is prepared to operate without repairs during the wind turbine's planned lifespan. NFPA. [s.f.]. NFPA 780.

Traditional mechanical design methods for gearbox design

Traditional mechanical design methods for gear design specify that the first thing to be known are design environment conditions which are key input and output: input speed, torque, power, direction of rotation, output speed, torque, power and type of motion desired, operating conditions [temperature, lubrication, duty cycle], space constraints, weight, noise and efficiency are essential to select the gear type, gear ratio and materials.

Select the gear geometry that best suits your application: spur, helical, helical, bevel, worm. Consider load carrying capacity, size, noise, and mounting configuration when making your decision.

ISSN: 2531-2979
RENIECYT: 1702902

Berra-Ceballos, Raúl, Cruz-Gómez, Marco Antonio, Mejía-Pérez, José Alfredo and Castillo- Pensado, Juan Luis. [2025]. Design and maintenance analysis of wind turbine amplifier gearboxes systems exposed to lightning discharges. Journal-Mathematical and Quantitative Methods. 9[15]1-16: e3915116.
https://doi.org/10.35429/JMQM.2025.9.15.3.1.16

Determine the gear ratio, select the standard tooth size [modulus or diametral pitch], calculate pitch diameters, verify center distances, select the appropriate pressure angle, clearance for the lubricant to be used, tooth profile, interference and clearance [involute profile], radial height above the pitch circle [addendum], radial depth under the pitch circle [dedendum], clearance between the tip and root [clearance], angle between the line of action and the tangent on the pitch circle [pressure angle], contact depth [working depth].

Avoid interference by ensuring the minimum number of teeth meets AGMA 2001-D04 for a given pressure angle and profile offset. Clearance [typically 0.05 to 0.15 mm] ensures smooth rotation and compensates for thermal expansion and tooth deflection. Strength analysis and AGMA classifications, strength checks; bending stress, contact stress [Hertzian], applying dynamic, load, size, and reliability factors, converting these allowable stresses into a safety factor against fatigue and pitting. material selection and heat treatment, manufacturing methods, assembly, alignment and lubrication, maintain correct center distance and shaft alignment to minimize vibration and noise, adjust backlash within recommended limits for thermal expansion and tooth deflection, choose lubricant type [oil, grease, solid film] based on speed, load and temperature and finally prototype verification and testing, stress re-evaluation with refined loads [dynamic, impact], finite element analysis and continuous evaluation of the system based on its experimental development until the expected performance target is reached in a sustainable and sustainable optimization. AGMA. [2004]. AGMA 2001-D04 and Araya, N., et al. [2025].

Design of gearboxes for wind turbines.

The wind power propulsion system has a turbine whose load is not perfectly uniform. Implementing an equivalent load with various load levels must be done with multifunctional design models and safety factors against fatigue and pitting, based on the environment and exposure to chaos theory phenomena, as this can lead to inaccurate results when assessing fatigue. AGMA 6006 includes a method for calculating gearbox reliability and also addresses how to address other failure modes. AGMA. [s.f.]. AGMA 6006 and Jiang, L., et al. [2020].

Numerical simulation combines finite element gear stress models with plasma arc CFD to predict local heating and erosion, in-situ monitoring incorporates thin-film sensors on critical tooth surfaces to detect arc events and quantify material loss over time, multidisciplinary cross-sector collaboration analyzing experience from the wind turbine and aerospace sectors, where plasma arcs on metal frequently result in advanced mitigation tactics.

By combining gear geometry, load rating standards, lightning protection protocols, and high-energy discharge testing, drives can be created that are resilient to the mechanical stresses and extreme conditions of lightning-induced plasma.

Multidimensional failure modeling and optimization based on the classic Stribeck curve of planetary gearbox bearings, pins to prevent wear failures and reduce friction in wind turbines, have proposed a unified failure model based on a tribodynamic framework for full-size gearbox bearings. The proposed multidimensional designs achieve reductions of more than 90% in friction and wear failures, closely matching wear patterns that improve stability and wear resistance of the radial clearance observed in tests. This represented an improvement in the regulation of oil film thickness in the critical transition zone.

Hydrodynamic and mixed lubrication regimes in gear shafts, bearings, and bushings reduce friction coefficients at contacts, thermal effects, and thermoelastic deformation. Lower clearance ratios and higher width-to-diameter ratios alleviate stress concentrations at the edge. Al-Bedhany, J. H., et al. [2024].

Replacing rolling bearings with plain bearings and integrating them with planetary gears can increase the torque density of wind turbine transmission systems. However, planetary gears are subjected to complex forces and moments arising from the dynamic meshing of internal and external gear pairs. This results in edge contact in the plain bearings, feedback effects in the mesh, load skew, strong inter-gear coupling, and critical lubrication.

Asymmetric deformation of the support pins under dynamic meshing forces results in skewed mesh loading and edge contact, which intensifies the increase in input torque.

ISSN: 2531-2979
RENIECYT: 1702902

Berra-Ceballos, Raúl, Cruz-Gómez, Marco Antonio, Mejía-Pérez, José Alfredo and Castillo- Pensado, Juan Luis. [2025]. Design and maintenance analysis of wind turbine amplifier gearboxes systems exposed to lightning discharges. Journal-Mathematical and Quantitative Methods. 9[15]1-16: e3915116.
https://doi.org/10.35429/JMQM.2025.9.15.3.1.16

Optimizing skewed mesh loading and edge contact of the bearing reduces loading conditions, improving load distribution and the performance of the wind turbine gearbox shown in Figure 1.

Box 1

Gearbox test bench top view diagram:

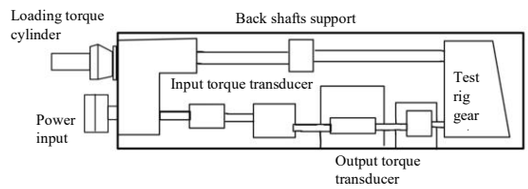

Figure 1
Gearbox system for wind turbine
Source: Own elaboration

Lightning strikes on wind turbines.

Lightning strikes to wind turbines over their lifetime were estimated by previous studies at 20 years and are divided into low-risk scenarios with 12 events, medium-risk scenarios with 20 events, and high-risk scenarios with 200 events. Factors affecting the number of strikes include turbine height, geographic location, and lifetime.

Lightning and high-voltage faults can create a transient plasma arc carrying tens to hundreds of kiloamperes and temperatures exceeding 20,000 K. This plasma expands supersonically, emits intense electromagnetic fields, and generates powerful shock waves. When such an arc touches a gear system or gearbox housing, it can cause complex damage that goes far beyond simple superficial burns.

Factors influencing the severity of lightning damage: current waveform: short, high-peak return strokes [μs] cause deeper, sharper craters; longer continuous currents [hundreds of μs] provide more total heat and wider melting zones, resulting in greater total charge transfer; greater charge results in higher energy deposits, thicker melt layers, and larger heat-affected zones. Cernalevschi, G., et al. [2025], and Farrando, M., et al. [2024].

Gears made of high-conductivity steel and hardened alloys are more prone to cracking. Protective and lubricating coatings: Dielectric paints delay arc formation but can trap energy, causing the coating to explode. Grounding and enclosure design: Well-sealed housings deflect arc paths away from sensitive gear surfaces.

Transient currents induce electromagnetic Lorentz forces that can bend fine metal teeth or demagnetize bearings. Bruce, T., et al. [2015] and Cernalevschi, G., et al. [2025].

Mitigation strategies include installing a robust ground and bonding system to provide a low-resistance arc path to the chassis or ground, thus avoiding the gears; enclosing gear trains in conductive housings or Faraday cages to intercept arcs externally; and applying arc-resistant coatings [thin, high-hardness, conductive films] that vaporize in a controlled manner, thereby reducing direct damage to the steel. Agbogo, V. U., et al. [2025].

Recommendations after a lightning strike: install surge protection on nearby power supplies to minimize stray current faults; implement condition monitoring [ultrasonic inspection, ink penetration testing, hardness mapping] after any severe electrical event.

Beyond immediate repairs, arc erosion test benches are worth exploring to quantify material loss under current waveforms. This data helps predict service life after an impact and refine maintenance intervals for critically damaged gear systems. Cernalevschi, G., et al. [2025] and Zhang, W., et al. [2025].

Standards for the design of gearboxes, bearing and bushings exposed to lightning discharges.

International standards for wind turbines exposed to lightning strikes. IEC 61400-24:2019 Wind power generation systems Part 24: Lightning protection specifies requirements and guidelines for the protection of wind turbines and complete wind power systems against the direct and indirect effects of lightning. It defines the lightning discharge environment for wind turbines, establishes risk assessment procedures, and sets out protective measures, test methods, and recommendations. Alipio et al. [2021] and IEC. [2019]. IEC 61400-24:2019.

To design mechanical or electromechanical gear systems that may be exposed to lightning strikes, two families of international standards are used: general lightning protection principles and test methods, and application-specific requirements [for wind turbines, vehicles, aircraft, etc.].

ISSN: 2531-2979
RENIECYT: 1702902

Berra-Ceballos, Raúl, Cruz-Gómez, Marco Antonio, Mejía-Pérez, José Alfredo and Castillo- Pensado, Juan Luis. [2025]. Design and maintenance analysis of wind turbine amplifier gearboxes systems exposed to lightning discharges. Journal-Mathematical and Quantitative Methods. 9[15]1-16: e3915116.
https://doi.org/10.35429/JMQM.2025.9.15.3.1.16

General rules for lightning protection and surge immunity; IEC 62305-1 - 2021, Lightning protection - General principles, risk management, definitions, and lightning parameters. IEC 62305-2 - 2021; Lightning protection - Risk management methodology for assessing lightning risk to structures/equipment. IEC 62305-3 - 2021; Lightning protection - Physical damage to structures and life-threatening lightning strikes - Protection of external systems [air termination, downconductor, earthing]. IEC. [2021]. IEC 62305-1:2021, IEC. [2021]. IEC 62305-2:2021, IEC. [2021] and IEC 62305-3:2021.

Wind turbine gearboxes IEC 61400-24:2019; Wind turbine generator systems - Part 24: Lightning protection addresses lightning strikes to blades, nacelles, and internal surge mitigation for control and power electronics. IEC. [2019]. IEC 61400-24:2019.

International standards for the design of gears that may be exposed to lightning-induced plasma arcs require combining traditional gear engineering standards with lightning protection and high-energy discharge testing standards. ISO 6336, Load-carrying capacity calculation of spur and helical gears, defines safety factors for bending and pitting, material properties, and design formulas. ISO 1328, Precision of involute cylindrical gears, specifies tolerances for tooth profile, helix, and pitch to ensure accurate meshing. AGMA 2001-D04, Fundamental classification factors and calculation methods, the American equivalent of ISO 6336, which includes fatigue factors for surface cracking and wear. AGMA. [2004]. AGMA 2001-D04, Bru, K., et al. [2020], ISO. [2019]. ISO 1328 and ISO. [2019]. ISO 6336.

Lightning protection and risk management IEC 62305 lightning protection, NFPA 780 standard for the installation of lightning protection systems and guides on air terminals, down conductors, bonding and grounding. IEC. [2021]. IEC 62305-1:2021.

High-energy discharge and plasma testing IEC 60068-2-60 Environmental testing - Mixed gas flow corrosion test, adapts to electrode erosion testing by simulating the impact of a plasma jet. IEC 61000-4-5 Electromagnetic compatibility, Surge immunity test defines the generator output for high-energy transients, useful for emulating impact currents. IEC 61400-24 Wind turbines, Lightning protection, although focused on blades, details plasma arc adhesion and material erosion.

Aerospace and Transportation Applications RTCA DO-160, Section 22 Environmental Conditions and Test Procedures - Lightning-Induced Transient Susceptibility addresses the indirect effects of lightning strikes on mechanical and electrical assemblies. SAE ARP5412A Guidelines for Aircraft Lightning Protection describes test setups for direct-strike plasma arc interaction with metallic parts. Bru, K., et al. [2020], Cernalevschi, G., et al. [2025], IEC. [2000]. IEC 60068-2-60, IEC. [2014]. IEC 61000-4-5 and SAE. [s.f.]. SAE ARP5412A.

Integrating standards into the gear design workflow: Risk assessments apply IEC 62305-2 to determine the likelihood and severity of lightning strikes at the facility. Mechanical design: Use ISO 6336/AGMA 2001 to size gears for torque and fatigue life, considering potential plasma erosion. Material and coating selection: Choose steels or nickel-based alloys with proven resistance to plasma arc erosion; consider thermal spray coatings according to ISO 14916. Protective measures: Connect gear housings to down conductors; ensure equipotential bonding according to IEC 62305-4. Laboratory tests: Overcurrent simulation according to IEC 61000-4-5 on gear shafts.

Perform plasma jet erosion tests according to the modified IEC 60068-2-60 standard. Check the accuracy of the gears after testing against the tolerances of ISO 1328. AGMA. [2004]. AGMA 2001-D04, IEC. [2000]. IEC 60068-2-60, IEC. [2014]. IEC 61000-4-5, IEC. [2021]. IEC 62305-1:2021, IEC. [2021]. IEC 62305-2:2021, IEC. [s.f.]. IEC 62305-4, ISO. [2010]. ISO 14916, ISO. [2019]. ISO 1328, ISO. [2019]. ISO 6336 and ISO/AGMA. [s.f.]. ISO 6336/AGMA 2001.

The ISO 4406:99 4/6/14 µm standard is used to classify the cleanliness of hydraulic oil [or similar fluids] based on the amount of particles it contains in µm. ISO. [1999]. ISO 4406:99.

ISSN: 2531-2979
RENIECYT: 1702902

Berra-Ceballos, Raúl, Cruz-Gómez, Marco Antonio, Mejía-Pérez, José Alfredo and Castillo- Pensado, Juan Luis. [2025]. Design and maintenance analysis of wind turbine amplifier gearboxes systems exposed to lightning discharges. Journal-Mathematical and Quantitative Methods. 9[15]1-16: e3915116.
https://doi.org/10.35429/JMQM.2025.9.15.3.1.16

Failure rate in onshore and offshore wind turbine gearboxes

A previous assessment of offshore, floating, semi-submersible, and stationary wind turbines estimated that the failure rate for electrical and electronic components and blade systems is seven times higher than that of land-based turbines. However, the approximate annual failure rate for the gearbox and drive train system was estimated to be about four times higher than that of land-based turbines. Baragetti, S., et al. [2011].

The adverse operating conditions of semi-submersible and fixed floating offshore wind turbines determined that failures have a greater incidence in the support structures, hydraulic system, gearbox, generator, and other systems.

These are due to factors such as salt spray, waves, high wind speed, and others. Early fault detection allowed for the implementation of predictive maintenance strategies for the most critical systems, such as corrective maintenance in gearboxes, generators, turbine blades, and hydraulic systems that require longer downtimes. Maintenance strategies were implemented with cause-and-effect analysis of failures, as part of a plan to improve the design and optimize maintenance programs.

In semi-submersible and fixed floating offshore wind turbines, it was identified that the mooring system - support structures [mooring line breakage, abnormal tension of turnbuckles, failure of anchor, buoys and fairleads] were the most prone to failure components with a rate of 17%, failures to hydraulic and pitch systems have a failure frequency around 13%, the generator with a frequency 12%, the gearbox and speed train with 8% representing the failures with the greatest downtime due to repair that influence the performance of the wind turbine with impacts on the production of the wind farm.

On the other hand, failures of lesser incidence are electronic components, blades, and blade yaw system. Cardoni, M., et al. [2021] and Farrando, M., et al. [2024].

The frequency of failure in wind turbine amplifier box systems considering a useful life of 20 years, with respect to CMMS/SCADA [Computerized Maintenance Management System/ Supervisory Control and Data Acquisition] inspection databases, manufacturer recommendations and statistics is; oil change and filter replacement every [0.1, 0.25] complete gearbox disassembly and rebuild every [0.15, 0.4], drive train failure 0.03 and bearing failure 0.028, media leakage 0.78, mechanical vibration 0.13, sensor failure 0.001, abrasive wear 0.24, gear fatigue 0.06, bearing pitting 0.06, poor lubricating oil quality 0.04, abnormal filter 0.04, gear pitting 0.04, poor gear tooth design 0.04, excessive pressure 0.04, gear tooth deterioration 0.02, and over temperature 0.018. you can see figure 2. Hu, Q., et al. [2017].

Box 2

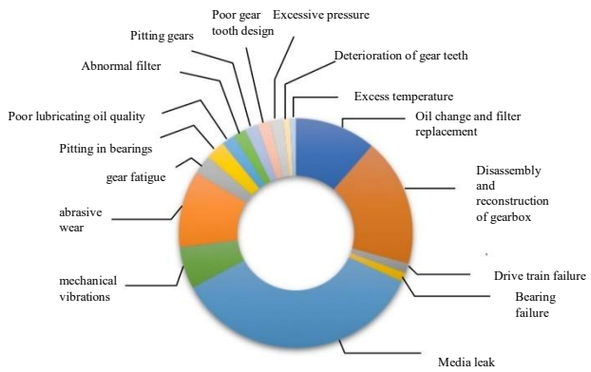

Figure 2

Failure frequency in wind turbine amplifier box systems considering a useful life of 20 years.

Source: Own elaboration

Damage mechanisms in gears, bearings and bushings of wind turbines

Gear damage mechanisms generated by thermal effects cause localized melting and vaporization at the arc junction, producing craters, pitting, grain growth, hardness reduction, and embrittlement. Repeated or prolonged current pulses deepen the molten layer and widen the heat-affected zone, developing mechanical effects; supersonic plasma expansion, pressure shocks in the metal, microcracks, and subsurface delamination. Furthermore, magnetic [Lorentz] forces from the arc current can deform thin-walled gear teeth or initiate fatigue cracks. High-velocity plasma jets erode sharp edges and surface asperities.

ISSN: 2531-2979
RENIECYT: 1702902

Berra-Ceballos, Raúl, Cruz-Gómez, Marco Antonio, Mejía-Pérez, José Alfredo and Castillo- Pensado, Juan Luis. [2025]. Design and maintenance analysis of wind turbine amplifier gearboxes systems exposed to lightning discharges. Journal-Mathematical and Quantitative Methods. 9[15]1-16: e3915116.
https://doi.org/10.35429/JMQM.2025.9.15.3.1.16

Eddy currents induced in specific areas of the gear cause volumetric heating, intensifying thermal, stress and electromagnetic gradients, and distorting tolerances between parts and within the part.

Chemical and metallurgical effects promote rapid oxidation of the freshly molten metal, forming brittle oxides that delaminate under load.

Nitrogen and other atmospheric ions can be absorbed by the heat-affected zone, altering the microstructure and corrosion resistance.

Thin films and their properties at high temperatures applied to mechanical transmissions of wind turbines.

Thin films are a mitigation strategy, using plasma-resistant alloy substrates [stainless steel such as 316L or nickel-based superalloys], hard ceramic or diamond-like carbon [DLC] coatings to protect against sputtering and arc pitting, alumina insulating barrier coatings on non-drive surfaces to prevent unwanted discharges, round tooth edges and avoid sharp corners to reduce field intensification factors, introduce local grounding electrodes or Faraday cages around the gearbox to deflect stray discharges from the gears, implement adequate insulation on shafts or housings to control where plasma can form, use solid lubricants [molybdenum disulfide and graphite or those that resist plasma attack. Agbogo, V. U., et al. [2025], Amaro, R. I., et al. [2005], Bobzin, K., et al. [2015], Bobzin, K., et al. [2015] and Yu, B., et al. [2024].

Plasma ion nitriding is used to harden gears and shafts in the aerospace industry operating in high-altitude, low-pressure environments. Plasma-resistant coatings [ceramic thermal barriers] protect rotating components from ionized gas erosion and thermal cycling in the industry. Gear systems near plasma-exposed components are coated with tungsten carbide or DLC to resist neutron bombardment and plasma-induced erosion.

High-temperature ceramic matrix composites are used in gear housings and bearing housings to withstand extreme thermal loads. Originally developed for turbine blades, these composites have now been adapted for compact, high-temperature gearboxes to operate at temperatures up to 1200°C without significant thermal deformation.

Diamond-like carbon [DLC] surface engineering coatings offer a combination of mechanical and chemical benefits. This amorphous carbon material with diamond-like properties, extreme hardness, low friction, and high chemical resistance. It contains mixtures of sp^2 [graphite] and sp^3 [diamond] carbon bonds, giving it a unique balance of toughness and lubricity. DLC is deposited by physical vapor deposition [PVD] or chemical vapor deposition [CVD]. Substrates are placed in a vacuum chamber where carbon ions are accelerated and implanted onto the surface, forming a uniform, ultra-thin film a few microns thick. DLC coatings offer a low coefficient of friction <0.1, reducing wear and energy loss, which is essential for automotive and aerospace parts.

High hardness protects components from abrasion and corrosion resistance, and is applied under ISO 4406:99, ISO 14577-1/-2/-3:2015, and ASTM F1578-18 standards. ASTM. [2018]. ASTM F1578-18, Baragetti, S., et al. [2011], Bobzin, K., et al. [2015], ISO. [1999]. ISO 4406:99, ISO. [2015]. ISO 14577-1/-2/-3, Latha, S., & Surendar, S. [2023], Latha, S., & Surendar, S. [2023] and Yu, B., et al. [2024].

Lubricants for transmission exposed to plasma environments.

Lightning discharges generate plasma channels with ion bombardment that dislodge atoms from gear teeth and rolling elements/races in bearings, altering profiles and increasing clearance. High-energy neutrals and radicals chemically erode surfaces over time. The sharp edges of deformed teeth and rolling elements on bearing races concentrate electric fields, causing microarcs that pit the metal. Return currents or discharge paths can traverse lubricated spaces, degrading gears, bearings, and lubricants.

Reactive plasma species [O, OH, F, Cl] attack and degrade conventional lubricants [semi-solid, liquid, gaseous-nebula states], acidifying them, or carbonizing them to form sludge. Vacuum or low-pressure plasmas completely eliminate lubricants, generating thermal and mechanical stress. Localized heating of the discharges can induce thermal cycling and microcracks. Increased friction due to surface roughness amplifies wear. Araya, N., et al. [2025].

ISSN: 2531-2979
RENIECYT: 1702902

Berra-Ceballos, Raúl, Cruz-Gómez, Marco Antonio, Mejía-Pérez, José Alfredo and Castillo- Pensado, Juan Luis. [2025]. Design and maintenance analysis of wind turbine amplifier gearboxes systems exposed to lightning discharges. Journal-Mathematical and Quantitative Methods. 9[15]1-16: e3915116.
https://doi.org/10.35429/JMQM.2025.9.15.3.1.16

Gears exposed to plasma environments use solid lubrication [MoS_2 or graphite], which performs better than fluid lubricants. Ag-Mo, $FeTiO_3$, composite coatings form lubricating films that can withstand over 800°C under plasma exposure, ideal for hypersonic vehicle gearboxes. Extreme temperatures can exceed 1000°C.

Gearbox housings and internal components must resist thermal distortion and maintain lubricant integrity. Motors and actuators require compact gearboxes that deliver hundreds of kW per kilogram. Achieving high torque in a confined space tests gear strength and bearing life. Araya, N., et al. [2025], González Prieto, D., et al. [2021], Kozień, E., & Grzegorczyk, M. [2020] and Ma, Y., et al. [2020].

In vacuum or low-pressure plasmas, it is advisable to use thin films of ionic-coated MoS_2 or gold-coated coatings as a solid-film solution. It uses self-healing lubricants, such as ionic liquids with high oxide stability that resist radical bombardment. Smart lubrication systems; nano-enhanced lubricants [incorporating graphene or boron nitride, polytetrafluoroethylene [PTFE], to reduce friction and wear at high temperatures], self-healing lubricants [which react chemically to repair microabrasions on gear surfaces], and real-time oil condition monitoring [sensors integrated into the gearbox detect degradation and trigger adaptive responses]. Graphenes in oils increase the heat transfer rate by 31.91%, increase viscosity and performance, strengthen lubricants for wind turbine gearboxes, optimal graphene loading varies between [0.1, 4] wt% depending on base oil viscosity and operating conditions, high shear mixing or ultrasonic treatment ensures uniform distribution. Ahsan, A., et al. [2025], Gulzar, M., et al. [2015], Jin, X., et al. [2024], Kozień, E., & Grzegorczyk, M. [2020], Ma, Y., et al. [2020] and Zouina, O., et al. [2025].

Previous studies of oils in wind turbine amplifier gearboxes identified oil properties. The oil degrades for up to 16 years, but does not lose its lubricating properties, making it functional for use. However, the addition of additives [corrosion inhibitors and antifoam agents] is recommended to improve its properties. It is also worth mentioning that these studies were conducted in a laboratory under controlled environmental conditions and without the presence of lightning strikes.

They also identified premature failure of the gearbox bearings, which continue to fail between 5% and 20% of their useful life. This indicates that the lubricant loses shear properties and, tribologically, loses load conditions that are fundamental to the contact clearance damping phenomenon. Kozień, E., & Grzegorczyk, M. [2020] and Kumar, R., et al. [2023].

Autonomous base balancing and leveling systems for industrial machinery

Gearboxes in wind turbines accelerate the slow rotation of the turbine blades to the high speed required by electric generators. A gear ratio of 90:1 transforms [7, 16] rpm in the rotor into 1500 rpm in the generator.

Design challenges: it must withstand large moments, torque fluctuations, and severe transient loads from power grid startups, shutdowns, and events. Misalignment under high loads causes stress concentrations, leading to gear or bearing failures, as shown in Figure 3. Al-Bedhany, J. H., et al. [2024] and Bruce, T., et al. [2015].

Box 3

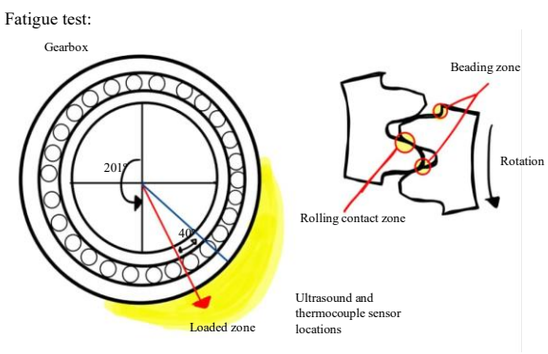

Figure 3
Areas of greatest damage in bearings and gears.
Source: Own elaboration

Offshore wind energy takes advantage of the high intensity of oceanic winds. As energy demand grows, larger turbines are required to optimize generation and reduce the cost of renewable electricity. On the other hand, the engineering challenge, particularly in the design of pedestal-type structures, is that they must withstand greater structural loads such as wind gusts while maintaining structural integrity, profitability, and transportability.

ISSN: 2531-2979
RENIECYT: 1702902

Berra-Ceballos, Raúl, Cruz-Gómez, Marco Antonio, Mejía-Pérez, José Alfredo and Castillo- Pensado, Juan Luis. [2025]. Design and maintenance analysis of wind turbine amplifier gearboxes systems exposed to lightning discharges. Journal-Mathematical and Quantitative Methods. 9[15]1-16: e3915116.
https://doi.org/10.35429/JMQM.2025.9.15.3.1.16

A sustainable development analysis supported by monitoring using digital twin technology, powered by artificial intelligence, can revolutionize the optimization of tower design based on zonal deformation under radial and mixed loads that influence the leveling of the wind turbine and its components, as shown in Figure 4. Ding, Y., et al. [2025].

Box 4

Deformation diagram of wind towers:

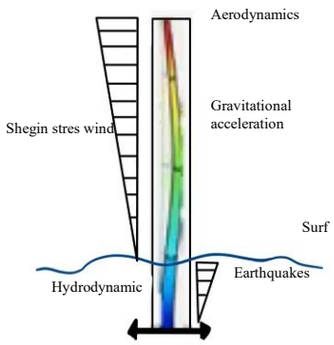

Figure 4

Deformation of towers by zones under radial and mixed environmental loads

Source: Own elaboration

Autonomous balancing and leveling systems for industrial or aerospace machines automatically monitor and correct imbalance and misalignment of rotating aerospace components [propellers, turbine rotors, driveshafts] during operation. By integrating real-time sensors, control algorithms, and actuators, these systems ensure optimal rotor dynamics, reducing vibration, noise, and structural fatigue. Aerospace components operate at very high speeds and within tight tolerances. Unbalanced rotors amplify vibration, reduce performance, and accelerate wear. An automatic balancing and leveling system seeks lightweight, highly stable structural designs that minimize additional mass and part count, meeting the stringent requirements of aeroengines and transmissions.

High-precision accelerometers, or vibration probes, measure synchronous vibration amplitudes and phase angles in one or more planes. These have aerospace applications, such as gyroscopes for inertial navigation and satellite stabilization platforms, microturbines and high-speed ventilation devices in avionics cooling, helicopter rotors [main and tail] and fixed-wing propellers, turbine and compressor discs in jet engines, drive shafts and power take-off assemblies. Coronado, D., & Kupferschmidt, C. [2014].

The working principle of a self-contained balancing and leveling loop captures the amplitude and phase of vibration via vibration sensors, base mounted piezoelectric accelerometers detect the amplitude and phase of the unbalanced vibration in real time, inclinometers/gyroscopes, MEMS [Microelectromechanical Systems] or fiber optic gyroscopes continuously measure the roll and pitch angles of the base enabling angulation leveling control, control unit, real-time signal processor, a high-speed DSP [Digital Signal Processors] or FPGA [Programmable Gate Arrays] reads the sensor data, executes balancing/leveling algorithms, and issues actuator commands with millisecond latency adaptive algorithms, combination of PID [Proportional-Integral-Derivative control] loops for fast correction with model-based observers that distinguish between true unbalance and transient disturbances, actuation layer, Electromagnetic balance actuators generate counter-rotating magnetic forces that directly oppose imbalance vectors, ideal for high-frequency corrections without adding moving mass.

Hydraulic/pneumatic leveling cylinders. High-rigidity cylinders adjust base height at multiple corners; solenoid valves regulate flow according to control needs. Adjustable mass carriers: Motorized sleds carrying removable masses are repositioned around the spindle to rebalance rotating components. AI-based adaptive controls: Hybrid controllers that combine the simplicity of PID with the adaptability of reinforcement learning, automatically adapting to changing dynamics. Edge computing and 5G [machine learning or blockchain]: Offloading heavy estimation and planning tasks to edge servers, enabling lighter embedded computers and more complex algorithms. Bio-inspired mechanisms for optimization offer forward-looking learning capabilities. González, M. J., et al. [2021].

International standards for autonomous balancing and leveling systems applicable to wind turbine systems: SAE ARP 4048; Horizontal rigid bearing balancer for aero-components, SAE ARP 4050; Vertical rigid bearing balancer for discs and rings, SAE ARP 5323; Test methods for vibration measurement on rotating machinery, ISO 1940-1; Balance quality and permissible residual unbalance, IEC 62832.

ISSN: 2531-2979
RENIECYT: 1702902

Berra-Ceballos, Raúl, Cruz-Gómez, Marco Antonio, Mejía-Pérez, José Alfredo and Castillo- Pensado, Juan Luis. [2025]. Design and maintenance analysis of wind turbine amplifier gearboxes systems exposed to lightning discharges. Journal-Mathematical and Quantitative Methods. 9[15]1-16: e3915116.
https://doi.org/10.35429/JMQM.2025.9.15.3.1.16

Establishes a framework for digital factory architectures, including digital twin elements for level sensing modules and adaptive control systems that maintain machine or platform levelness in real time; and IEC 60204-1; Covers the safety of machine electrical equipment, specifying requirements for control circuits and monitoring devices used in automated leveling systems. Al-Bedhany, J. H., et al. [2024], Bruce, T., et al. [2015], Ding, Y., et al. [2025], Hu, Q., et al. [2017], IEC. [2016]. IEC 60204-1, IEC. [2016]. IEC 60204-1, IEC. [2016]. IEC 62832, IEC. [2016]. IEC 62832, ISO. [2006]. ISO 1940-1, SAE. [s.f.]. SAE ARP4048, SAE. [s.f.]. SAE ARP4050, SAE. [s.f.]. SAE ARP5323 and SAE. [s.f.]. SAE ARP5412A.

Proactive maintenance of wind turbine amplifier boxes with the support of artificial intelligence [AI]

Wind turbine maintenance programs begin at the beginning of their useful life, in an initial phase of 0-5 years; manufacturing defects are identified, a performance baseline is established. In the intermediate life phase, corresponding to 5-20 years, uptime is maximized and wear is addressed. Finally, in the final life stage of 20-25 years, conservation maintenance is carried out to enable safe and profitable operation with a planning approach to a decommissioning program aligned with circular economy objectives. Verma, P., & Kumar, N. [2021].

Strategies to extend service life: dust and moisture-proof housing sealing, high-reliability HVAC or fan systems, surge protection units, remote monitoring: SCADA status indicators for early warnings, solid-state MOSFET or SSR [MTBF] replacements. Digital twins: simulating thermal and vibration profiles to optimize preventive maintenance. Consider amplifier enclosures as mid-life consumables. Agbogo, V. U., et al. [2025], Araya, N., et al. [2025], Arias Velásquez, R. M. [2024], Bobzin, K., et al. [2015] and Ding, Y., et al. [2025]. For monitoring and maintenance, install active cooling [liquid or conduction] near high-flow areas to buffer temperature spikes; incorporate voltage/current sensors to detect the onset of electrical arcing in real time; schedule periodic inspections using optical profilometry or scanning acoustic microscopy to detect early erosion; implement a predictive maintenance algorithm based on operating hours, discharge counts, or cumulative plasma exposure.

Digital twins: Virtual replicas of geared powertrains that enable real-time load optimization. You can see Figure 5. Doostmohammadi, M., et al. [2020], González Prieto, D., et al. [2021], Gulzar, M., et al. [2015], Jin, X., et al. [2024], Verma, P., & Kumar, N. [2021], Yu, B., et al. [2024] and Zouina, O., et al. [2025].

Box 5

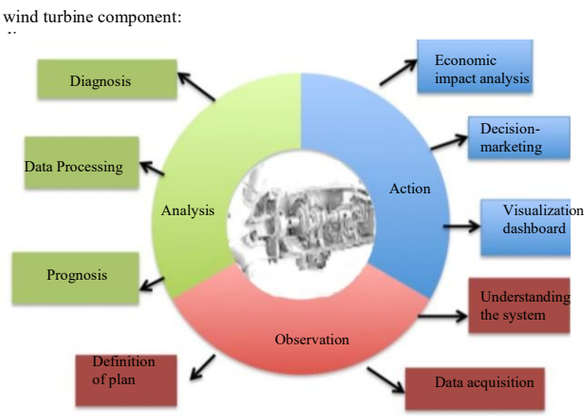

Figure 5

Real-time monitoring of wind turbine systems and components.

Source: Own elaboration

Wind turbulence can cause enormous stress on wheels and bearings. The faster the wind, the more vulnerable the gearboxes; offshore turbines are more exposed than onshore ones.

Wind turbine gearboxes face severe stresses due to temperature fluctuations, humidity, vibrations, and system transients. The presence of 0.01% water in the oil reduces oil life to 66%, 0.05% to 38%, and 0.15% to 20%. This represents a latent problem in gearbox systems, shortening gearbox life.

AI models predict failure modes before they occur, enabling proactive maintenance. Gearboxes now include integrated vibration and temperature sensors. Surface roughness measurement provides valuable information on slippage failures; the shape of the roller impact zone confirms deflection and misalignment throughout the bearing's rotation. Indentation, on the other hand, depends on contact pressure rather than debris size. Coronado, D., & Kupferschmidt, C. [2014], Farrando, M., et al. [2024], González, M. J., et al. [2021], Hu, Q., et al. [2017] and Zhang, W., et al. [2025].

ISSN: 2531-2979
RENIECYT: 1702902

Berra-Ceballos, Raúl, Cruz-Gómez, Marco Antonio, Mejía-Pérez, José Alfredo and Castillo- Pensado, Juan Luis. [2025]. Design and maintenance analysis of wind turbine amplifier gearboxes systems exposed to lightning discharges. Journal-Mathematical and Quantitative Methods. 9[15]1-16: e3915116.
https://doi.org/10.35429/JMQM.2025.9.15.3.1.16

Replacing a turbine gearbox represents approximately 10% of the cost. Turbines are designed for a 20-year lifespan, but many gearboxes fail after about five years due to fatigue, micropitting, and lubrication failure. The downtime from replacement impacts profitability and energy efficiency. Arias Velásquez, R. M. [2024] and Cardoni, M., et al. [2021].

Gearbox efficiency affects net power output; advanced tooth profiles and low-viscosity lubricants are key to increasing efficiency. Gearbox design varies for marine and onshore turbines; the role of digital twins in proactive maintenance. Ding, Y., et al. [2025], Kumar, R., et al. [2023] and Zhang, W., et al. [2025].

Conclusions

This research study fulfills its objective of analyzing the design and maintenance of wind turbine gearbox systems exposed to lightning strikes. It presents the contribution that wind turbine gearbox systems have evolved to meet the growth and expansion of the wind energy industry, along with the challenges it faces. The results of the analysis determined that traditional design methods under international standards establish the design bases for wind turbine amplifier boxes based on dynamic safety factors for each of their components. However, the wind turbine gearbox system and its components face a major challenge in lightning strikes [transient currents].

In the event of this phenomenon, the mechanical transmission is part of the grounding plasma channel, exposing its components to high temperatures, causing premature wear and reducing their useful life. In order to solve this problem, this research contributes that existing technologies for the aerospace industry should be used, such as the coating of thin films of ceramic or diamond-like carbon [DLC] on stainless and duplex steel superalloy substrates, to protect against sputtering and plasma-resistant arc pitting, in addition to the use of nano-enhanced intelligent lubrication systems [incorporating graphene or boron nitride, solid MoS_2 or graphite, Ag-Mo, $FeTiO_3$, PTFE [Polytetrafluoroethylene] that resist high temperatures in the event of transient discharges.

It is worth mentioning that the authors' proposal to incorporate an autonomous gyroscopic balancing and leveling system used in the aerospace industry and that has not been used for the anchoring system of equipment inside the machine room of wind turbines, will allow intermittent wind gusts and bending of the pedestal of the base of the wind turbine to mitigate the impacts on the rotodynamic systems, greatly reducing cracking.

The impact of materials, abrasive, adhesive, and corrosive wear, fatigue failures, and surface pitting will extend the lifespan of the gearbox system, similar to the lifespan of the wind turbine. The growth of wind turbines means that the technologies that must be used are the same as those used in the aerospace industry, with their adaptations to international standards, and the idea that a wind turbine is a simple machine for generating electrical energy with reduced costs that can be scaled with the same basic infrastructure conditions is abandoned.

The sustainable development of a wind farm lies in generating a sustainable balance based on the advanced technologies demanded by the equipment's operating environment.

Declarations

Conflict of interest

The authors declare no interest conflict. They have no known competing financial interests or personal relationships that could have appeared to influence the article reported in this article.

Author contribution

Berra-Ceballos, Raúl: Contributed to the research idea, information gathering, and writing of several sections of the article, based on his professional experience.

Cruz-Gómez, Marco Antonio: Contributed to the revision of the project's writing and provided general improvement suggestions, based on his professional experience.

Mejía-Pérez, José Alfredo: Contributed to the revision and writing of various sections, based on his professional experience.

Castillo-Pensado, Juan Luis: Contributed to the revision and writing of various sections, based on his professional experience.

ISSN: 2531-2979
RENIECYT: 1702902

Berra-Ceballos, Raúl, Cruz-Gómez, Marco Antonio, Mejía-Pérez, José Alfredo and Castillo- Pensado, Juan Luis. [2025]. Design and maintenance analysis of wind turbine amplifier gearboxes systems exposed to lightning discharges. Journal-Mathematical and Quantitative Methods. 9[15]1-16: e3915116.
https://doi.org/10.35429/JMQM.2025.9.15.3.1.16

Availability of data and materials

This article is a literature review based on previously published data and documents. No new datasets were generated during this study.

Funding

This work was self-funded by the authors.

Acknowledgements

To the Benemérita Universidad Autónoma de Puebla; Engineering Faculty for the support in the use of its infrastructure., To the Tribology and Transport Group, BUAP, for their support in the analysis and development of the work, and 189 Disaster Prevention, Sustainable Development and Tribology Academic body, BUAP.

Abbreviations

AI - Artificial Intelligence

References

Antecedents

Adedeji, P. A., Olatunji, O. O., Madushele, N., Rasmeni, Z. Z., & Janse van Rensburg, N. [2024]. Effectiveness of evolutionary-tuned neurofuzzy inference system in predicting wind turbine gearbox oil temperature. Materials Today: Proceedings, 105, 126–130.

Alves Ribeiro, J., Alves Ribeiro, B., Pimenta, F., Tavares, S. M. O., Zhang, J., & Ahmed, F. [2025]. Offshore wind turbine tower design and optimization: A review and AI-driven future directions. Applied Energy, 397, 126294.

Arias Velásquez, R. M. [2024]. Bearings faults and limits in wind turbine generators. Results in Engineering, 21[101891], 101891.

Banihabib, R., & Assadi, M. [2023]. Towards a low-carbon future for offshore oil and gas industry: A smart integrated energy management system with floating wind turbines and gas turbines. Journal of Cleaner Production, 423, 138742.

Bruce, T., Rounding, E., Long, H., & Dwyer-Joyce, R. S. [2015]. Characterisation of white etching crack damage in wind turbine gearbox bearings. Wear, 338–339, 164–177.

Coronado, D., & Kupferschmidt, C. [2014]. Assessment and validation of oil sensor systems for on-line oil condition monitoring of wind turbine gearboxes. Procedia Technology, 15, 747–754.

Fridman, A., Gutsol, A., & Cho, Y. I. [2007]. Non-Thermal Atmospheric Pressure Plasma. In Advances in Heat Transfer Volume 40 [pp. 1–142]. Elsevier.

Gulzar, M., Masjuki, H. H., Kalam, M. A., Varman, M., Zulkifli, N. W. M., Mufti, R. A., Zahid, R., & Anuar, H. [2015]. Tribological performance of nanoparticles as lubricating oil additives. Journal of Nanoparticle Research, 17[7], 1–26.

Hu, Q., Yang, H., & Ding, K. [2017]. Remaining useful life prediction of wind turbine bearings based on non-stationary vibration signal using adaptive redundant multiscale morphological decomposition. Renewable Energy, 116, 447–456.

Jiang, L., Zhu, J., Jin, Z., Jiang, Z., Song, Y., & Feng, D. [2020]. A review on reliability analysis of wind turbine gearbox. Engineering Failure Analysis, 115, 104692.

Kumar, R., Chatterjee, S., & Dhar, A. [2023]. Role of nanoparticles as additives in lubricants: A comprehensive review. Tribology International, 179, 108092.

Basics

AGMA. [2004]. AGMA 2001-D04: Fundamental rating factors and calculation methods for involute spur and helical gear teeth. American Gear Manufacturers Association.

AGMA. [n.d.]. AGMA 6006: Specification for design, rating and application of gearboxes for wind turbines. American Gear Manufacturers Association.

Alipio, R., Conceição, D., De Conti, A., Yamamoto, K., Dias, R. N., & Visacro, S. [2019]. A comprehensive analysis of the effect of frequency-dependent soil electrical parameters on the lightning response of wind-turbine grounding systems. Electric Power Systems Research, 175[105927], 105927.

ISSN: 2531-2979
RENIECYT: 1702902

Berra-Ceballos, Raúl, Cruz-Gómez, Marco Antonio, Mejía-Pérez, José Alfredo and Castillo- Pensado, Juan Luis. [2025]. Design and maintenance analysis of wind turbine amplifier gearboxes systems exposed to lightning discharges. Journal-Mathematical and Quantitative Methods. 9[15]1-16: e3915116.
https://doi.org/10.35429/JMQM.2025.9.15.3.1.16

Amaro, R. I., Martins, R. C., Seabra, J. O., Renevier, N. M., & Teer, D. G. [2005]. Molybdenum disulphide/titanium low friction coating for gears application. Tribology International, 38[4], 423–434.

ASTM. [2018]. ASTM F1578-18: Standard specification for turbines, hydraulic. ASTM International.

González Prieto, D., Díaz Domínguez, J., & Carou, D. [2021]. Tribological behavior of MoS_2-based coatings under different loads and lubricants. Coatings, 11[2], 213.

IEC. [2000]. IEC 60068-2-60: Environmental testing – Part 2-60. International Electrotechnical Commission.

IEC. [2014]. IEC 61000-4-5: Electromagnetic compatibility – Surge immunity test. International Electrotechnical Commission.

IEC. [2016]. IEC 60204-1: Safety of machinery – Electrical equipment of machines. International Electrotechnical Commission.

IEC. [2016]. IEC 62832: Digital factory framework. International Electrotechnical Commission.

IEC. [2019]. IEC 61400-24: Wind energy generation systems – Lightning protection. International Electrotechnical Commission.

IEC. [2021]. IEC 62305-1 to 4: Protection against lightning. International Electrotechnical Commission.

ISO. [1999]. ISO 4406:99: Hydraulic fluid power – Fluids – Method for coding the level of contamination by solid particles. International Organization for Standardization.

ISO. [2006]. ISO 1940-1: Mechanical vibration – Balance quality requirements for rotors in a constant [rigid] state – Part 1: Specification and verification of balance tolerances. International Organization for Standardization.

ISO. [2010]. ISO 14916: Thermal spraying – Determination of tensile adhesive strength. International Organization for Standardization.

ISO. [2015]. ISO 14577-1/-2/-3: Instrumented indentation test for hardness and materials parameters. International Organization for Standardization.

ISO. [2019]. ISO 1328: Cylindrical gears – ISO system of accuracy. International Organization for Standardization.

ISO. [2019]. ISO 6336: Calculation of load capacity of spur and helical gears. International Organization for Standardization.

ISO/AGMA. [n.d.]. ISO 6336/AGMA 2001: Standard for gear capacity calculations. International Organization for Standardization / American Gear Manufacturers Association.

NFPA. [n.d.]. NFPA 780: Standard for the Installation of Lightning Protection Systems. National Fire Protection Association.

Supports

Araya, N., Arenhart, R., Neves, G. O., Aguilar, C., Binder, C., Klein, A. N., & de Mello, J. D. B. [2025]. The influence of solid lubricant reservoir's morpho-dimensional evolution on the sliding wear of sintered iron-based self-lubricant composites. Wear, 570, 206032.

Ahsan, A., Zanj, A., Zafar, A., Iqbal, N., Fatima, A., Khan, W., Yousaf, M. Z., Khan, B., & Guerrero, J. M. [2025]. Predicting the impact of graphene oxide and its shapes on the thermal efficiency of Polyalphaolefin-40 using a mathematical model for wind turbine gearboxes. Case Studies in Thermal Engineering, 72[106307], 106307.

Baragetti, S., Cavalleri, S., & Tordini, F. [2011]. A numerical method to predict the RCF behaviour of PVD-coated transmission gears and experimental results. Procedia Engineering, 10, 1485–1490.

Bobzin, K., Brögelmann, T., Stahl, K., Stemplinger, J.-P., Mayer, J., & Hinterstoißer, M. [2015]. Influence of wetting and thermophysical properties of diamond-like carbon coatings on the frictional behavior in automobile gearboxes under elasto-hydrodynamic lubrication. Surface & Coatings Technology, 284, 290–301.

ISSN: 2531-2979
RENIECYT: 1702902

Berra-Ceballos, Raúl, Cruz-Gómez, Marco Antonio, Mejía-Pérez, José Alfredo and Castillo- Pensado, Juan Luis. [2025]. Design and maintenance analysis of wind turbine amplifier gearboxes systems exposed to lightning discharges. Journal-Mathematical and Quantitative Methods. 9[15]1-16: e3915116.
https://doi.org/10.35429/JMQM.2025.9.15.3.1.16

Cardoni, M., Pau, D., Falaschetti, L., Turchetti, C., & Lattuada, M. [2021]. Synthetic image dataset of shaft junctions inside wind turbines in presence or absence of oil leaks. Data in Brief, 39, 107538.

Cernalevschi, G., Ratoi, M., Mellor, B. G., & Cai, Y. [2025]. Effect of current discharges across MTM and MPR tribological contacts with negatively charged MTM ball and MPR roller. Tribology International, 210, 110776.

Farrando, M., Pané, S., & Pons, M. [2024]. Failure detection and diagnosis in wind turbine generators: A comprehensive review of recent trends and challenges. Renewable Energy, 212, 1270–1289.

González, M. J., Gómez-Gil, J., Bravo-Muñoz, I., & García-Prada, J. C. [2021]. Bearing fault detection using envelope analysis and dynamic pressure sensors in wind turbines. Energies, 14[8], 2342.

Jin, X., Qu, X., Zhang, X., Wang, X., & Liu, Y. [2024]. Effect of nano-lubricants on friction and wear performance of wind turbine gear materials. Tribology International, 190, 108060.

Differences

Agbogo, V. U., Sadiku, E. R., Mavhungu, L., Kupolati, W. K., & Injor, O. M. [2025]. Nanotechnology coatings in the defense and aerospace industry. Next Nanotechnology, 7[100197], 100197.

Akgül, E. F. [2024]. Navigating decarbonization: Examining shipping companies' fleet modernization strategies worldwide. Dokuz Eylül Üniversitesi Denizcilik Fakültesi Dergisi, 16[1], 1–21.

Al-Bedhany, J. H., Mankhi, T. A., & Legutko, S. [2024]. A surface study of failed planetary wind turbine gearbox bearings to investigate the causes of the bearing premature failure issue. Heliyon, 10[4], e25860.

Bru, K., Beaulieu, M., Sousa, R., Leite, M. M., Botleho de Sousa, A., Kol, E., Rosenkranz, J., & Parvaz, D. B. [2020]. Comparative laboratory study of conventional and Electric Pulse Fragmentation [EPF] technologies on the performances of the comminution and concentration steps for the beneficiation of a scheelite skarn ore. Minerals Engineering, 150, 106302.

Doostmohammadi, M., Moghadam, S. A., & Khonsari, M. M. [2020]. Surface defects and pitting formation in lubricated point contacts under sliding. Wear, 442–443, 203121.

Discussions

Ding, Y., Zhu, F., Li, H., Parlikad, A. K., & Xie, M. [2025]. A failure knowledge graph learning framework for offshore wind turbines with incomplete knowledge. Renewable and Sustainable Energy Reviews, 215, 115561.

Kozień, E., & Grzegorczyk, M. [2020]. Wind turbine lubrication systems: Review and future challenges. Energies, 13[9], 2272.

Verma, P., & Kumar, N. [2021]. Wear mechanisms in wind turbine gearbox: A comprehensive review. Tribology International, 155, 106765.

ISSN: 2531-2979
RENIECYT: 1702902

Berra-Ceballos, Raúl, Cruz-Gómez, Marco Antonio, Mejía-Pérez, José Alfredo and Castillo- Pensado, Juan Luis. [2025]. Design and maintenance analysis of wind turbine amplifier gearboxes systems exposed to lightning discharges. Journal-Mathematical and Quantitative Methods. 9[15]1-16: e3915116.
https://doi.org/10.35429/JMQM.2025.9.15.3.1.16

Journal-Mathematical and Quantitative Methods 9[15]1-9: e4915109
Article

Modelling of the lifting platform braking mechanism for autonomous vertical parking

Modelado del mecanismo de frenado de plataforma de elevación para un estacionamiento vertical autónomo

Betanzos-Castillo, Francisco * [a], Fuentes-Castañeda, Pilar [b], Cortez-Solis, Reynaldo [c] and Rodriguez-Cortes, Aldo [d]

[a] Tecnológico Nacional de México – TES Valle de Bravo • AIE-1532-2022 • 0000-0002-7245-703X • 206209
[b] Tecnológico Nacional de México – TES Valle de Bravo • KUD-2889-2024 • 0000-0001-6567-9614 • 428699
[c] Tecnológico Nacional de México – TES Valle de Bravo • KUD-2900-2024• 0000-0001-7519-1815 • 1113392
[d] Tecnológico Nacional de México – TES Valle de Bravo • MTG-1051-2025• 0009-0000-4009-6340

Classification:

Area: Engineering
Field: Engineering
Discipline: Mechanical Engineering
Subdiscipline: Mechanical design

https://doi.org/10.35429/JMQM.2025.9.15.4.1.9
History of the article:
Received: October 30, 2025
Accepted: December 30, 2025

* ✉ [francisco.bc@vbravo.tecnm.mx]

Abstract

Autonomous vertical parking lots [AVP] are fully automated systems that allow vehicles to be stored efficiently and securely. These systems offer an innovative solution for fast access and reliable storage of automobiles. In this work, the conceptual design of an AVP was developed with a vision oriented towards Industry 5.0. The design, modeling and structural analysis, using computer-aided engineering [CAE] tools, of a braking system for the central platform where vehicles are housed upon arrival was carried out. This platform is raised and transfers the vehicles to a structure divided into several levels, evaluating different configurations and design parameters. Finally, the behavior of the braking mechanism under loads was studied by finite element analysis [FEA]. The results obtained demonstrate and verify the feasibility of the system under real operating conditions, improving both safety and operational efficiency.

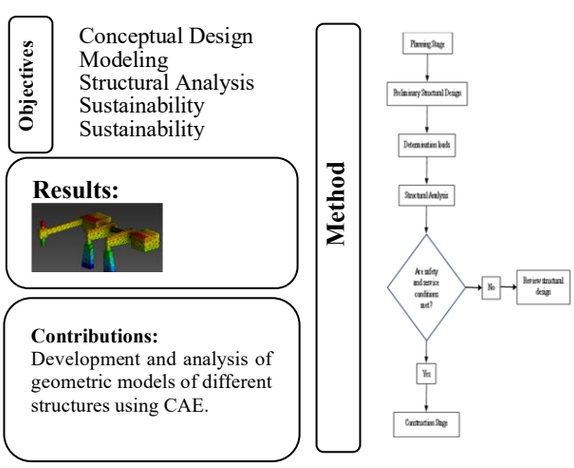

Braking mechanism, Load modelling, I5.0.

Resumen

Los estacionamientos verticales autónomos [AVP] son sistemas completamente automatizados que permiten almacenar vehículos de manera eficiente y segura. Estos sistemas ofrecen una solución innovadora para el acceso rápido y el resguardo confiable de automóviles. En este trabajo, se desarrolló el diseño conceptual de un AVP con una visión orientada hacia la Industria 5.0. Se llevó a cabo el diseño, modelado y análisis estructural, utilizando herramientas de ingeniería asistida por computadora [CAE], de un sistema de frenado para la plataforma central donde se alojan los vehículos al llegar. Esta plataforma se eleva y transfiere los vehículos a una estructura dividida en varios niveles, evaluando diferentes configuraciones y parámetros de diseño. Finalmente, se estudió el comportamiento del mecanismo de frenado bajo cargas mediante análisis por elementos finitos [FEA]. Los resultados obtenidos demuestran y verifican la viabilidad del sistema en condiciones reales de operación, mejorando tanto la seguridad como la eficiencia operativa.

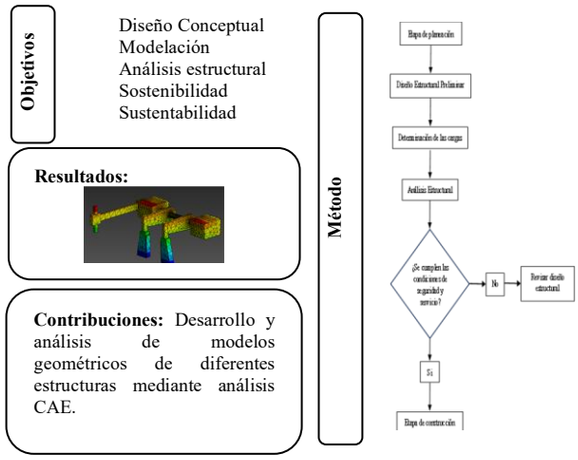

Mecanismo de frenado, Modelización de la carga, I5.0.

Area: Promotion of frontier research and basic science in all fields of knowledge

Citation: Betanzos-Castillo, Francisco, Fuentes-Castañeda, Pilar, Cortez-Solis, Reynaldo and Rodriguez-Cortes, Aldo. [2025]. Modelling of the lifting platform braking mechanism for autonomous vertical parking. Journal-Mathematical and Quantitative Methods. 9[15]1-9: e4915109.

Introduction

Autonomous vertical parking systems have evolved significantly since their introduction, especially in urban areas where space is limited, traditional parking systems require a lot of space and cause pollution and traffic jams, as drivers often keep circling to find an empty space (Guangmei Wu, 2019). These systems combine quick access and safe storage of vehicles, with minimal space requirements. A notable early example is the Auto Zuri West in Switzerland, an automated system that employs a combination of lifts and platforms to maximize the use of vertical space.

These systems are part of a trend toward more efficient and technologically advanced parking solutions that seek to reduce environmental impact and improve accessibility in densely populated environments. Nowadays it is very important to know that urban space is becoming more and more limited, the need for innovative solutions to optimize the use of land is more and more constant. In this context, the conceptualization of vertical parking support structures emerges as an efficient and practical response to the growing demand for parking spaces. Aiming to mitigate the limitations in the current parking infrastructure and address the global challenge of traffic congestion, they propose a vehicle design scheme with vertical lifting mechanisms and folding wings, which represents an innovative change for environmental protection, sustainable development and artificial intelligence (Yixu, Junying, & Kun, 2024).

Other researchers propose as an alternative solution, the development of a conceptual design of a vertical autonomous parking with a vision oriented to the I4.0 industry (Betanzos-Castillo, Fuentes-Castañeda, & Cortez-Solis, 2024).

Emerging technologies are used during the machine design process, such as simulation, which substantially improves performance by facilitating the detection of anomalies not foreseen in the design phase, reducing the number of tests under real conditions and, in addition, enables the analysis and evaluation of the safety factor, reducing the probability of generating failures due to fatigue or overload.

Today, finite element methods are widely used to numerically solve structural, fluid and multiphysics problems (Bathe, 2003). Engineers and scientists can mathematically model and numerically solve very complex problems, such as to evaluate designs, which allows to a large extent to gain insight into phenomena and ideally predict them. Designs can be made safer and more cost-effective, and can help prevent catastrophes during operation.

Finite Element Analysis [FEA] is referred to as Finite Element Method [FEM], which is used in engineering to reduce the number of physical prototypes and run virtual experiments to optimize their designs (Rameshrao Yawale & Nivrutti Naik, 2021). The basic idea of FEM is to divide the complex structure into a finite number of interconnected elements, to determine the loads acting on each node and to calculate the displacements in the direction of those loads, and thus obtain a result for the whole (Oguz Örmecioglu, Aydogdu, & Tugba Örmecioglu, 2024).

Throughout the history of braking systems, from the earliest wooden blocks to modern disc brakes and specific spring brake systems designed for elevators, one fundamental principle has remained constant: the intrinsic reliance on friction. In addition, the concept of mechanical advantage, whether through levers, pulleys, or hydraulic systems, has been consistently employed to amplify the force applied to friction surfaces, making braking more effective and less dependent on brute human strength. The present work deals with the structural analysis of the braking mechanism for a lifting platform of an autonomous vertical parking lot, simulating the behaviour under load conditions.

The analysis is performed using software such as Ansys Workbench, the results obtained demonstrate and verify the feasibility of the system in real operating conditions, improving both safety and operational efficiency. A general description of the research is given in the first section of this article.

The second part includes the introduction to the project, in which the reader will understand the comparative and the main point of analysis.

ISSN: 2531-2979
RENIECYT: 1702902

Betanzos-Castillo, Francisco, Fuentes-Castañeda, Pilar, Cortez-Solis, Reynaldo and Rodriguez-Cortes, Aldo. [2025]. Modelling of the lifting platform braking mechanism for autonomous vertical parking. Journal-Mathematical and Quantitative Methods. 9[15]1-9: e4915109.
https://doi.org/10.35429/JMQM.2025.9.15.4.1.9

The third shows the theoretical framework as the main support of the project to know terms and concepts that will be addressed in the CAE simulation, then, in the fourth section you will find the FEA methodology to be applied in the analysis of the mechanism, materials added to the 3D model, parameters, types of models to be used, meshing and comparisons made, finally the fifth section shows the results and conclusions found.

Methodology

Structural engineering is the science and art of safely and economically planning, designing and constructing structures to serve those purposes. Structural analysis is an integral part of any structural engineering project, whose function begins with the prediction of the behaviour of the structure. Structural analysis is the prediction of the performance of a structure under prescribed loads and/or external effects, such as support movements and temperature changes. The characteristics of interest in the design performance of structures are [1] stresses or stress results, such as axial forces, shear forces, and bending moments; [2] deflections; and [3] support reactions, therefore, the analysis of structures usually involves the determination of these quantities as the cause of a loading condition.

Box 1

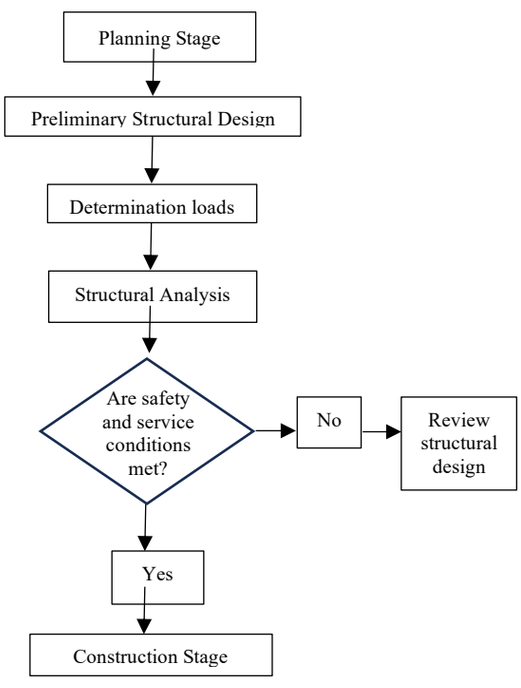

Figure 1
Stages of structural design, adopted from (Kassimali, 2015); (Betanzos-Castillo, Fuentes-Castañeda, & Cortez-Solis, 2024).
Source: Own elaboration, 2025

A structural engineering study is described by various stages using a flow chart, this indicates that it is an iterative process, and generally consists of the following steps (Kassimali, 2015):

1. Planning Stage. The planning phase usually involves the establishment of the functional requirements of the proposed structure, the general layout and dimensions of the structure, general considerations of the possible types of structures [e.g., rigid frames or trusses] that may be used, and the types of materials to be used [e.g., structural steel or reinforced concrete].This stage may also take into account other considerations of non-structural factors, such as aesthetic aspects, environmental impact of the structure and some others. Its result is generally a structural system that meets the functionality requirements and is expected to be the most economical.

This stage is perhaps the most crucial of the entire project and requires experience and knowledge of construction practices, as well as a thorough understanding of the behaviour of structures.

2. Preliminary structural design. In the preliminary structural design stage, the size of the structural system elements selected in the planning stage is estimated based on an approximate analysis, previous experience and code or regulation requirements. Thus, the sizes of the selected elements are used in the next stage to calculate the weight of the structure.

3. Determination of loads. Load estimation involves the determination of all loads that can be expected to act on the structure.

4. Structural analysis. In the structural analysis, the load values are used to develop an analysis to determine the resulting stresses in the elements and the deflections at different points of the structure.

5. Safety and serviceability check. The results of the analysis are used to determine whether or not a structure meets the safety and serviceability requirements of the design code. If these requirements are satisfied, then the design drawings and construction specifications are executed and the construction phase begins.

ISSN: 2531-2979
RENIECYT: 1702902

Betanzos-Castillo, Francisco, Fuentes-Castañeda, Pilar, Cortez-Solis, Reynaldo and Rodriguez-Cortes, Aldo. [2025]. Modelling of the lifting platform braking mechanism for autonomous vertical parking. Journal-Mathematical and Quantitative Methods. 9[15]1-9: e4915109.
https://doi.org/10.35429/JMQM.2025.9.15.4.1.9

6. Structural design review. If the requirements of the structure are not satisfied, then the element sizes are reviewed, and phases 3 to 5 are repeated until all safety and serviceability requirements are met (Kassimali, 2015).

Mathematical model FEM

Different problems treated in science and engineering are often described in terms of differential equations, formulated by using continuous mechanics models. In general, elasticity problems are reduced to solving the differential equations, known as equilibrium equations together with stress-strain relations or the strain-displacement relations and the compatibility equation under given boundary conditions.

Equilibrium equations in an elastic body in two dimensions:

$$\frac{\partial \sigma_x}{\partial x} + \frac{\partial \tau_{xy}}{\partial y} + F_x = 0 \quad [1]$$

$$\frac{\partial \tau_{yx}}{\partial x} + \frac{\partial \sigma_y}{\partial y} + F_y = 0 \quad [2]$$

Where σ_x and σ_y are normal forces in the x and y axes respectively, τ_{xy} and τ_{yx} are shear forces acting in the xy plane.

The strain-displacement relationships are:

$$\varepsilon_x = \frac{\partial u}{\partial x} \quad [3]$$

$$\varepsilon_y = \frac{\partial v}{\partial y} \quad [4]$$

$$\gamma_{xy} = \frac{\partial v}{\partial x} + \frac{\partial u}{\partial y} \quad [5]$$

Where ε_x and ε_y are the normal deformations in the x- and y-axis directions respectively, the engineering shear deformation in the xy plane is γ_{xy}; u and v are infinitesimal displacements in the x- and y-axis directions respectively.

Constitutive equations [stress-strain relationships]. These relationships describe the state of deformation, deformations induced by internal forces or stresses resisting against applied loads. These relationships depend on the materials properties; they are determined experimentally. Hooke's law relates six components of the three-dimensional stress tensors to the strain tensors, as follows:

$$\sigma_x = \frac{vE}{(1+v)(1-2v)} e_v + 2G\varepsilon_x \quad [6]$$

$$\sigma_y = \frac{vE}{(1+v)(1-2v)} e_v + 2G\varepsilon_y \quad [7]$$

$$\sigma_z = \frac{vE}{(1+v)(1-2v)} e_v + 2G\varepsilon_z \quad [8]$$

$$\tau_{xy} = G\gamma_{xy} = \frac{E}{2(1+v)}\gamma_{xy} \quad [9]$$

$$\tau_{yz} = G\gamma_{yz} = \frac{E}{2(1+v)}\gamma_{yz} \quad [10]$$

$$\tau_{xz} = G\gamma_{zx} = \frac{E}{2(1+v)}\gamma_{zx} \quad [11]$$

Or inversely:

$$\varepsilon_x = \frac{1}{E}\left[\sigma_x - v(\sigma_y + \sigma_z)\right] \quad [12]$$

$$\varepsilon_y = \frac{1}{E}\left[\sigma_y - v(\sigma_z + \sigma_x)\right] \quad [13]$$

$$\varepsilon_z = \frac{1}{E}\left[\sigma_z - v(\sigma_x + \sigma_y)\right] \quad [14]$$

$$\gamma_{xy} = \frac{\tau_{xy}}{G} \quad [15]$$

$$\gamma_{yz} = \frac{\tau_{yz}}{G} \quad [16]$$

$$\gamma_{zx} = \frac{\tau_{zx}}{G} \quad [17]$$

Where E is Young's modulus, v is Poisson's ratio, G is the shear modulus and e_v the volumetric strain expressed by the sum of the three normal strain components, $e_v = \varepsilon_x + \varepsilon_y + \varepsilon_z$.

The FEM assumes an object of analysis as a set of elements having arbitrary shapes and finite sizes [called finite element], approximates partial differential equations by simultaneous algebraic equations and numerically solves various elasticity problems (Nakasone, Yoshimoto, & Stolarski, 2006).

The Finite Element Analysis method requires the following main steps:

- Discretization of the domain into a finite number of subdomains [elements].
- Selection of interpolation functions.
- Development of the elementary matrix for the subdomain [element].

ISSN: 2531-2979
RENIECYT: 1702902

Betanzos-Castillo, Francisco, Fuentes-Castañeda, Pilar, Cortez-Solis, Reynaldo and Rodriguez-Cortes, Aldo. [2025]. Modelling of the lifting platform braking mechanism for autonomous vertical parking. Journal-Mathematical and Quantitative Methods. 9[15]1-9: e4915109.
https://doi.org/10.35429/JMQM.2025.9.15.4.1.9

- Assembly of the elementary matrices of each subdomain to obtain the global matrix of the complete domain.
- Imposition of the boundary conditions.
- Solution of the equations.
- Additional calculations [if required].

Computational Model

A computational model is a computer program designed to simulate and study complex systems using an algorithmic or mechanistic approach. These models are widely used across various fields, including physics and engineering. The ability to discretize irregular domains with finite elements makes the [FEA] method a valuable and practical analysis tool for the solution of boundary, initial and eigenvalue problems arising in different engineering disciplines (Madenci & Guven, 2015).

Simulation programs, over time, have improved their analysis, using improvements in the meshing processes, acceptance criteria, implementation of variables and presentation of results, where it is absolutely essential that the user acquires skills and can identify its operation, to have a command of the software (Díaz Iglesias, 2021). In order to perform simulation and structural analysis, some design software is used, such as: Ansys Workbench® which is an engineering simulation software, provides a wide range of tools and resources for post-processing and visualization of simulation results, allowing to understand and analyze the results effectively (SEMCOCAD, 2024). Ansys Workbench® was used for this study.

Table 1 shows the initial conditions for configuring the computational model, which are essential for structural analysis in ANSYS.

Box 2

Table 1

Key elastic mechanical properties of ASTM A36 structural steel.

Mechanical Properties	*Symbol*	*Recommended Value [ASTM A36]*	*Units*
Modulus of Elasticity [Young's Modulus]	***E***	*200*	GPa
Poisson ratio	***v***	*0.30*	Dimensi-onless
Shear Module	***G***	*78*	GPa
Density	***ρ***	*7850*	kg/m³

Source: Own elaboration, 2025

Results

The support structure and central platform were designed, which will lift and transfer vehicles in the available space. The lifting mechanism and braking system were also designed, taking into account the mechanics of the structure, creating a model and simulation in software, and considering the sensors, controllers, and electromechanical drives. To obtain the structural behaviour of the lifting platform, where the vehicles will be housed and later transferred to their final available location, a bridge type structure was designed, without lateral perforations, square profile 127 mm per side, 12.7 mm thick, 25.4 mm plate, upper and lower central part without plate and lower sides without plate. This can be seen in Figure 2.

To determine the structural behaviour of the lifting platform model, a load distributed along the entire structure was configured.

The necessary components for the lifting and braking systems were selected, and then the calculation was developed for a total load $W = 11{,}000\ kg$, considering 2 lifting systems.

We found that the force needed to lift the load is $Fs = 53{,}955\ N$ and the torque required by the system on the pulley shaft is Tp = 10,791 Nm.

Box 3

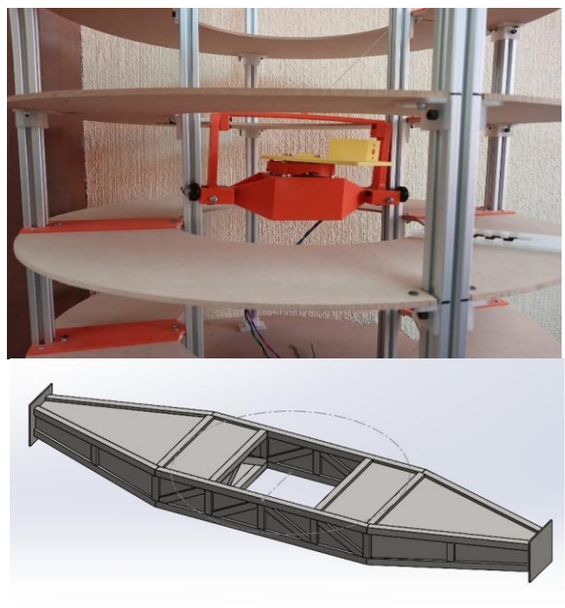

Figure 2

Support structure and central platform.

Source: Own elaboration, 2025

ISSN: 2531-2979
RENIECYT: 1702902

Betanzos-Castillo, Francisco, Fuentes-Castañeda, Pilar, Cortez-Solis, Reynaldo and Rodriguez-Cortes, Aldo. [2025]. Modelling of the lifting platform braking mechanism for autonomous vertical parking. Journal-Mathematical and Quantitative Methods. 9[15]1-9: e4915109.
https://doi.org/10.35429/JMQM.2025.9.15.4.1.9

A fundamental part of a lifting system is the braking system, which consists of two different types of brakes: the continuous-use brake, which is the electromagnetic brake, and the emergency brake, which is the mechanical brake.

The lifting system must be capable of lifting heavy loads. One might think that a hydraulic system would be the best option; however, it must be taken into account that this system does not allow for lifting to great heights, such as the 22 levels contemplated for the project. In contrast, an electric system represents a better alternative.

In addition, the electrical system offers greater performance, precise control, and energy savings, which is why this system was selected, demonstrating concern for its environmental impact, as the oil required in hydraulic systems is highly polluting. Figure 3 shows the parachute brake mechanism and its components and the properties of its materials, which is connected to the lifting platform and the motor by means of cables and pulleys.

Box 3

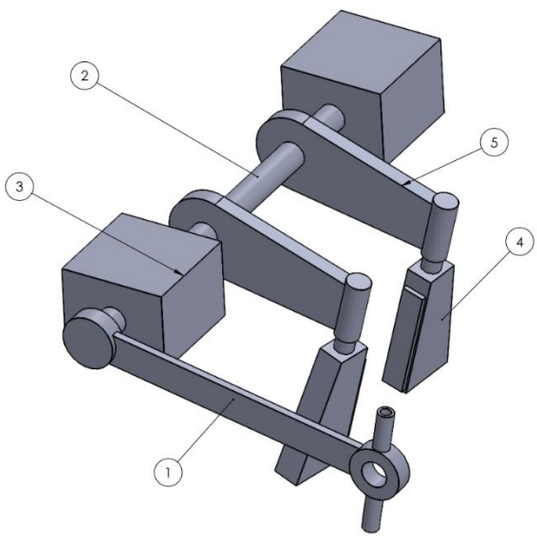

N.° DE ELEMENTO	N.° DE PIEZA	DESCRIPCIÓN	CANTIDAD
1	BrazoCable	Aleacion de acero - Endurecimiento superficial	1
2	BrazoFrenos	Aleacion de acero - Endurecimiento superficial	1
3	SoporteFreno	Aleacion de acero - Endurecimiento superficial	2
4	FrenoParacaidas	Fundicion gris o acero aleado - Endurecimiento por induccion	2
5	SoporteFrenos	Aleacion de acero - Endurecimiento superficial	2

Figure 3

Freno Paracaidas.

Source: Own elaboration, 2025

Simulation in Ansys Workbench

To translate the behaviour from a physical model to a computational model, the problem must be understood, which leads to obtaining an analytical solution using the theory of simple stresses and stress concentration factors. The computational model of the platform for an autonomous vertical parking was designed in DesignModeler of Ansys Workbench, considering the geometry, load, boundary conditions and structural materials, in this case a ASTM A36 structural steel was used.

In Figure 4, using the Static Structural module of Ansys Workbench 2024 R1 Student software, which was configured to use ASTM A36 structural steel for the proposed computational model, the static structural analysis of the elevation platform supporting the parking transfer was performed, which allowed determining the total deformation, this is shown in Figure 5.

Box 5

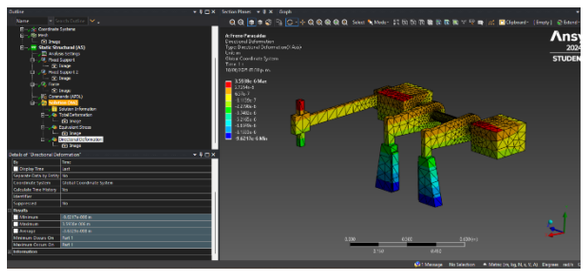

Figure 4

Configuration for static structural analysis simulation.

Source: Own elaboration, 2025

Box 6

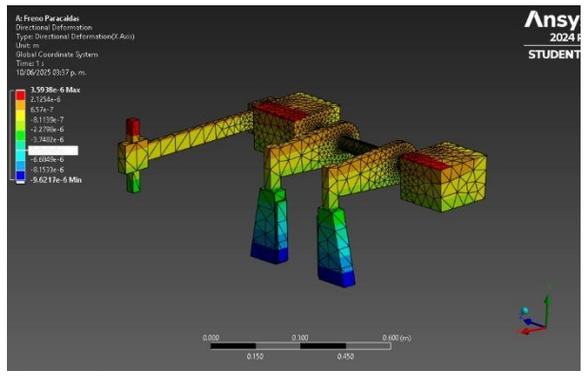

Figure 5

Minimum and maximum total deformation, analysis simulation.

Source: Own elaboration, 2025

ISSN: 2531-2979
RENIECYT: 1702902

Betanzos-Castillo, Francisco, Fuentes-Castañeda, Pilar, Cortez-Solis, Reynaldo and Rodriguez-Cortes, Aldo. [2025]. Modelling of the lifting platform braking mechanism for autonomous vertical parking. Journal-Mathematical and Quantitative Methods. 9[15]1-9: e4915109.
https://doi.org/10.35429/JMQM.2025.9.15.4.1.9

Box 7

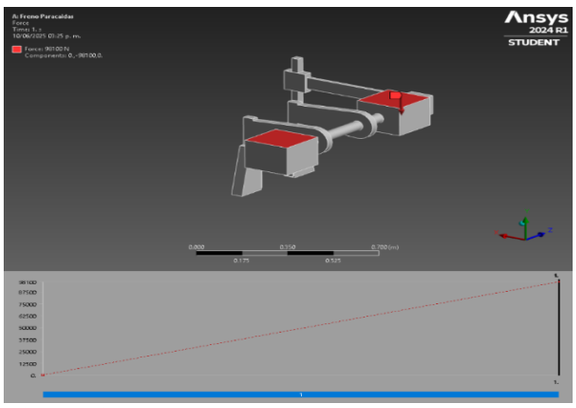

Figure 6

Configuration of forces and supports.

Source: Own elaboration, 2025

For the static structural analysis, an input force of 98100 N was used on faces of the structure shown in red in Figure 6.

Box 8

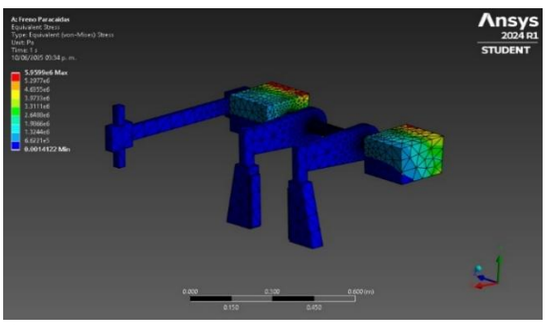

Figure 7

Equivalent [von-Mises] Stress.

Source: Own elaboration, 2025

Finally, Figure 7 shows the minimum and maximum equivalent stress values, i.e., using the Von Mises criterion, these were 1.4122e-3 Pa and 5.9599e6 Pa, respectively, which are found at the end of the fastening element of the brake mechanism support structure.

Discussion of results

A braking system for a lifting platform was modeled, and the behavior of the stresses and total deformation was determined. which were determined numerically using the finite element technique. This type of analysis is very suitable for structural analysis, which made it possible to determine the mechanical behavior of the braking mechanism for the vertical parking lift platform, which, as a conceptual proposal, will be used for an autonomous vertical parking system with a view towards Industry 5.0.

In addition, this technique saves time and money in performing material strength calculations, as well as in the construction and prototyping of physical models.

Computational modelling allowed us to represent and describe the behaviour of total deformation and equivalent stress when subjected to loads equivalent to actual working conditions, allowing us to visualize structural behaviour under different working and limit conditions, which gives an idea of what that behaviour would be like in reality and saves time and money.

The results found in this research allow us to conclude that it is feasible to use computational models with the help of CAD software and perform CAE analysis, which makes it relatively easy to carry out various simulations, thereby imitating the real physical conditions of this type of mechanical element, as well as comparing the results obtained.

It is recommended to continue working on the analysis of these findings and take advantage of these tools to support research in the field of engineering by implementing physical prototypes and verifying and optimizing the current design.

Conclusions

The implementation of electromechanical elevators in this type of parking system offers advantages in terms of energy efficiency and reduced operating costs, providing greater speed and lower energy consumption thanks to the incorporation of advanced electric motors and counterweight systems.

This efficiency not only allows for more economical operation in the long term, but also contributes to reducing the carbon footprint associated with parking infrastructure. In a context where environmental policies demand lower emissions and responsible energy use, electromechanical elevator systems are aligned with current sustainability standards.

Future work should focus on studying new conceptual designs and comparing them with theoretical calculations in order to optimize results and resources. This will make it possible to predict the behavior of the braking mechanism in different materials subjected to different working conditions.

ISSN: 2531-2979
RENIECYT: 1702902

Betanzos-Castillo, Francisco, Fuentes-Castañeda, Pilar, Cortez-Solis, Reynaldo and Rodriguez-Cortes, Aldo. [2025]. Modelling of the lifting platform braking mechanism for autonomous vertical parking. Journal-Mathematical and Quantitative Methods. 9[15]1-9: e4915109.
https://doi.org/10.35429/JMQM.2025.9.15.4.1.9

Finally, this project highlights the importance of incorporating innovative technological solutions into city planning and management.

Autonomous vertical parking systems with electromechanical lifts are a practical and sustainable solution to mobility and space problems in densely populated urban environments.

Declarations

Conflict of interest

The authors declare no interest conflict. They have no known competing financial interests or personal relationships that could have appeared to influence the article reported in this article.

Author contribution

The presente project contribute Development of strategic leading-edge technologies and open innovation for social transformation.

Betanzos-Castillo, Francisco: Contributed to the project idea, research method and technique.

Fuentes-Castañeda, Pilar: wrote the manuscript with input from all authors and developed the theoretical formalism.

Cortez-Solis, Reynaldo: designed the model and the computational framework and analyzed the data.

Rodriguez-Cortes, Aldo: documented and designed the project components.

Funding

The research did not receive funding, although it has received support from the Tecnológico Nacional de México - TES Valle de Bravo in terms of technical support.

Acknowledgements

Special thanks to the Tecnológico Nacional de México - TES Valle de Bravo, since their support has allowed the development of this project, important stages have been achieved that lead to an advance in technological development and in the training of human resources.

References

Basics

Díaz, C. A. & Rosas, J. c. [2021]. Tutorial de Ansys Fluid Flow Polyflow [WORKBENCH]: Moldeo por soplado de una botella PET.

Guangmei Wu, Xianhao Xu, Yeming [Yale] Gong, René De Koster, Bipan Zou. [2019]. Optimal design and planning for compact automated parking systems. European Journal of Operational Research.

K. J. Bathe, ed., Computational Fluid and Solid Mechanics. New York: Elsevier, 2003.

SEMCOCAD. [16 de 09 de 2025]. Soluciones y capacitación CAD/BIM. Obtenido de SEMCOCAD:

Kassimali, A. [2015]. Structural Analysis. 5th Edition. Cengage Learning. ISBN.

Supports

Betanzos-Castillo, Francisco, Fuentes-Castañeda, Pilar and Cortez-Solis, Reynaldo. [2024]. Structural analysis of a lifting platform for autonomous vertical vehicular parking. Journal of Architecture and Design. 8[19]-1-8: e10819108.

Madenci, E., & Guven, I. [2015]. The Finite Element Method and Applications in Engineering Using ANSYS. New York: Springer.

Nakasone, Y., Yoshimoto, S., & Stolarski, T. [2006]. Engineering Analysis with ANSYS Software. Oxford: Elsevier.

Differences

Oguz Örmecioglu, T., Aydogdu, Í., & Tugba Örmecioglu, H. [2024]. GPU-based parallel programming for FEM analysis in the optimization of steel frames. Journal of Asian Architecture and Buikding Engineering, 1-22.

Rameshrao Yawale, V., & Nivrutti Naik, N. [2021]. Static structural and modal analysis of mechanical component using FEA approach. International Journal of Creative Research Thoughts, 9, 4003-4012.

ISSN: 2531-2979
RENIECYT: 1702902

Journal-Mathematical and Quantitative Methods 9[15]1-9: e4915109
Article

Yixu Chu, Junying Lin, Kun Li. Design and Simulation of Foldable Wing eVTOL UAV. Academic Journal of Engineering and Technology Science [2024] Vol. 7, Issue 4: 136-143.

ISSN: 2531-2979
RENIECYT: 1702902

Betanzos-Castillo, Francisco, Fuentes-Castañeda, Pilar, Cortez-Solis, Reynaldo and Rodriguez-Cortes, Aldo. [2025]. Modelling of the lifting platform braking mechanism for autonomous vertical parking. Journal-Mathematical and Quantitative Methods. 9[15]1-9: e4915109.
https://doi.org/10.35429/JMQM.2025.9.15.4.1.9

[[Title in TNRoman and Bold No. 14 in English and Spanish]

Surname, Name 1st Author*[a], Surname, Name 1st Co-author[b], Surname, Name 2nd Co-author[c] and Surname, Name 3rd Co-author[d] [No.12 TNRoman]

[a] Affiliation institution, Researcher ID, ORC ID, SNI-CONAHCYT ID or CVU PNPC [No.10 TNRoman]
[b] Affiliation institution, Researcher ID, ORC ID, SNI-CONAHCYT ID or CVU PNPC [No.10 TNRoman]
[c] Affiliation institution, Researcher ID, ORC ID, SNI-CONAHCYT ID or CVU PNPC [No.10 TNRoman]
[d] Affiliation institution, Researcher ID, ORC ID, SNI-CONAHCYT ID or CVU PNPC [No.10 TNRoman]

All ROR-Clarivate-ORCID and CONAHCYT profiles must be hyperlinked to your website.
Prot- University of South Australia • 7038-2013• 0000-0001-6442-4409 • 416112

CONAHCYT classification:
https://marvid.org/research_areas.php [No.10 TNRoman]
Area:
Field:
Discipline:
Subdiscipline:

DOI: https://doi.org/
Article History:
Received: [Use Only ECORFAN]
Accepted: [Use Only ECORFAN]
Contact e-mail address:
* ✉ [example@example.org]

Abstract [In English]
Must contain up to 150 words
Graphical abstract [In English]

Authors must provide an original image that clearly represents the article described in the article. Graphical abstracts should be submitted as a separate file. Please note that, as well as each article must be unique. File type: the file types are MS Office files.No additional text, outline or synopsis should be included. Any text or captions must be part of the image file. Do not use unnecessary white space or a "graphic abstract" header within the image file.

Keywords [In English]
Indicate 3 keywords in TNRoman and Bold No. 10

Abstract [In Spanish]
Must contain up to 150 words
Graphical abstract [In Spanish]

Authors must provide an original image that clearly represents the article described in the article. Graphical abstracts should be submitted as a separate file. Please note that, as well as each article must be unique. File type: the file types are MS Office files.No additional text, outline or synopsis should be included. Any text or captions must be part of the image file. Do not use unnecessary white space or a "graphic abstract" header within the image file.

Keywords [In Spanish]
Indicate 3 keywords in TNRoman and Bold No. 10

Citation: Surname, Name 1st Author, Surname, Name 1st Co-author, Surname, Name 2nd Co-author and Surname, Name 3rd Co-author. Article Title. Journal-Agrarian and Natural Resource Economics. Year. V-N: Pages [TN Roman No.10].

Introduction

Text in TNRoman No.12, single space.

General explanation of the subject and explain why it is important.

What is your added value with respect to other techniques?

Clearly focus each of its features.

Clearly explain the problem to be solved and the central hypothesis.

Explanation of sections Article.

Development of headings and subheadings of the article with subsequent numbers

[Title No.12 in TNRoman, single spaced and bold]

Products in development No.12 TNRoman, single spaced.

Including figures and tables-Editable

In the article content any table and figure should be editable formats that can change size, type and number of letter, for the purposes of edition, these must be high quality, not pixelated and should be noticeable even reducing image scale.

[Indicating the title at the bottom with No.10 and Times New Roman Bold]

Box

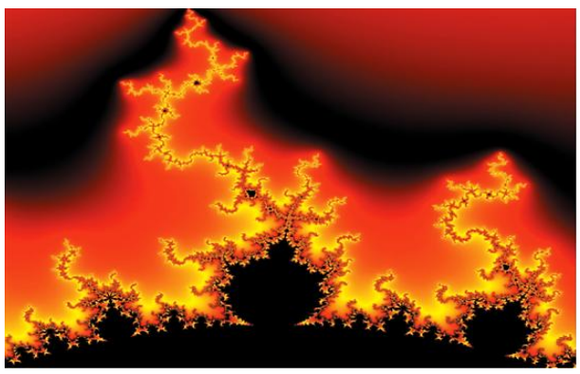

Figure 1

Title [Should not be images-everything must be editable]

Source [in italic]

Box

Table 1

Title [Should not be images-everything must be editable]

Source [in italic]

The maximum number of Boxes is 10 items

For the use of equations, noted as follows:

$$Y_{ij} = \alpha + \sum_{h=1}^{r} \beta_h X_{hij} + u_j + e_{ij} \qquad [1]$$

Must be editable and number aligned on the right side.

Methodology

Develop give the meaning of the variables in linear writing and important is the comparison of the used criteria.

Results

The results shall be by section of the article.

Conclusions

Clearly explain the results and possibilities of improvement.

Annexes

Tables and adequate sources.

The international standard is 7 pages minimum and 14 pages maximum.

Declarations

Conflict of interest

The authors declare no interest conflict. They have no known competing financial interests or personal relationships that could have appeared to influence the article reported in this article.

ISSN 2524-2091

Author contribution

Specify the contribution of each researcher in each of the points developed in this research.

Prot-
Benoit-Pauleter, Gerard: Contributed to the project idea, research method and technique.

Availability of data and materials

Indicate the availability of the data obtained in this research.

Funding

Indicate if the research received some financing.

Acknowledgements

Indicate if they were financed by any institution, University or company.

Abbreviations

List abbreviations in alphabetical order.

Prot-

ANN	Artificial Neural Network

References

Use APA system. Should not be numbered, nor with bullets, however if necessary numbering will be because reference or mention is made somewhere in the Article.

Use the Roman alphabet, all references you have used should be in Roman alphabet, even if you have cited an article, book in any of the official languages of the United Nations [English, French, German, Chinese, Russian, Portuguese, Italian, Spanish, Arabic], you should write the reference in Roman alphabet and not in any of the official languages.

Citations are classified the following categories:

Antecedents. The citation is due to previously published research and orients the citing document within a particular scholarly area.

Basics. The citation is intended to report data sets, methods, concepts and ideas on which the authors of the citing document base their work.

Supports. The citing article reports similar results. It may also refer to similarities in methodology or, in some cases, to the reproduction of results.

Differences. The citing document reports by means of a citation that it has obtained different results to those obtained in the cited document. This may also refer to differences in methodology or differences in sample sizes that affect the results.

Discussions. The citing article cites another study because it is providing a more detailed discussion of the subject matter.

The URL of the resource is activated in the DOI or in the title of the resource.

Prot-
Mandelbrot, B. B. [2020]. Negative dimensions and Hölders, multifractals and their Hölder spectra, and the role of lateral preasymptotics in science. Journal of Fourier Analysis and Applications Special. 409-432.

Intellectual Property Requirements for editing:

- Authentic Signature in Color of Originality Format Author and Coauthors.
- Authentic Signature in Color of the Acceptance Format of Author and Coauthors.
- Authentic Signature in blue color of the Conflict of Interest Format of Author and Co-authors.

ISSN 2524-2091

Reservation to Editorial Policy

RINOE Journal-Mathematical and Quantitative Methods reserves the right to make editorial changes required to adapt the Articles to the Editorial Policy of the Journal. Once the Article is accepted in its final version, the Journal will send the author the proofs for review. RINOE® will only accept the correction of errata and errors or omissions arising from the editing process of the Journal, reserving in full the copyrights and content dissemination. No deletions, substitutions or additions that alter the formation of the Article will be accepted.

Code of Ethics - Good Practices and Declaration of Solution to Editorial Conflicts

Declaration of Originality and unpublished character of the Article, of Authors, on the obtaining of data and interpretation of results, Acknowledgments, Conflict of interests, Assignment of rights and Distribution.

The RINOE® Management claims to Authors of Articles that its content must be original, unpublished and of Scientific, Technological and Innovation content to be submitted for evaluation.

The Authors signing the Article must be the same that have contributed to its conception, realization and development, as well as obtaining the data, interpreting the results, drafting and reviewing it. The Corresponding Author of the proposed Article will request the form that follows.

Article title:

- The sending of an Article to RINOE Journal-Mathematical and Quantitative Methods emanates the commitment of the author not to submit it simultaneously to the consideration of other series publications for it must complement the Format of Originality for its Article, unless it is rejected by the Arbitration Committee, it may be withdrawn.

- None of the data presented in this article has been plagiarized or invented. The original data are clearly distinguished from those already published. And it is known of the test in PLAGSCAN if a level of plagiarism is detected Positive will not proceed to arbitrate.

- References are cited on which the information contained in the Article is based, as well as theories and data from other previously published Articles.

- The authors sign the Format of Authorization for their Article to be disseminated by means that RINOE® in its Holding Spain considers pertinent for disclosure and diffusion of its Article its Rights of Work.

- Consent has been obtained from those who have contributed unpublished data obtained through verbal or written communication, and such communication and Authorship are adequately identified.

- The Author and Co-Authors who sign this work have participated in its planning, design and execution, as well as in the interpretation of the results. They also critically reviewed the paper, approved its final version and agreed with its publication.

- No signature responsible for the work has been omitted and the criteria of Scientific Authorization are satisfied.

- The results of this Article have been interpreted objectively. Any results contrary to the point of view of those who sign are exposed and discussed in the Article.

Copyright and Access

The publication of this Article supposes the transfer of the copyright to RINOE® in its Holding Spain for its RINOE Journal-Mathematical and Quantitative Methods, which reserves the right to distribute on the Web the published version of the Article and the making available of the Article in This format supposes for its Authors the fulfilment of what is established in the Law of Science and Technology of the United Mexican States, regarding the obligation to allow access to the results of Scientific Research.

Article Title:

Name and Surnames of the Contact Author and the Coauthors	Signature
1.	
2.	
3.	
4.	

Principles of Ethics and Declaration of Solution to Editorial Conflicts

Editor Responsibilities

The Publisher undertakes to guarantee the confidentiality of the evaluation process, it may not disclose to the Arbitrators the identity of the Authors, nor may it reveal the identity of the Arbitrators at any time.

The Editor assumes the responsibility to properly inform the Author of the stage of the editorial process in which the text is sent, as well as the resolutions of Double-Blind Review.

The Editor should evaluate manuscripts and their intellectual content without distinction of race, gender, sexual orientation, religious beliefs, ethnicity, nationality, or the political philosophy of the Authors.

The Editor and his editing team of RINOE® Holdings will not disclose any information about Articles submitted to anyone other than the corresponding Author.

The Editor should make fair and impartial decisions and ensure a fair Double-Blind Review.

Responsibilities of the Editorial Board

The description of the peer review processes is made known by the Editorial Board in order that the Authors know what the evaluation criteria are and will always be willing to justify any controversy in the evaluation process. In case of Plagiarism Detection to the Article the Committee notifies the Authors for Violation to the Right of Scientific, Technological and Innovation Authorization.

Responsibilities of the Arbitration Committee

The Arbitrators undertake to notify about any unethical conduct by the Authors and to indicate all the information that may be reason to reject the publication of the Articles. In addition, they must undertake to keep confidential information related to the Articles they evaluate.

Any manuscript received for your arbitration must be treated as confidential, should not be displayed or discussed with other experts, except with the permission of the Editor.

The Arbitrators must be conducted objectively, any personal criticism of the Author is inappropriate.

The Arbitrators must express their points of view with clarity and with valid arguments that contribute to the Scientific, Technological and Innovation of the Author.

The Arbitrators should not evaluate manuscripts in which they have conflicts of interest and have been notified to the Editor before submitting the Article for Double-Blind Review.

Responsibilities of the Authors

Authors must guarantee that their articles are the product of their original work and that the data has been obtained ethically.

Authors must ensure that they have not been previously published or that they are not considered in another serial publication.

Authors must strictly follow the rules for the publication of Defined Articles by the Editorial Board.

The authors have requested that the text in all its forms be an unethical editorial behavior and is unacceptable, consequently, any manuscript that incurs in plagiarism is eliminated and not considered for publication.

Authors should cite publications that have been influential in the nature of the Article submitted to arbitration.

Information services

Indexation - Bases and Repositories

LATINDEX (Scientific Journals of Latin America, Spain and Portugal)
RESEARCH GATE (Germany)
GOOGLE SCHOLAR (Citation indices-Google)
MENDELEY (Bibliographic References Manager)
V|LEX (Global Legal Intelligence Platform)

Publishing Services

Citation and Index Identification H
Management of Originality Format and Authorization
Testing Article with PLAGSCAN
Article Evaluation
Certificate of Double-Blind Review
Article Edition
Web layout
Indexing and Repository
Article Translation
Article Publication
Certificate of Article
Service Billing

Editorial Policy and Management

38 Matacerquillas, CP-28411. Moralzarzal - Madrid – Spain. Phones: +52 1 55 1260 0355, +52 1 55 6159 2296, +52 1 55 6034 9181; E-mail: contact@rinoe.org www.rinoe.org

RINOE® Journal-Mathematical and Quantitative Methods

Site Licences

03-2010-032610094200-01-For printed material, 03-2010-031613323600-01-For Electronic material,03-2010-032610105200-01-For Photographic material,03-2010-032610115700-14-For the facts Compilation,04-2010-031613323600-01-For its Web page,19502-For the Iberoamerican and Caribbean Indexation,20-281 HB9-For its indexation in Latin-American in Social Sciences and Humanities,671-For its indexing in Electronic Scientific Journals Spanish and Latin-America,7045008-For its divulgation and edition in the Ministry of Education and Culture-Spain,25409-For its repository in the Biblioteca Universitaria-Madrid,16258-For its indexing in the Dialnet,20589-For its indexing in the edited Journals in the countries of Iberian-America and the Caribbean, 15048-For the international registration of Congress and Colloquiums. financingprograms@rinoe.org

Management Offices

38 Matacerquillas, CP-28411. Moralzarzal - Madrid - Spain.

Journal-Mathematical and Quantitative Methods

2531 2979
ISSN 2531-2979
www.rinoe.org